

# START

0033732

5

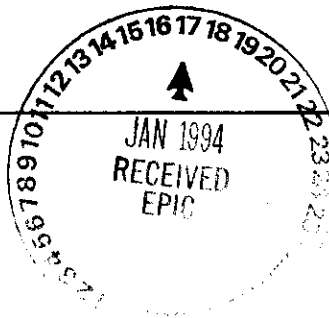
## ENGINEERING DATA TRANSMITTAL

Page 1 of 1

DEC 20 1993


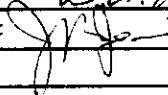
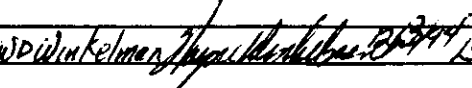
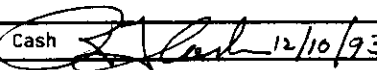
1. EDT 600454

2. To: (Receiving Organization) Characterization & Safety Technology	3. From: (Originating Organization) Process Chemistry Laboratory	4. Related EDT No.: N/A
5. Proj./Prog./Dept./Div.: Characterization & Safety Technology	6. Cog. Engr.: B. A. Crawford	7. Purchase Order No.: N/A
8. Originator Remarks:  N/A		9. Equip./Component No.: N/A
11. Receiver Remarks:		10. System/Bldg./Facility: 222-S Laboratory
		12. Major Assm. Dwg. No.: N/A
		13. Permit/Permit Application No.: N/A
		14. Required Response Date:




15. DATA TRANSMITTED					(F)	(G)	(H)	(I)
(A) Item No.	(B) Document/Drawing No.	(C) Sheet No.	(D) Rev. No.	(E) Title or Description of Data Transmitted	Impact Level	Reason for Transmittal	Originator Disposition	Receiver Disposition
1	WHC-SD-WM-TI-580		0	EVALUATION OF DISPERSIVE RAMAN SPECTROSCOPY FOR CHARACTERIZATION OF HLW TANK WASTE IN THE LABORATORY	4	1	1	

16. KEY					
Impact Level (F)		Reason for Transmittal (G)			Disposition (H) & (I)
1, 2, 3, or 4 (see MRP 5.43)		1. Approval 2. Release 3. Information	4. Review 5. Post-Review 6. Dist. (Receipt Acknow. Required)		1. Approved 2. Approved w/comment 3. Disapproved w/comment 4. Reviewed no/comment 5. Reviewed w/comment 6. Receipt acknowledged

(G)	(H)	17. SIGNATURE/DISTRIBUTION (See Impact Level for required signatures)								(G)	(H)
Reason	Disp.	(J) Name	(K) Signature	(L) Date	(M) MSIN	(J) Name	(K) Signature	(L) Date	(M) MSIN	Reason	Disp.
1	1	Cog.Eng. BA Crawford		9/4/93							
1	1	Cog. Mgr. JR Jewett		9/24/93							
		QA									
		Safety				WD Winkelman		1/5/94		1	1
		Env.									
1	1	Program R. Cash		12/10/93							

18. BA Crawford <i>[Signature]</i> 9/4/93 Signature of EDT Originator	19. RJ Cash <i>[Signature]</i> 12/10/93 Authorized Representative Date for Receiving Organization	20. JR Jewett See Block 17 Cognizant/Project Engineer's Manager	21. DOE APPROVAL (if required) Ltr. No. <input type="checkbox"/> Approved <input type="checkbox"/> Approved w/comments <input type="checkbox"/> Disapproved w/comments
---	---	---	--

**THIS PAGE INTENTIONALLY  
LEFT BLANK**

Date Received: <u>12/14/93</u> <u>KMB</u>		<b>INFORMATION RELEASE REQUEST</b>		Reference: WHC-CM-3-4	
Complete for all Types of Release					
Purpose <input type="checkbox"/> Speech or Presentation <input type="checkbox"/> Full Paper (Check only one suffix) <input type="checkbox"/> Summary <input type="checkbox"/> Abstract <input type="checkbox"/> Visual Aid <input type="checkbox"/> Speakers Bureau <input type="checkbox"/> Poster Session <input type="checkbox"/> Videotape			ID Number (include revision, volume, etc.) WHC-SD-WM-TI-580, REV. 0 List attachments. N/A Date Release Required 9/30/93		
Title <b>EVALUATION OF DISPERSIVE RAMAN SPECTROSCOPY FOR CHARACTERIZATION OF HLW TANK SAMPLES IN THE LABORATORY</b>				Unclassified Category UC-	
New or novel (patentable) subject matter? <input checked="" type="checkbox"/> No <input type="checkbox"/> Yes If "Yes", has disclosure been submitted by WHC or other company? <input type="checkbox"/> No <input type="checkbox"/> Yes (Disclosure No(s)).			Information received from others in confidence, such as proprietary data, trade secrets, and/or inventions? <input checked="" type="checkbox"/> No <input type="checkbox"/> Yes (Identify)		
Copyrights? <input checked="" type="checkbox"/> No <input type="checkbox"/> Yes If "Yes", has written permission been granted? <input type="checkbox"/> No <input type="checkbox"/> Yes (Attach Permission)			Trademarks? <input checked="" type="checkbox"/> No <input type="checkbox"/> Yes (Identify)		
Complete for Speech or Presentation					
Title of Conference or Meeting N/A			Group or Society Sponsoring N/A		
Date(s) of Conference or Meeting N/A		City/State N/A		Will proceedings be published? <input type="checkbox"/> Yes <input type="checkbox"/> No Will material be handed out? <input type="checkbox"/> Yes <input type="checkbox"/> No	
Title of Journal N/A					
CHECKLIST FOR SIGNATORIES					
Review Required per WHC-CM-3-4		Yes      No		Reviewer - Signature Indicates Approval Name (printed)      Signature      Date	
Classification/Uncontrolled Nuclear Information		<input type="checkbox"/> Yes <input checked="" type="checkbox"/> No		S. W. Berglin <u>[Signature]</u> 9/27/93	
Patent - General Counsel		<input checked="" type="checkbox"/> Yes <input type="checkbox"/> No		S. W. Berglin <u>[Signature]</u>	
Legal - General Counsel		<input checked="" type="checkbox"/> Yes <input type="checkbox"/> No		R. J. Cash <u>[Signature]</u> 9-24-93	
Applied Technology/Export Controlled Information or International Program		<input type="checkbox"/> Yes <input checked="" type="checkbox"/> No		R. F. Christensen <u>[Signature]</u> 12/16/93	
WHC Program/Project		<input checked="" type="checkbox"/> Yes <input type="checkbox"/> No		C. Collins <u>[Signature]</u> 12/20/93	
Communications		<input type="checkbox"/> Yes <input checked="" type="checkbox"/> No			
RL Program/Project		<input checked="" type="checkbox"/> Yes <input type="checkbox"/> No			
Publication Services		<input checked="" type="checkbox"/> Yes <input type="checkbox"/> No			
Other Program/Project		<input type="checkbox"/> Yes <input checked="" type="checkbox"/> No			
Information conforms to all applicable requirements. The above information is certified to be correct.					
References Available to Intended Audience <input checked="" type="checkbox"/> Yes <input type="checkbox"/> No Transmit to DOE-HQ/Office of Scientific and Technical Information <input checked="" type="checkbox"/> Yes <input type="checkbox"/> No Author/Requestor (Printed/Signature)      Date B. A. Crawford <u>[Signature]</u> 9/6/93				INFORMATION RELEASE ADMINISTRATION APPROVAL STAMP Stamp is required before release. Release is contingent upon resolution of mandatory comments. 	
Intended Audience <input type="checkbox"/> Internal <input type="checkbox"/> Sponsor <input checked="" type="checkbox"/> External Responsible Manager (Printed/Signature)      Date J. R. Jewett <u>[Signature]</u> 12/24/93					
Date Cancelled      Date Disapproved					

**THIS PAGE INTENTIONALLY  
LEFT BLANK**

## SUPPORTING DOCUMENT

1. Total Pages 111

## 2. Title

EVALUATION OF DISPERSIVE RAMAN SPECTROSCOPY FOR CHARACTERIZATION OF HLW TANK SAMPLES IN THE LABORATORY

## 3. Number

WHC-SD-WM-TI-580

## 4. Rev No.

0

## 5. Key Words

Raman spectroscopy, dispersive Raman spectroscopy, hot cell, screening, argon ion laser, fiber optic probe, waste tanks, high-level waste samples, diode laser, ferrocyanide, speciation

APPROVED FOR  
PUBLIC RELEASE

*EMB 12/20/93*

## 6. Author

Name: B. A. Crawford *B.A. Crawford*  
F. L. Kohlasch *F.L. Kohlasch*  
G. L. Troyer *G.L. Troyer*  
D. A. Dodd *D.A. Dodd*

Signature

Organization/Charge Code 12110/N232P

## 7. Abstract

This document describes the development and assessment of laser Raman spectrometric methods for analysis of anions in HLW samples in laboratory hot cells and hoods. It has been successfully demonstrated that selected equipment and methods may provide for routine use of dispersive Raman in laboratory sample screening at weight percent concentrations. Detection limits for ferrocyanide, chemical identity of major components in salt-containing tank wastes, baseline assay for organic species and library development are discussed.

~~PURPOSE AND USE OF DOCUMENT - This document was prepared for use within the U.S. Department of Energy and its contractors. It is to be used only to perform, direct, or integrate work under U.S. Department of Energy contracts. This document is not approved for public release until reviewed.~~

~~PATENT STATUS - This document copy, since it is transmitted in advance of patent clearance, is made available in confidence solely for use in performance of work under contracts with the U.S. Department of Energy. This document is not to be published nor its contents otherwise disseminated or used for purposes other than specified above before patent approval for such release or use has been secured, upon request, from the Patent Counsel, U.S. Department of Energy Field Office, Richland, WA.~~

DISCLAIMER - This report was prepared as an account of work sponsored by an agency of the United States Government. Neither the United States Government nor any agency thereof, nor any of their employees, nor any of their contractors, subcontractors or their employees, makes any warranty, express or implied, or assumes any legal liability or responsibility for the accuracy, completeness, or any third party's use or the results of such use of any information, apparatus, product, or process disclosed, or represents that its use would not infringe privately owned rights. Reference herein to any specific commercial product, process, or service by trade name, trademark, manufacturer, or otherwise, does not necessarily constitute or imply its endorsement, recommendation, or favoring by the United States Government or any agency thereof or its contractors or subcontractors. The views and opinions of authors expressed herein do not necessarily state or reflect those of the United States Government or any agency thereof.

## 10.

## RELEASE STAMP

OFFICIAL RELEASE	
BY WHO	
DATE	DEC 20 1993
<i>Sta 4</i>	

## 9. Impact Level 4

**THIS PAGE INTENTIONALLY  
LEFT BLANK**

**EVALUATION OF DISPERSIVE RAMAN SPECTROSCOPY FOR  
CHARACTERIZATION OF HIGH LEVEL WASTE  
TANK SAMPLES IN THE LABORATORY**

**B. A. Crawford  
D. A. Dodd  
F. L. Kohlsh  
G. L. Troyer**

**ABSTRACT**

*This report describes (1) the development and assessment of laser Raman spectrometric methods for analysis of anions in high-level waste samples in laboratory hot cells and hoods, (2) the successful demonstration of selected equipment and methods that have provided preliminary procedures that may facilitate the routine use of the Raman instrument in the laboratory, and (3) the introduction of a suitable analytical tool for direct screening of ferrocyanide species in weight percent concentrations. Oxyanions and ferrocyanide anions have been identified qualitatively in pure reagents, simulants, and real tank matrices. This report summarizes the results of evaluation and features testing of Raman spectroscopy completed in cold and hot cell environments at the Hanford Site. The hot cell analyses performed for this work are the first application of a Raman system with a remote fiber optic probe in Hanford Site hot cells with real tank waste samples. Direct analysis has application as both a qualitative and quantitative sample screening tool in the laboratory, and may be developed as a means of in situ characterization in waste tanks once appropriate tank standards are established and calibration transfer has been demonstrated. Future work will center on generation of reference spectra of pure reagents expected in these materials and assessment of tank wastes as extrusion and sampling proceeds through the laboratory.*

This page intentionally left blank.

943205 328



## EXECUTIVE SUMMARY

This report provides a status of studies performed during fiscal year 1993 toward implementing a Raman optical spectroscopy system, one technology to be incorporated into a multi-discipline tool to provide this screening for molecular species. This screening methodology must be capable of deployment in harsh environments where ambient temperature is not well controlled and where chemical vapors and radiation are present (i.e., in laboratory hot cells). This technology may be extended to nonlaboratory screening applications in the future if the technology is proven reliable and effective in supporting program needs.

This technology is complimentary to infrared spectroscopy (e.g., chemical species may be detectable by one technology and obscured in the other). For example, Raman spectroscopy is more suitable for aqueous samples, while infrared spectroscopy is strongly implicated for use in moisture monitoring. Raman technology has been demonstrated in remote operations using fiber optics.

Although the work reported in this document is preliminary, the activities performed in fiscal year 1993 provide strong indication that the technology is viable and beneficial to the intended EM-50 and EM-30 programmatic objectives. The following paragraphs describe achievements attained.

System Integration. Experts in the field of Raman spectroscopy, outside Westinghouse Hanford Company (WHC), assisted WHC in obtaining and testing state-of-the-art dispersive Raman system technology within a compressed time

span. Extensive technical interactions were nurtured between scientists from the Savannah River Site, Lawrence Livermore National Laboratories, Naval Research Laboratories, Florida State University, and WHC. Collectively, these scientists developed a plan for instrument purchase and implementation. Instruments that were purchased to provide an operating system included a dispersive Raman spectrometer, charge-coupled device (CCD) detectors, diode and argon ion laser sources, a Savannah River Site "tapered probe," vendor-supplied operating software, and custom-designed data manipulation software.

Test Strategy. Limited testing was initially conducted in a nonradioactive environment, before proceeding to a radioactive environment in laboratory hoods and finally into hot cells. These tests provided operating experience from which an initial operating procedure was developed (Appendix B).

This testing was sufficient to conclude that the near infrared diode laser source, initially used with the WHC Raman system, performed acceptably on pure reagents; however, it provided insufficient excitation power through the fiber optic for adequate response from constituents of interest in some solid samples. Therefore, testing was initiated using an argon ion laser source producing light in the visible spectral region. Data currently available is insufficient to make conclusions about the adequacy of this excitation source. However, preliminary data showed oxyanions and possible cyanide breakdown products in actual ferrocyanide waste tank samples.

Preliminary data strongly suggest that Raman methods can be useful for identification of differences in material composition within a sample, such as

061 502616  
941305.130



This page intentionally left blank.

943205.132

## CONTENTS

1.0	INTRODUCTION . . . . .	1-1
2.0	OBJECTIVE . . . . .	2-1
3.0	RAMAN SYSTEM DESCRIPTION . . . . .	3-1
3.1	PRINCIPLE . . . . .	3-1
3.2	SYSTEM CONFIGURATION . . . . .	3-1
4.0	TEST MATERIALS . . . . .	4-1
5.0	DIODE LASER SYSTEM RESULTS . . . . .	5-1
5.1	SPECTRA AND COMPARISON OF ASSIGNMENTS OF PURE REAGENTS . . . . .	5-1
6.0	ARGON ION LASER RESULTS . . . . .	6-1
7.0	MATRIX SPIKING . . . . .	7-1
8.0	DETECTION LIMITS FOR CYANIDE SPECIES . . . . .	8-1
9.0	QUALITY ASSURANCE . . . . .	9-1
9.1	SOFTWARE QUALITY ASSURANCE . . . . .	9-6
9.2	QUALITY ASSURANCE IN SAMPLE ANALYSES . . . . .	9-6
10.0	DATA TREATMENT PROTOCOLS AND NOISE SOURCES . . . . .	10-1
11.0	RECOMMENDATIONS AND CONCLUSIONS . . . . .	11-1
12.0	ACKNOWLEDGEMENTS . . . . .	12-1
13.0	REFERENCES . . . . .	13-1

## APPENDIXES

A	SPECTRA OF PURE REAGENTS . . . . .	A-1
B	PRELIMINARY LABORATORY TECHNICAL PROCEDURE . . . . .	B-1

# LIST OF FIGURES

1-1	Homogeneity in an Archived Sample of Tank 241-T-107 Waste Material . . . . .	1-3
3-1	Remote Raman Spectroscopy System . . . . .	3-3
5-1	Sodium Ferrocyanide Obtained in the Hot Cell . . . . .	5-2
5-2	Quantum Efficiency of CCD Detector for Mononickel Ferrocyanide Speciation . . . . .	5-3
5-3	Spectra of Tank 241-BX-107 Samples . . . . .	5-4
6-1	Cyclohexane Diode vs. Argon Ion Laser Excitation . . . . .	6-2
6-2	Spectrum of Sodium Nickel Ferrocyanide . . . . .	6-3
6-3	Spectrum of Tank 241-T-111 . . . . .	6-4
6-4	Comparison of Tank 241-BY-104 Simulant and Real Waste Spectra . . . . .	6-5
6-5	FTIR Spectra of Ferrocyanide Process Simulants . . . . .	6-7
6-6	Raman Spectra of Ferrocyanide Process Simulants at Different Excitation Frequencies . . . . .	6-8
6-7	Raman Spectra of Tank 241-T-107 Waste Sample . . . . .	6-10
7-1	Internal Standard $\text{NaClO}_3$ with Diode Laser Excitation . . . . .	7-2
7-2	Spiking Tank 241-BY-104 Simulant with $\text{Na}_2\text{NiFe}(\text{CN})_6$ . . . . .	7-3
7-3	Spiking Tank 241-BX-107 Real Tank Waste. . . . .	7-4
8-1	$\text{K}_4\text{Fe}(\text{CN})_6$ and $\text{Na}_4\text{Fe}(\text{CN})_6$ in $\text{NaNO}_3$ . . . . .	8-3
8-2	Calibration Curve of $\text{K}_3\text{Fe}(\text{CN})_6$ in Tank 241-BY-104 Simulant . . . . .	8-4
8-3	Tank 241-BX-107 Real Waste Sample Spiked with $\text{Na}_4\text{Fe}(\text{CN})_6$ and $\text{Na}_2\text{NiFe}(\text{CN})_6$ . . . . .	8-5
10-1	Background with Known Sources . . . . .	10-2
10-2	Raman Gama Spike Comparison: Upper Trace is Direct Sum of Unprocessed Scans; Lower Trace is Sum of Scans with Spikes Removed . . . . .	10-4

3-1	Remote Raman Configurations Investigated . . . . .	3-2
4-1	Ferrocyanide Process Simulants . . . . .	4-2
4-2	Tank 241-BY-104 Simulant Makeup . . . . .	4-2
4-3	Tank 241-BY-104 Sample Analysis . . . . .	4-3
4-4	Real Waste Weight Percent Total Analytes . . . . .	4-5
5-1	Peak Assignment Comparisons . . . . .	5-5
9-1	Instrumental Parameters . . . . .	9-2
9-2	File Data Types and File Extensions . . . . .	9-5
9-3	Documentation Methods . . . . .	9-5
9-4	Data Comparisons by Analyte . . . . .	9-7

This page intentionally left blank.

9413205.1336



LIST OF TERMS

ANSI	American National Standards Institute
ASTM	American Society for Testing and Materials
CCD	Charge-coupled device
EM	U.S. Department of Energy, Office of Environmental Restoration and Waste Management
FSU	Florida State University
FT	Fourier transform
FY	Fiscal year
FTIR	Fourier transform infrared
HPT	Health Physics Technician
IC	Ion chromatography
ICP	Inductively coupled plasma spectroscopy
IEEE	Institute of Electrical and Electronics Engineers
LOD	Limits of detection
NIST	National Institute of Standards and Technology
PCL	Process Analytical Chemistry Laboratories
PNL	Pacific Northwest Laboratory
RWP	Radiation Work Permit
TOC	Total organic carbon
USQ	Unreviewed safety question
UV	Ultraviolet
WHC	Westinghouse Hanford Company

This page intentionally left blank.

9413205.1338

**EVALUATION OF DISPERSIVE RAMAN SPECTROSCOPY FOR  
CHARACTERIZATION OF HIGH LEVEL WASTE  
TANK SAMPLES IN THE LABORATORY**

**1.0 INTRODUCTION**

The development of the Raman technology follows a phased iterative approach supported through EM-50 and EM-30 budget tasks. These tasks involve a progression of cold testing, hot cell testing, hot cell applications, and eventually in situ waste tank applications. This phased, interactive approach supports the development of a Raman applications knowledge base in a progressive manner that should minimize risks in applying the technology to tank waste materials and environments. This work has focused on cold laboratory and hot cell testing, and on hot cell applications. Support for this work was jointly supplied by the U.S. Department of Energy Office of Environmental Restoration and Waste Management (EM), Office of Technology Development, Underground Storage Tank Integrated Demonstration (EM-50), Tank Waste Remediation Systems, and Tank Safety (EM-30) programs.

The long-range goal of this evaluation is to develop a system for remote characterization and analysis of materials in waste tank applications. A short-range goal is to provide an overview of the Raman technique as a laboratory screening method. A collection of archived samples and simulants provides a reasonable means to prove that screening with an argon ion laser-based dispersive Raman system is suitable for detection of oxyanions and ferrocyanide salts in weight percent quantities in laboratory hoods and hot cells. In this work, core sample screening is based on observation of analytes that are known to be present and to have spectra that have been stored for comparison. Therefore, an experience base and an archive of data for applying and comparing remotely obtained Raman spectra has been established.

A feasibility study of the use of Raman spectroscopy to provide analytical screening data on Hanford Site waste tank constituents was performed by Florida State University (FSU) in fiscal year (FY) 1992. The results of that study were documented in *Detection and Quantitative Analysis of Ferrocyanide and Ferricyanide*, WHC-SD-TD-RPT-003, Revision 0 (WHC 1992). The study results showed that the detection limits of a Raman spectroscopy system were sufficient to provide valuable data on ferrocyanide and ferricyanide salts and selected oxyanions in Hanford Site tank waste samples. Tests conducted during the study were performed on waste simulants and pure materials.

With the successful completion of the FSU study, work continued toward the routine use of Raman spectroscopy analysis with high-level waste materials from Hanford Site tank waste samples. The *Preliminary Evaluation of Raman Spectroscopy for the Hot Cell*, WHC-SD-WM-TP-157 (Crawford 1993a) described the protocol for the development of Raman spectroscopy for qualitative screening of tank samples in laboratory hot cells and hoods. The results of this evaluation are in this report. Protocols were established for calibration,

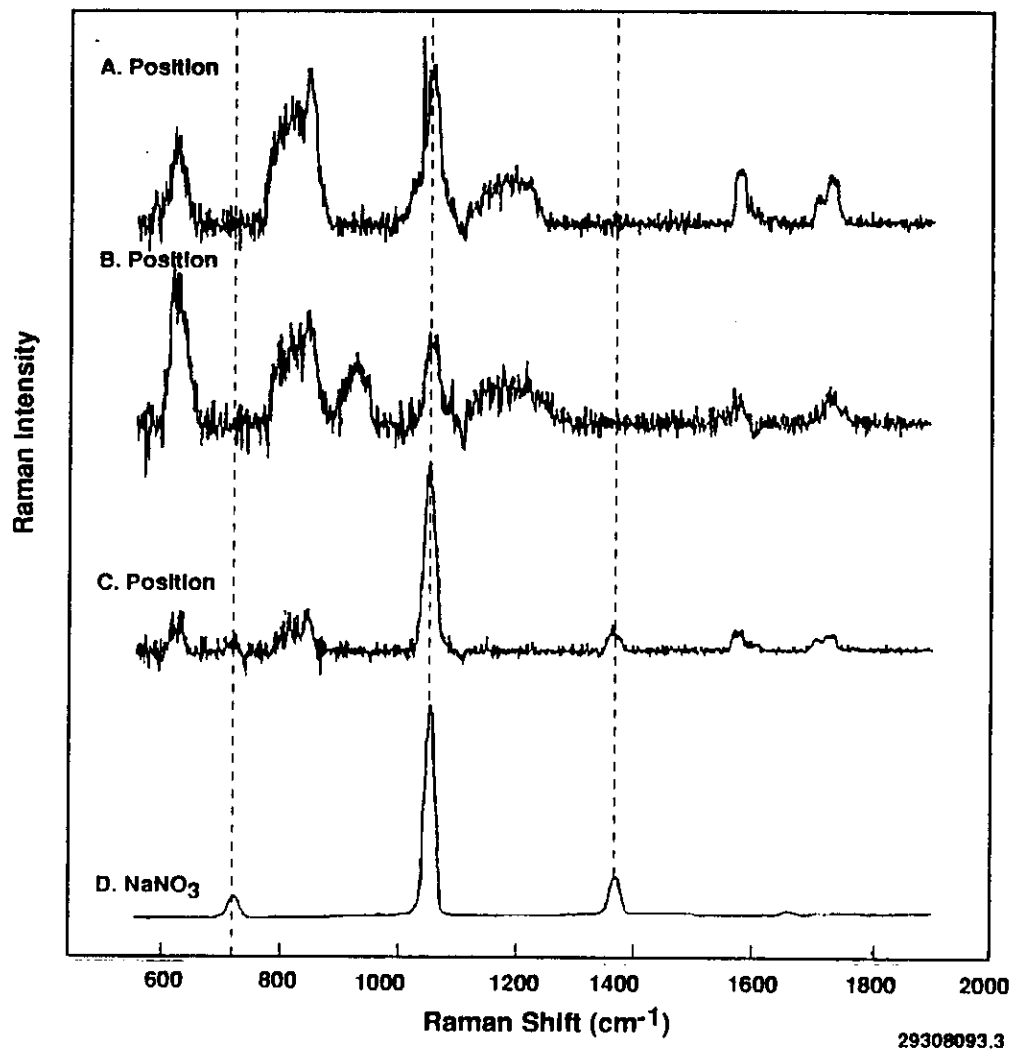
optimization, and analysis of pure material spectra and real tank wastes. The utility of Raman spectroscopy to ferrocyanide speciation and oxyanion analysis is also described.

Experts in the field of Raman spectroscopy have determined that chemical quantification may proceed in tank matrices (WHC 1992). However, it is important to understand sample matrix interference in order to determine the ultimate results. Some determination of homogeneity of samples is possible without full knowledge of matrix effects through simple spectral comparison. Data generated from the hot cell has provided fingerprint data from which a cursory level of homogeneity can be assessed. These data will be helpful in augmenting the selection of samples for detailed analysis, and effectively providing a process monitor that directs samples through the laboratory. A good illustration of how this may work is provided in Figure 1-1. The Raman fiber-optic probe was placed in three different sampling positions within a sample of archived tank 241-T-107 material. Three distinctly different spectra resulted from this experiment.

The major band appears to be from nitrate, which is variable in each spectrum with relation to other bands. The spectrum obtained from position 3 appears to be caused by nitrate with other weaker bands at 625, 850, 1,600 and 1,700  $\text{cm}^{-1}$ . In position 1 and 2, these weaker bands are more pronounced than the nitrate features, and another broad band at 1,150  $\text{cm}^{-1}$  is evident. In addition, spectra from position 2 differ by a band at 900  $\text{cm}^{-1}$ , which is nearly as intense as the nitrate band in the subsequent spectrum. This data clearly illustrates that, when used as a means to check sample homogeneity alone, this method may improve the quality of data obtained from the tank samples within the laboratory.

Figure 1-1. Homogeneity in an Archived Sample of Tank 241-T-107 Waste Material.

## Homogeneity in an Archived Sample of T-107 Tank Material



This page intentionally left blank.

9413205.342

## 2.0 OBJECTIVE

An analytical screening methodology is needed by the Westinghouse Hanford Company programs to provide additional assurance that significantly different materials in waste tank core segments are being analyzed. Raman spectroscopy has been identified as a technology that may provide this assurance. This report is a status of work performed in FY 1993 to implement this technology into hot cells at the Hanford Site 222-S Laboratory.

The work described in this document provides data for an initial technical assessment of both diode and argon ion laser-based remote Raman spectrometers for use in laboratory hot cells and hoods. Initial investigations focused on development of a system for direct ferrocyanide speciation. These studies included chemical identification and determination of limits of detection (LOD) for ferrocyanide species in simple salt matrices, simulants, and tank wastes. Work centered around analysis of oxyanions and ferrocyanide breakdown products. The results of these studies is intended to serve as valuable background for further development of the system for routine sample screening in the laboratory. Concurrently, the data provides a baseline for development of in situ characterization methods based on Raman spectroscopy. In particular, future characterization issues encountered in the hot cells in work with this system and others yield useful information for the deployment and operation of these systems at waste tanks.

This page intentionally left blank.

9403205.341



### 3.0 RAMAN SYSTEM DESCRIPTION

#### 3.1 PRINCIPLE

Raman spectroscopy is a vibrational form of molecular spectroscopy that provides information complementary to infrared spectroscopy on molecules. Unlike infrared spectra resulting from direct absorption of infrared radiation, Raman spectra result from inelastic light scattering. This light scattering is fundamentally dependent on the excitation source used, with the intensity of the Raman scattered light being proportional to the fourth power of the excitation frequency.

Raman scattered radiation produces light frequencies shifted from the source frequency for a given molecule. These shifted frequencies are unique for all normal modes of vibration in the molecule, depending on the polarizability of molecular bonds, neighboring atoms, molecules, and environment. Therefore, unique spectral fingerprints are possible for species depending on phase (i.e., aqueous versus solid), and in some cases, matrix.

Spectra are obtainable with laser excitation wavelengths ranging from the ultraviolet (UV) to the near infrared. This characteristic makes Raman-based techniques ideally suited for application with fiber optics because the source frequency can be tuned to favorable light transmission ranges for various fiber optic materials. Therefore, Raman excitation wavelengths of 514.5 nm in the visible region and the UV region provide spectral enhancements when a fluorescent background is not otherwise problematical.

#### 3.2 SYSTEM CONFIGURATION

This study examines the feasibility of remote dispersive Raman spectroscopy techniques. Because of the sensitivity constraints for ferrocyanide analysis, a dispersive Raman instrument has been selected. Dispersive Raman instruments with charge-coupled device (CCD) detectors provide spectral regions of information ranging from 400 to 700  $\text{cm}^{-1}$ , depending primarily on the grating used and the excitation frequency of the laser source. For this study, a 1,200-line/mm grating was used, yielding a 400  $\text{cm}^{-1}$  and a 700  $\text{cm}^{-1}$  spectral window for the diode and the argon ion laser respectively. The Savannah River tapered probe design (described below) was chosen because of the collection efficiency of the return fiber; this probe was used at all sites involved, in parallel, with efforts on this project. A list of the technologies examined are provided in Table 3-1.

Table 3-1. Remote Raman Configurations Investigated.

Instrumental components	Type
Spectrometer	Dispersive
Detector	CCD/Silicon
Probe	Tapered, 2-fiber
Laser source	Diode
	Argon ion
Software	Custom-designed
	Vendor-supported, standardized
CCD = charge-coupled device	

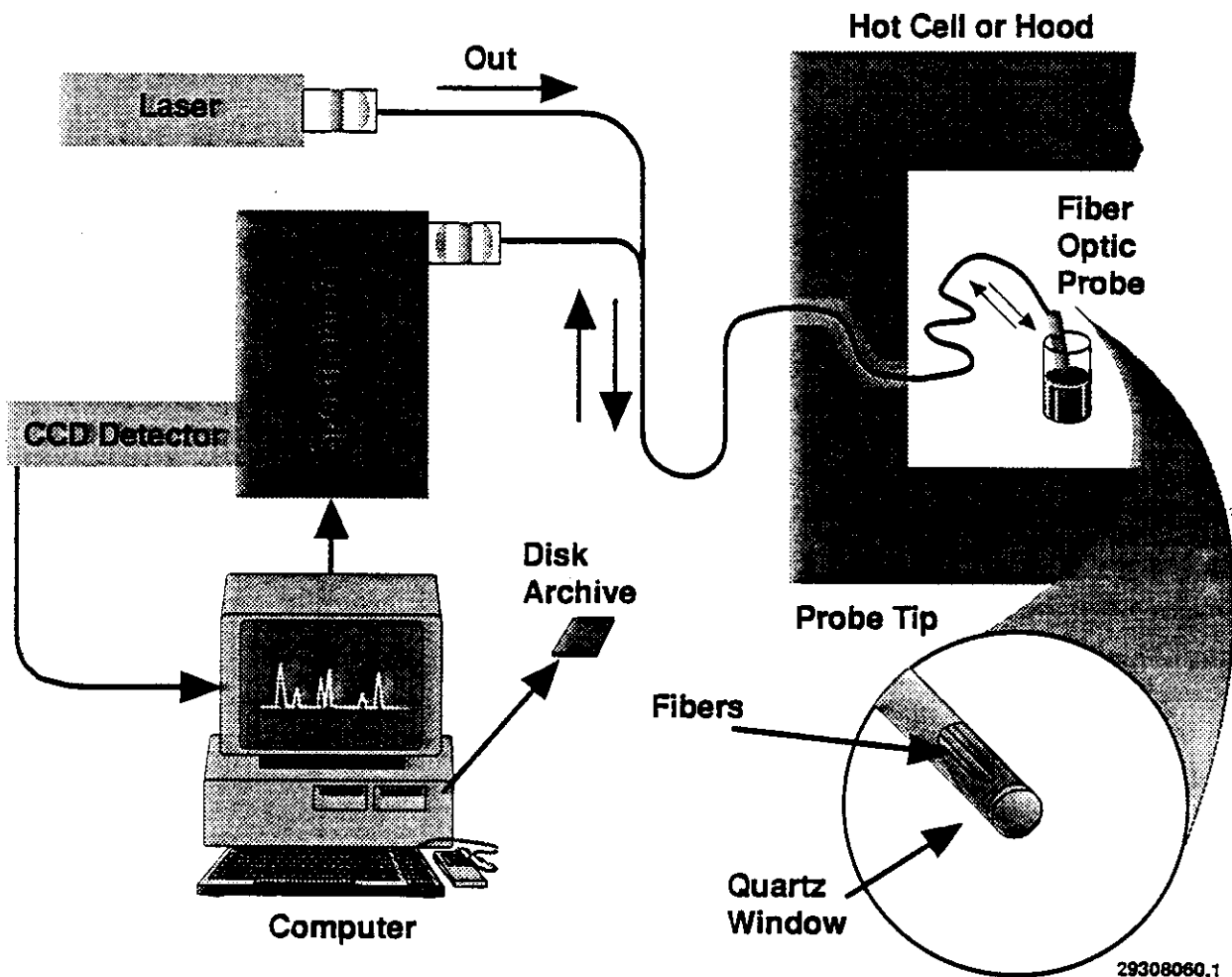
Two excitation sources were investigated: the diode laser (~842 nm) and the argon ion laser (514.5 nm) sources. The diode laser, originally intended for use on the project because of lower cost, was replaced by an argon ion laser source to improve signal quality. For application to other unknown analytes near infrared, fourier transform (FT) Raman spectroscopy may be more aptly suited. This is especially true when little or no process knowledge exists to indicate analyte content in widely diverse waste matrices other than waste tanks. In these situations, larger spectral windows are desired for library identification.

A diagram of the Raman system is provided in Figure 3-1. The system consists of (1) a dispersive, single-stage spectrometer with interchangeable gratings, (2) an argon ion laser or a diode laser source, (3) a silica fiber delivery system with an immersible probe tip, (4) a liquid nitrogen-cooled CCD detector, and (5) an IBM compatible personal computer.

The SPEX 0.5-m focal length, single-stage monochromator was fitted with a 1,200-line/mm holographic grating. The Princeton Instruments CCD chip contained 1,024 x 1,024 detector elements (pixels). Approximately 150 to 400 pixels were binned vertically to produce a single readout point. The detector was controlled by a Princeton Instruments CCD controller with an integrated temperature stabilizer. The spectrometer was fitted with a fiber optic couple by means of a standard mounting assembly connection, collimating lens, a holographic notch filter, and a focusing lens.

Initially, Raman excitation was provided by a diode laser, manufactured by Laser Diode, generating 25 to 38 mW at the end of a fiber optic cable with a tapered probe. Standard operating conditions for the diode laser were 120 mA input current with a 16.96 k $\Omega$  temperature resistance setting. Eventually, an Omnicrome air-cooled argon ion laser generating 140 mW of 514.5 nm radiation at the end of a 0.5 m fiber optic was used. The argon ion laser was operated at 4.95 V output as measured at the internal photodiode of the laser.

Figure 3-1. Remote Raman Spectroscopy System.



9413205.347

All fiber optic probes were designed and constructed at Savannah River Laboratories. These bifurcated, multi-mode fiber optic probes were made up of two 400- or 600- $\mu\text{m}$  (core diameter) pure silica fibers with a numerical aperture of 0.22. The distal ends of the fibers were ground to an angle (chiseled end) and fitted with quartz windows at the position of greatest overlap between spot size and observation area (coincidence plane).

Two specific software packages were used during the operation of the instrument: the vendor-supplied Princeton Instruments software (CSMA 2.0), and FSU's custom software. The FSU software was used to allow for collaboration and comparison of data with FSU. The software and system (i.e., shutter control and data collection) were operated from an IBM compatible computer (Figure 3-1).

9413205.348

#### 4.0 TEST MATERIALS

Efforts in this study focus on the need to carry out direct ferrocyanide salt speciation and quantitation to assist in the resolution of the ferrocyanide tank safety unreviewed safety questions (USQ). A portion of this testing and application is directed to quantitation and development of detection limits in the hot cell and laboratory hoods to effectively support ferrocyanide sample screening. This work is further verified by comparison with laboratory data generated during conventional characterization of the waste tanks using inductively coupled plasma (ICP) spectroscopy, ion chromatography (IC), and fourier transform infrared (FTIR) spectrometry.

A combination of simulants and archived tank materials have been characterized in this work to closely mimic those samples that are most likely to be taken from the ferrocyanide Watch List tanks. Simulants of one tank and two processes have been analyzed. Specifically, tank 241-BY-104 waste material, 241-BY-104 simulant, and in-farm and in-plant simulants have been used for characterization benchmarking. These matrices were selected based on the availability and likelihood for observation of ferrocyanide species in the samples.

Process simulants from in-farm and in-plant processes have been used to characterize mononickel ferrocyanide salts in matrices resembling tank conditions when treatment has been initiated (Bechtold and Jurgensmeier 1992). These process samples mimic the scavenging process flow sheets found in drawing HW-33536, *Nickel Ferrocyanide Scavenging Flow Sheet for Neutralized Concentrated RAW* (Smith and Coppinger 1954), and drawing HW-30399, *TBP Plant Nickel Ferrocyanide Scavenging Flow Sheet* (Sloat 1954). The three types of waste materials produced were described as follows (Bechtold and Jurgensmeier 1992):

1. "In-farm" (sample number CJ-93-B, Table 4-1) simulant represents the resultant material expected after in-tank treatment.
2. "Early in-plant" (sample number CJ-95-B, Table 4-1) waste represents waste resulting from the original uranium recovery plant effluent.
3. "In-plant" (sample number CJ-102-B, Table 4-1) waste represents effluent typical of the acidic uranium recovery plant as modified to include Sr-90 scavenging.

The composition of these samples as analyzed and constructed are provided in Table 4-1.

Table 4-2 provides the makeup concentrations of tank 241-BY-104 simulant material. Sample matrix spikes have been performed on tank 241-BY-104 simulant and are discussed in Sections 7.0 and 8.0. The laboratory characterized an auger sample of 241-BY-104 tank material in support of the ferrocyanide safety program (Beck 1992). The constituents and concentrations of Raman active analytes and major elements of interest are provided in Table 4-3 for the laboratory analyzed sample of tank 241-BY-104. Comparing the simulant to the analyzed results on the 241-BY-104 auger sample, a few

Table 4-1. Ferrocyanide Process Simulants

Analyte	Total moles	Molecular weight	Weight percent makeup	Weight percent analyzed
Sample Number CJ-93-B In-farm				
$\text{SO}_4^{2-}$	0.355	96.0576	2.44	2.26
$\text{PO}_4^{3-}$	0.250	94.9714	1.70	1.55
$\text{NO}_3^-$	6.25	62.0049	27.7	30.7
$\text{Fe}(\text{CN})_6^{4-}$	0.00480	211.9532	0.0727	0.537*
$\text{CN}^-$	0.0288	26.0177	0.0535	0.750*
Sample Number CJ-95-B Early In-plant				
$\text{SO}_4^{2-}$	0.239	96.0576	1.37	0.368
$\text{PO}_4^{3-}$	0.150	94.9714	1.02	0.297
$\text{NO}_3^-$	3.72	62.0049	16.5	17.9
$\text{Fe}(\text{CN})_6^{4-}$	0.0025	211.9532	0.0378	1.01*
$\text{CN}^-$	0.015	26.0177	0.0279	0.382*
Sample Number CJ-102-B In-plant				
$\text{SO}_4^{2-}$	0.239	96.0576	1.37	.0578
$\text{PO}_4^{3-}$	0.15	94.9714	1.02	.0407
$\text{NO}_3^-$	3.72	62.0049	16.5	.664
$\text{Fe}(\text{CN})_6^{4-}$	0.0025	211.9532	0.0378	8.55*
$\text{CN}^-$	0.015	26.0177	0.0279	0.389*

\*Water insoluble components analyzed in settled sludge by IC and FTIR analysis spectroscopy methods.

Table 4-2. Tank 241-BY-104 Simulant Makeup.

Analyte	Moles in Composite	Molecular Weight	Grams present	Weight percent
$\text{NO}_3^-$	1073.3	62.005	66549.97	4.960533
$\text{Al}(\text{OH})_4^-$	100.1	95.011	9510.601	0.708906
$\text{SiO}_3^{2-}$	13	76.084	989.092	0.073725
$\text{PO}_4^{3-}$	4.3	94.971	408.3753	0.03044

Table 4-3. Tank 241-BY-104 Sample Analysis.

Analysis	Expected species	Weight percent
TOC	Unknown	0.91
TIC	$\text{CO}_3^{2-}$	1.90
Total cyanide (modified)	$\text{Fe}(\text{CN})_6^{4-}$ $\text{CN}^-$	0.007
Al-ICP	$\text{Al}(\text{OH})_3$	8.00
Fe-ICP	$\text{Fe}(\text{CN})_6^{4-}$ $\text{FeO}(\text{OH})$	0.70
P-ICP	$\text{PO}_4^{3-}$	0.30
Cr-ICP	$\text{CrO}_4^{2-}$	1.40
$\text{NO}_2^-$ -IC	$\text{NaNO}_2$	1.19
$\text{NO}_3^-$ -IC	$\text{NaNO}_3$	4.90
$\text{PO}_4^{3-}$ -IC	$\text{BiPO}_4$ $\text{Na}_3\text{PO}_4$	0.58
$\text{SO}_4^{2-}$ -IC	$\text{Na}_2\text{SO}_4$ $\text{SrSO}_4$	2.65

discrepancies arise. The tank 241-BY-104 simulant selected was made without the addition of sulfate or nitrite, and the aluminum and phosphate content analyzed in the auger sample is much higher than that in the simulant. However, the composition of the component most prevalent in the simulant, nitrate, and the real tank material are nearly identical; spectral comparisons are provided in Section 6.3.

An effective, rapid screening tool is necessary to reduce the subjectivity of visual observations made on core segments. Extruded segments of real tank waste, about 48 cm (19 in.) in length, are supplied to the 222-S Laboratories by core drilling operations at the Tank Farms. The consistency of the waste varies from slurries or extremely wet solids to consistencies similar to peanut butter and hardened road tar. Dry crystalline solids are also received from rotary coring operations. Current observations and analytical results from sample duplicates indicate that tank wastes are known to be indistinguishably inhomogeneous on visual inspection (Herting et al. 1992). Segments may be divided into facies that are visually unique, and analyzed separately (Winters et al. 1990). When determination of layering or analysis of major tank components is important, segments are divided into sections (e.g., ferrocyanide core segments that are divided into quarter sections for analysis). In other single-shell tanks, and tanks in which all materials are expected to be similar, tank materials may be composited and analyzed as a complete core. Samples received for analysis of minor components require processing of larger sample sizes and often

necessitate core compositing. Therefore, some guidance provided in core preparation and sample homogeneity may lend increased confidence and credibility to results produced in the laboratory.

The majority of the wastes from the tanks consist of various types of metal hydroxides and phosphate and nitrate salts. These constituents have resulted from bismuth phosphate processing, uranium recovery, and plutonium and uranium extraction processes. In addition, several secondary waste streams have produced other types of waste in these tanks, such as lanthanum fluoride wastes, B Plant wastes, ferrocyanide scavenging wastes, and solidified wastes (Sasaki 1993).

There are no other simulants that have been constructed to best imitate the makeup of the real tank wastes observed in hoods and hot cells during this study. Results of analysis of these real samples are described in Table 4-4. These core results are listed as the average of all composite analyses for core 31 and 33 of tank 241-T-111 and core 51 and 52 from tank 241-T-107. Total organic carbon (TOC) analyses are performed on water digestates and do not reflect the concentration of the insoluble organic constituents that may be found in these tank materials. However, these concentrations provide a sense of the amount of chelating components and other polar organic species that are present in these waste materials.

Comparison of real-tank wastes (Table 4-4) with the in-farm and in-plant simulants (Table 4-1) provides a measure of the expected results of aging of wastes in ferrocyanide tanks. Most tank samples are generally lower in CN<sup>-</sup> content than the simulants. The degradation of ferrocyanide complexes is expected, to some extent, based on hydrolysis of cyanide in this caustic media (Robuck and Luthy 1989, Meeussen et al. 1992). At pH 12, micromolar concentrations of potassium ferrocyanide have been observed to decompose to free cyanide, in hours, when exposed to diffuse daylight (Meeussen et al. 1992). Furthermore, hydrolytic reactions have been observed in media of lower pH with photochemical initiation (Villanueva et al. 1992). Hydrolysis alone may cause spurious results in cyanide quantitation. However, the identification of some of the expected breakdown products like formamides and formates may be of benefit.

Other analyte concentrations vary from tank to tank and among simulant materials. Nitrate, phosphate, and sulfate concentrations vary from as high as 30 wt% to as little as 0.04 wt% in simulants, while the general concentration of oxyanions in real tank wastes appears to range between 0.1 to as much as 15 wt%. Typically, in both matrices nitrate is the major constituent. Phosphate appears as the second most abundant anionic species found in these real tank materials. Phosphate may be present in real waste material concentrations exceeding 10 wt%; however, the simulants of interest do not contain this concentration of phosphate. Sulfate is present in both simulants and real wastes in 0.5 to 2.5 wt% concentrations. In general, these simulants provide a wider range of anion concentrations and may underrepresent the concentration of phosphate present in tank samples. However, these matrix components are fairly representative of a blend of species expected to be analyzed, and are much more thoroughly understood than the real tank wastes being characterized.



Table 4-4. Real Waste Weight Percent Total Analytes.

Analyte	241-T-111 core 31	241-T-111 core 33	241-BX-107 composite	241-T-107 core 51	241-T-107 core 52
Al	0.00	---	1.20	0.41	2.46
Fe	2.00	1.60	0.94	3.32	2.98
NO <sub>3</sub> <sup>-</sup>	4.40	3.85	15.0	9.28	5.97
NO <sub>2</sub> <sup>-</sup>	---	---	0.92	1.53	0.86
PO <sub>4</sub> <sup>3-</sup>	1.68	1.44	1.50	9.45	13.3
SO <sub>4</sub> <sup>2-</sup>	0.37	0.34	1.42	1.26	0.75
CO <sub>3</sub> <sup>2-</sup>	0.04	0.10	0.12	0.57	0.28
Total organic carbon	0.37	0.25	0.06	0.14	0.19
CN <sup>-</sup>	0.00	0.00	0.00	0.01	0.006
H <sub>2</sub> O	75.3	76.8	56.4	51.9	47.8
Total (wt %)	84.2	84.4	77.6	77.9	74.6

This page intentionally left blank.

943205 35

## 5.0 DIODE LASER SYSTEM RESULTS

Results from the diode laser system have shown the system to be adequate for acquisition of data from pure reagents; however, it is not suitable for application on all tank waste samples. The diode laser system provided an independent means for comparison of spectral assignments made by FSU. In addition, spectra of oxyanions were obtained from tank 241-BX-107 samples.

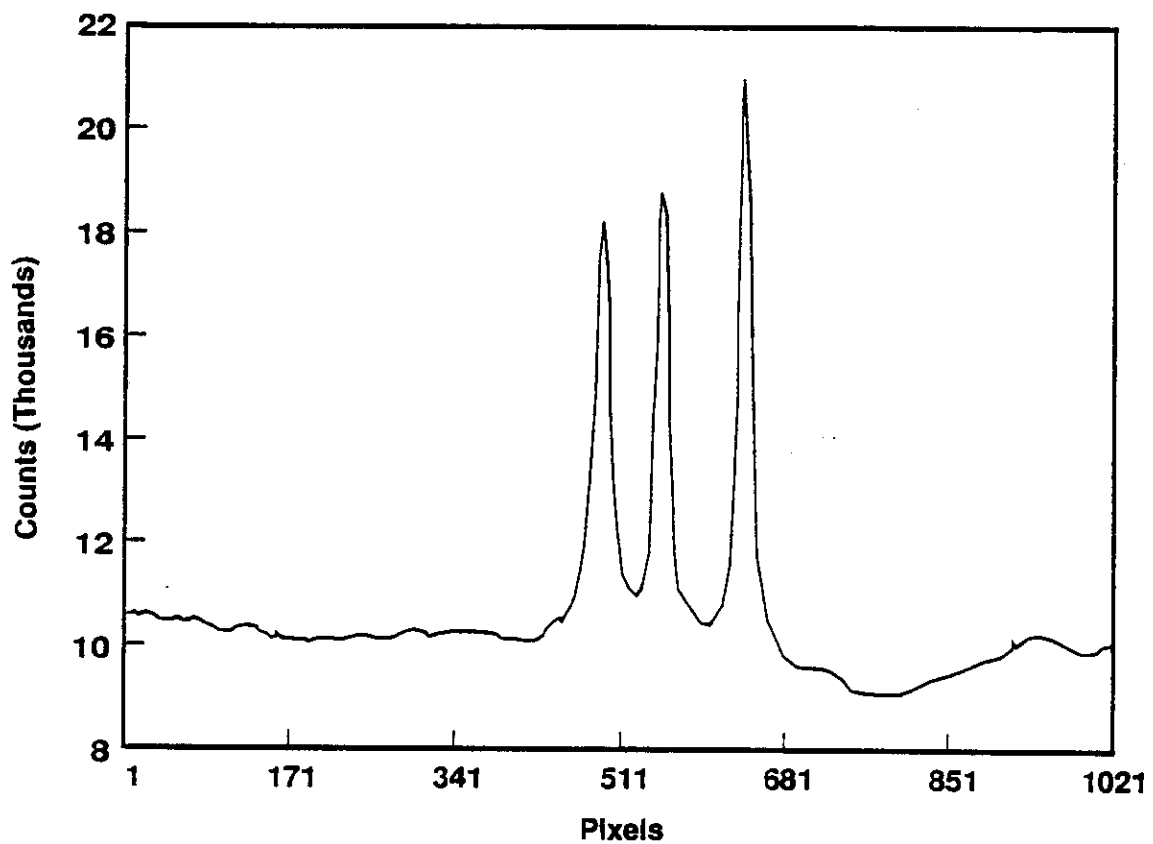
### 5.1 SPECTRA AND COMPARISON OF ASSIGNMENTS OF PURE REAGENTS

Spectra of pure ferrocyanide salts and oxyanions were obtained with the diode system in the cold laboratory and in hot cells. An example spectrum of sodium ferrocyanide obtained in the hot cell is provided in Figure 5-1. Reasonably clear signals are obtainable using the diode laser-based system on these pure reagents. Additional spectra are provided in Appendix A, as a compendium of materials which provide both clear spectra obtained with the diode laser and are similar to samples run at FSU with the argon ion laser. The spectra contained in Appendix A are of the dry salts of the pure reagents. Spectra of the following solid compounds were obtained with the diode laser:  $\text{NaNO}_3$ ,  $\text{NaNO}_2$ ,  $\text{Sr}(\text{NO}_3)_2$ ,  $\text{Na}_2\text{SO}_4$ ,  $\text{K}_4\text{Fe}(\text{CN})_6$ ,  $\text{Na}_4\text{Fe}(\text{CN})_5\text{NO}$ ,  $\text{Na}_4\text{Fe}(\text{CN})_6$ ,  $\text{K}_3\text{Fe}(\text{CN})_6$ , and  $\text{Na}_2\text{CO}_3$ . All peak assignments made were compared to previous assignments made on similar reagents at FSU with the exception of  $\text{Sr}(\text{NO}_3)_2$  and  $\text{Na}_2\text{CO}_3$ . This comparison is provided in Table 5-1. Values listed in Table 5-1 show reasonable deviations between wavenumber assignments, as two different spectrometer systems, and different vendor supplied reagents were used for data collection. Furthermore, assignment of Raman peaks from solid samples is not concretely established, and discrepancies are expected.

Spectra of the mononickel ferrocyanide species were not detectable because of the Raman-shifted position of the cyanide mode with respect to the excitation frequency of the diode laser. With a laser excitation source frequency of 826 nm, the linear dispersion of the instrument was 0.378 Å/pixel as indicated by a polynomial fit performed on neon line standards (Crawford 1993b). The Raman shift for mononickel ferrocyanide, using the diode laser, falls in the range of 1,010 nm. The recognized cut-off for silicon detectors is 1,100 nm at room temperature as illustrated in Figure 5-2. The quantum efficiency of the detector at 1,010 nm is approximately 18 percent, compared with 70 percent with 514.5 nm excitation, making the diode laser source a poor match for the detector.

Spectra of samples from tank 241-BX-107 were obtained with the diode laser system. Figure 5-3 shows the presence of a common peak in five core samples from tank 241-BX-107. Specifically, Segment 5 from core 40 and Segments 2, 3, 6 and 7 from core 41 reveal a prominent peak at approximately  $1,050\text{ cm}^{-1}$ . This peak does not match the solid  $\text{NaNO}_3$  band as illustrated, but does appear where a major mode of vibration in aqueous  $\text{NO}_3^-$  is expected (Herzberg 1945, Marston 1975, and Miller 1977). Other bands that are evident appear at the 950 to 970  $\text{cm}^{-1}$  range and may indicate the presence of sulfate (the second most abundant constituent) in the tank.

Figure 5-1. Sodium Ferrocyanide Obtained in the Hot Cell.



29308060.2

Figure 5-2. Quantum Efficiency of CCD Detector for Mononickel Ferrocyanide Speciation.

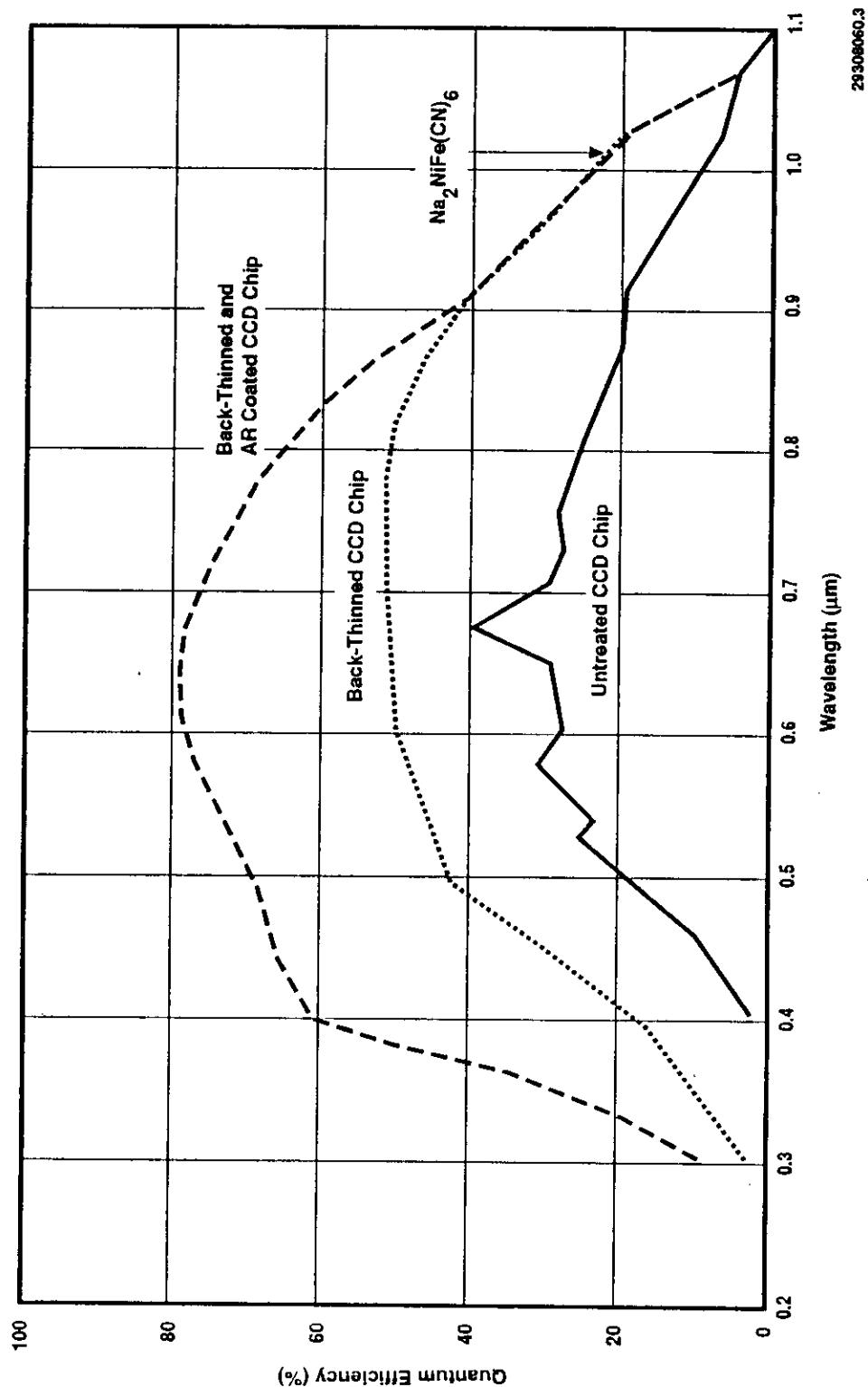
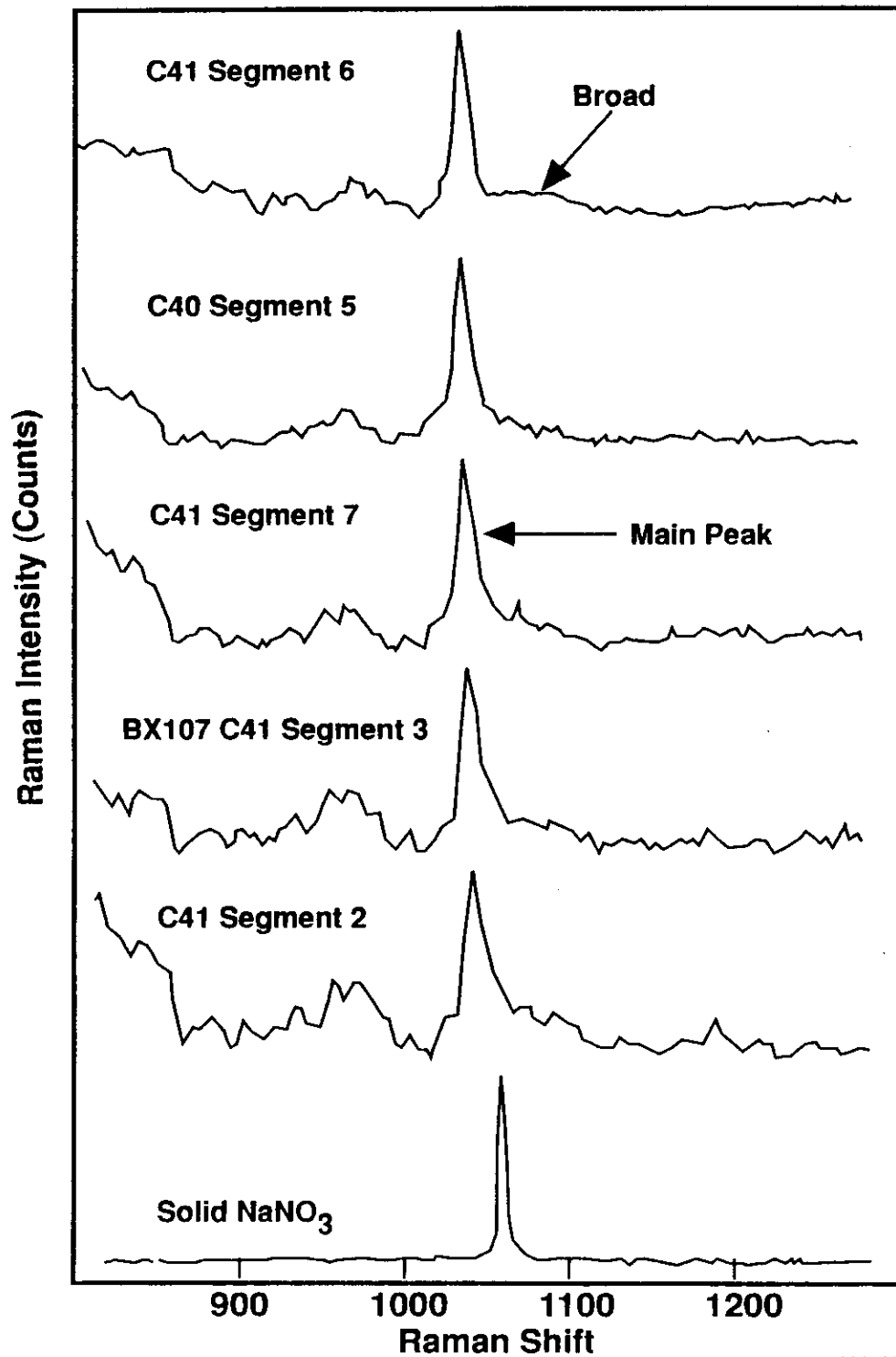


Figure 5-3. Spectra of Tank 241-BX-107 Samples.



29308060.4

9413205.353

Table 5-1. Peak Assignment Comparisons.

Analyte	Chemical formula	FSU assignment (cm <sup>-1</sup> )	WHC assignment (cm <sup>-1</sup> )	Difference (FSU - WHC)
Sodium Ferrocyanide	Na <sub>4</sub> Fe(CN) <sub>6</sub>	2,050 2,072 2,103	2,049 2,069 2,104	1 3 -1
Potassium Ferrocyanide	K <sub>4</sub> Fe(CN) <sub>6</sub>	2,064 2,093	2,055 2,093	9 0
Potassium Ferricyanide	K <sub>3</sub> Fe(CN) <sub>6</sub>	2,128	2,128	0
Sodium Nickel Ferrocyanide	Na <sub>2</sub> NiFe(CN) <sub>6</sub>	2,107 2,143	2,112* 2,148*	-5 -5
Cesium Nickel Ferrocyanide	Cs <sub>2</sub> NiFe(CN) <sub>6</sub>	2,104 2,143	---- ----	---- ----
Sodium Sulfate	Na <sub>2</sub> SO <sub>4</sub>	1,154 1,133 1,102 994	---- 1,131 1,101 997	---- 2 1 -3
Sodium Nitrate	NaNO <sub>3</sub>	724 1,068 1,386	1,068	0
Sodium Nitrite	NaNO <sub>2</sub>	1,329	1,325	4
TriSodium Phosphate	Na <sub>3</sub> PO <sub>4</sub>	430 550 940	---- ---- ----	---- ---- ----
Sodium Carbonate	Na <sub>2</sub> CO <sub>3</sub>	----	1,077	----

\*Determinations provided from argon ion laser-generated spectra.

Spectra of wastes from tank 241-T-111 have been obtained from laboratory hood work, and spectra from tanks 241-T-107 and 241-BY-104 have been obtained from the hot cell studies using the diode laser-based Raman system. These spectra, which were forwarded to FSU for data treatment, do not indicate the presence of oxyanions or ferrocyanide complexes. The laser power at the time the diode laser was operating was 26 mW at the end of the fiber optic. This power appears to be too low for adequate observation of backscatter on solid samples at low concentration (i.e., 5 wt% or less) such as the concentrations expected in tank 241-T-107 and tank 241-BY-104 samples. Therefore, arrangements were made for installation of an Ar<sup>+</sup> ion laser late in the project. Results from this laser-based system are provided in Section 6.0.

This page intentionally left blank.

943205-340



## 6.0 ARGON ION LASER RESULTS

The argon ion laser system produced an improvement of signal-to-noise and overall detection capability compared to the laser diode system. The anticipated fourth-order increase in frequency was very apparent as illustrated in Figure 6-1. The signal-to-noise ratio of the diode laser is 30.2 as measured for the  $1,029\text{ cm}^{-1}$  peak of cyclohexane. The argon ion laser exhibits a signal-to-noise ratio of 180 for the same peak (Crawford 1993d). Clearly, the spectra obtained with the two laser systems is different. This difference further demonstrates the advantage of the use of the argon ion laser as an excitation source. Linear dispersion at 514.5 nm vs. 830 nm provides a larger spectral window for peak observation.

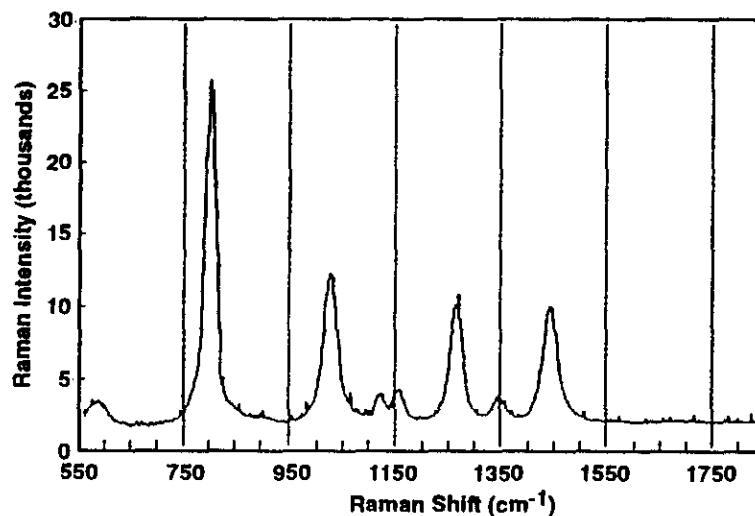
The advantage of shifting Raman excitation within a region of higher quantum efficiency for the detector is also depicted by the spectrum of sodium mononickel ferrocyanide provided in Figure 6-2. This spectrum was obtained with a 10-minute exposure time on reagent grade  $\text{Na}_2\text{NiFe}(\text{CN})_6$ . Reasonably clear spectra of mononickel ferrocyanide salts have been obtained from tank matrices, as well as described in Sections 7.0 and 8.0.

The argon ion laser was used to obtain spectra of waste from tank 241-T-111 and tank 241-BX-107. Spectra of the tank 241-T-111 sample were indistinguishable, consisting of noise on a broad background with no clear Raman peaks in the region from 800 to  $3,000\text{ cm}^{-1}$ . Signal processing performed at FSU on data obtained from tank 241-T-111 revealed that silica backgrounds did not adequately subtract from the signal spectrum obtained in the  $1,600$  to  $2,800\text{ cm}^{-1}$  range using interactive subtraction methods. This corroborated results obtained at WHC. However, the processed spectrum appeared to be very similar to that obtained for tank 241-T-107 samples, as shown in Figure 6-3. Spectra of wastes from tank 241-BX-107 were obtained in the nitrate and ferrocyanide spectral window region. Two broad peaks were evident in the nitrate spectral window which obscured the Raman signals. It has been speculated that these peaks may be caused by alumina or bismuth phosphate which are both prominent materials in this tank waste material (see Figure 6-4).

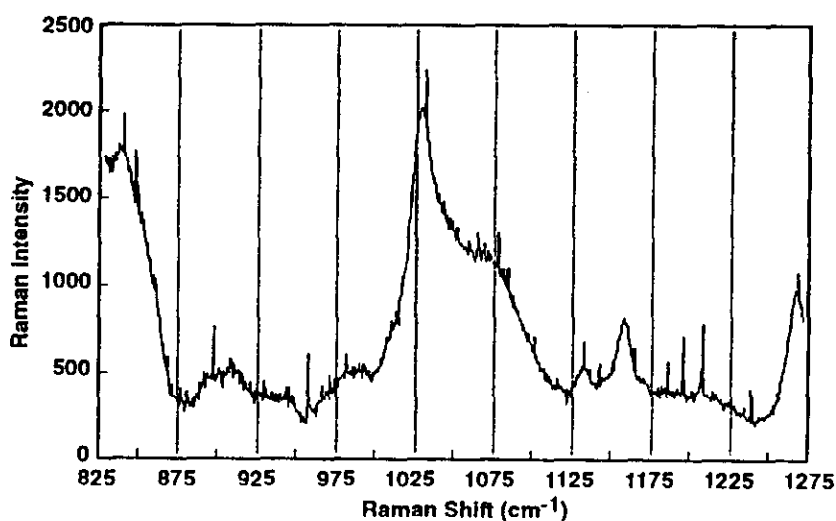
All spectra obtained from real tank samples showed some evidence of fluorescence or anomalous background. This is not surprising, as excitation at 514.5 nm occurs within electronic bands of many molecular species present in the tank wastes, especially organic compounds (Gerrard 1991). Fluorescence can be an indicator of sample homogeneity. When faced with pure spectral problems involving sample fluorescence, an operator must resort to chemically altering the system, physically changing the excitation source, or treating the data to extract the Raman signals. For the remote applications encountered in this study, chemical alternatives, including sample burn-out, are impossible, impractical, and defeat of the primary objective of remote "hands-off" analysis. Sample burn-out is not an option because the photochemistry involved changes the sample--an undesirable effect for these determinations. The physical methods of reducing fluorescence (i.e., laser pulsing and detector gating) remain restrictive because of costs for appropriate equipment. Expensive and delicate instrumentation are required for physically altering the spectrometer system, and procurement and

Figure 6-1. Cyclohexane Diode vs. Argon Ion Laser Excitation.

### Cyclohexane Signal with Argon Ion Laser for Signal to Noise Calculation



### Cyclohexane Signal with Diode Laser for Signal to Noise Calculation



29308093.11

Figure 6-2. Spectrum of Sodium Nickel Ferrocyanide.

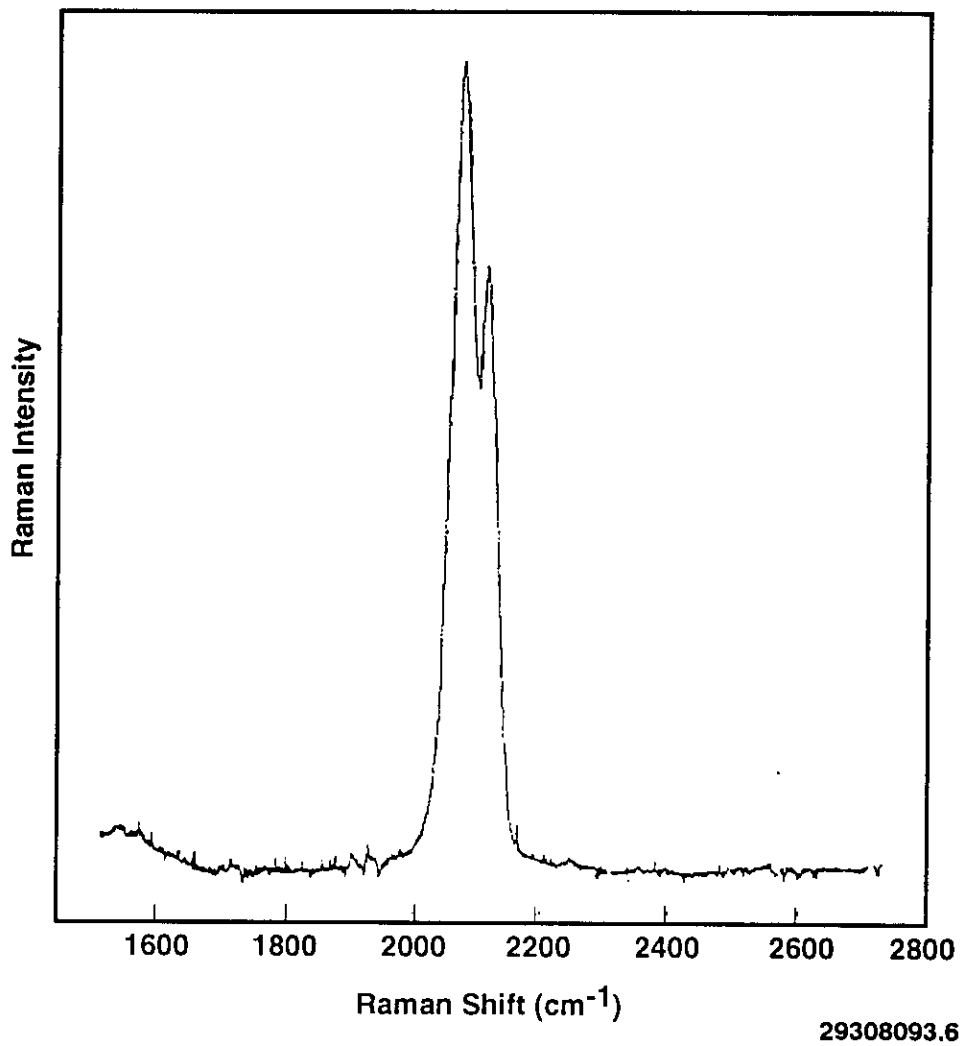


Figure 6-3. Spectrum of Tank 241-T-111.

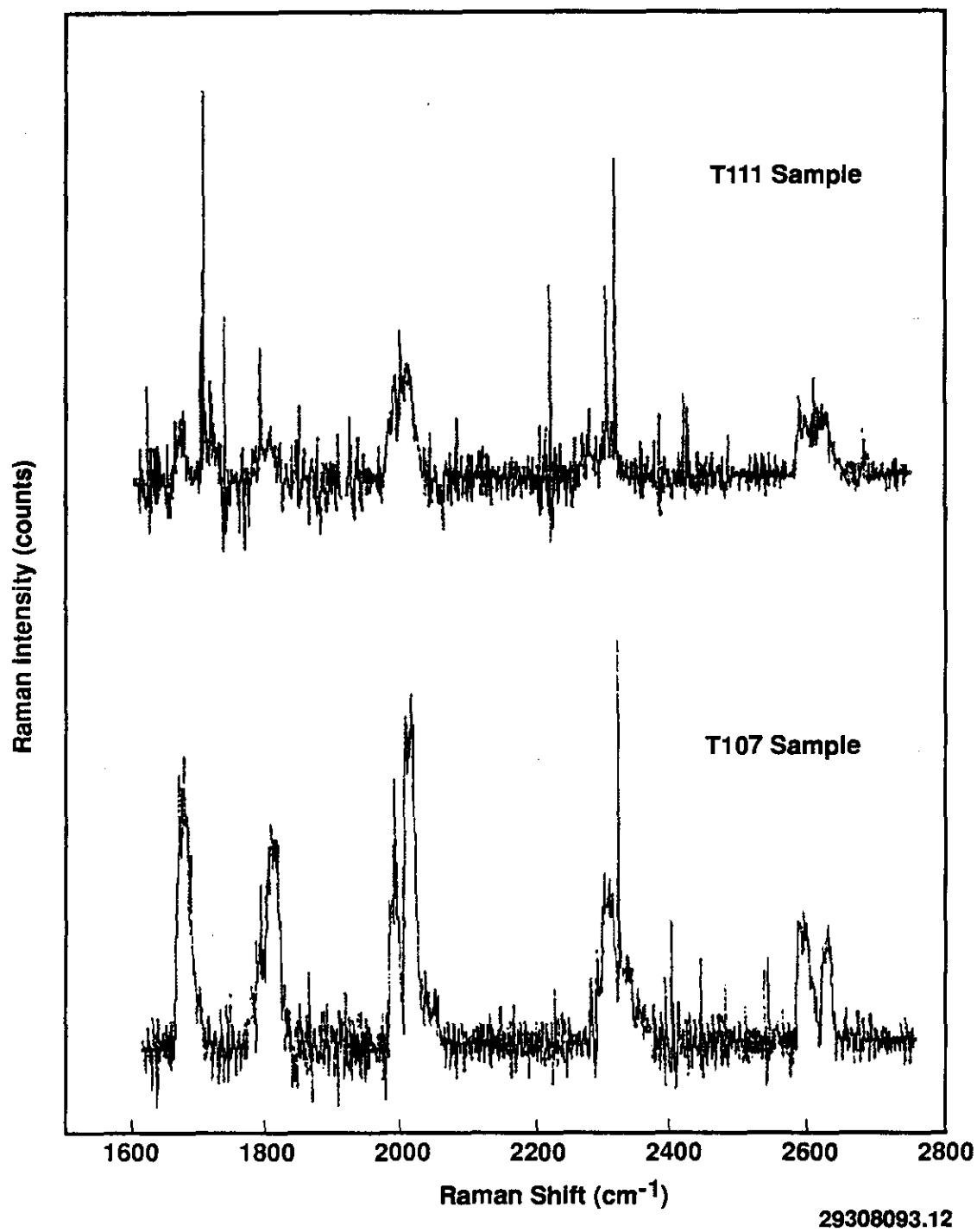
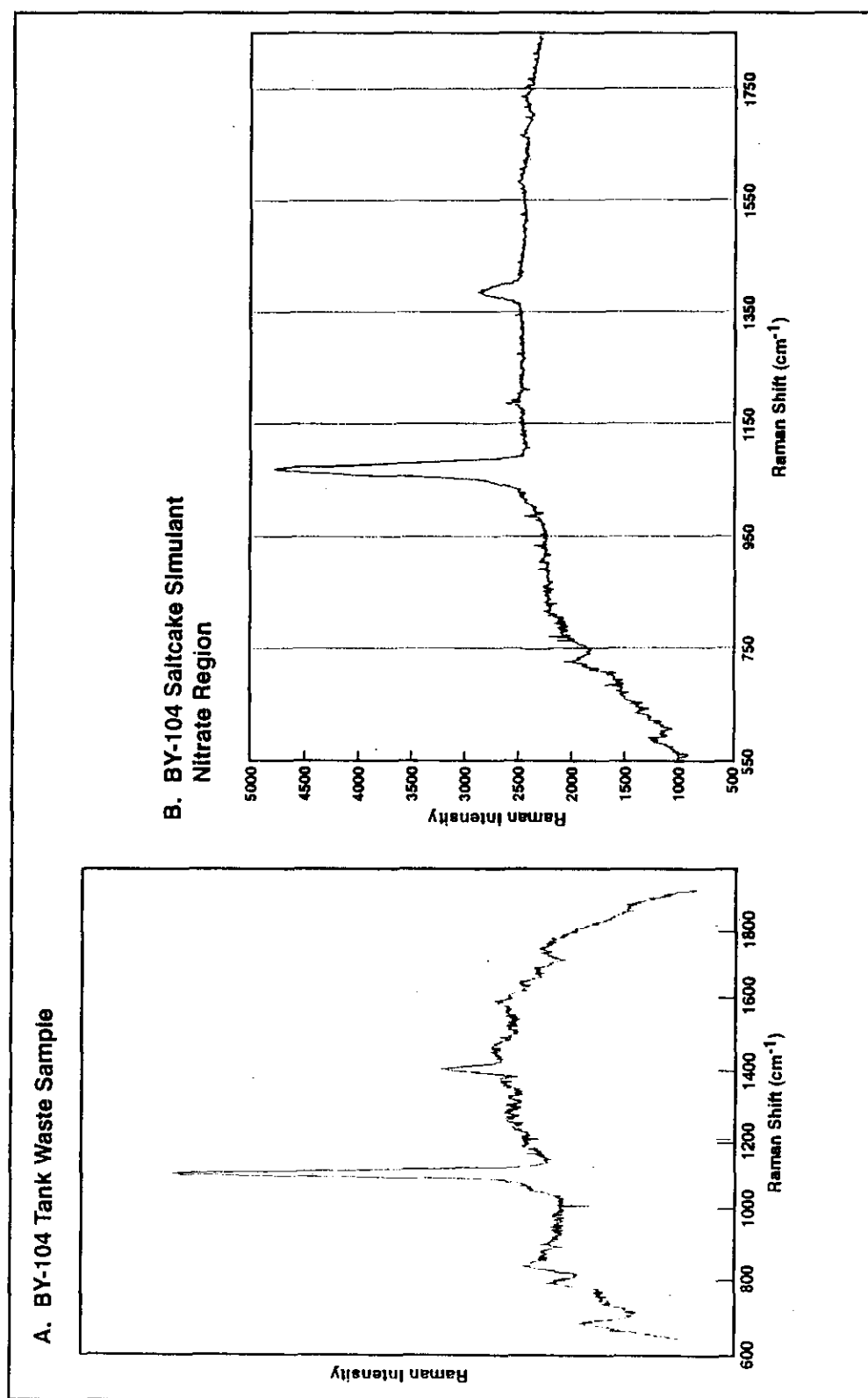


Figure 6-4. Comparison of Tank 241-BY-104 Simulant and Real Waste Spectra.



29309093.8

9413205.1365

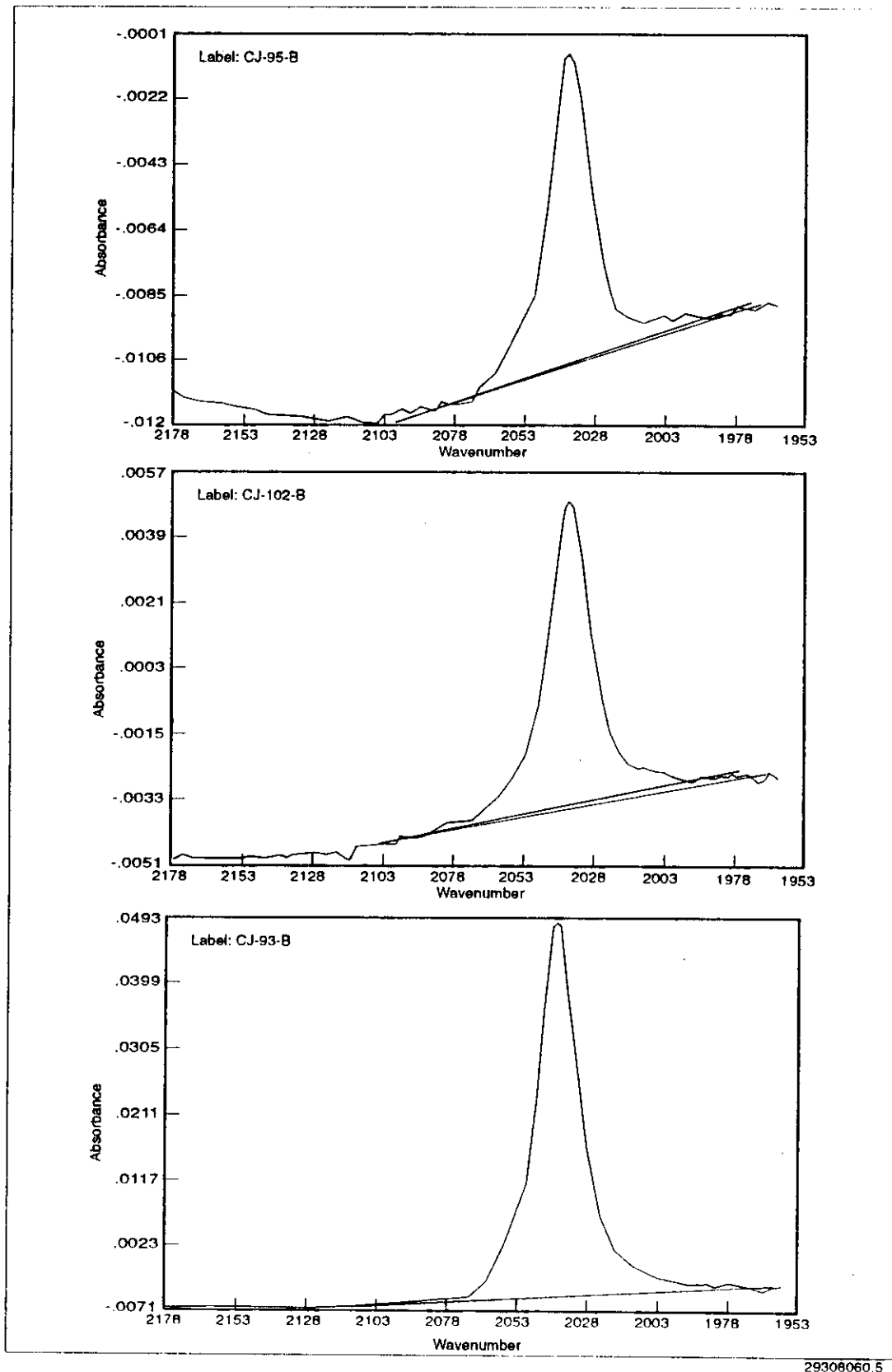
maintenance of such systems would be impractical for routine operating systems. Data removal of fluorescence, was the option used for these studies because there were no other alternatives available in the time limits of the study. Data manipulation does, however, have its own inherent weaknesses. This manipulation is subjective in nature, difficult to defend in an audit, and is often "frowned upon" during operations that demand stringent quality assurance protocols. For future work, a UV laser would produce attenuated signals caused by silica fiber absorbance (a fact that may also be functional in the clear appearance of silica bands in spectra generated with 514.5 nm excitation). Therefore, longer wavelength laser sources should be investigated (Greenwell et al. 1992).

Spectra of the oxyanions for tank 241-BY-104 simulant and real tank waste are shown in Figure 6-4. When comparing these spectra, there are strong similarities in the nitrate bands. In addition, there is a faint band in the simulant that is also in the real tank waste, and that may result from the presence of  $\text{Al}(\text{OH})_4^-$  in both samples. Ferrocyanide was not included in the original makeup of the simulant and there were no peaks observed in the real tank sample. The analyzed concentration of total cyanide in the auger sample taken from the tank was only 0.007 wt% of the sample. Samples of the simulant were spiked with ferrocyanide salts to determine a reasonable detection limit in this complex matrix. A discussion of matrix spiking is provided in Section 7.0.

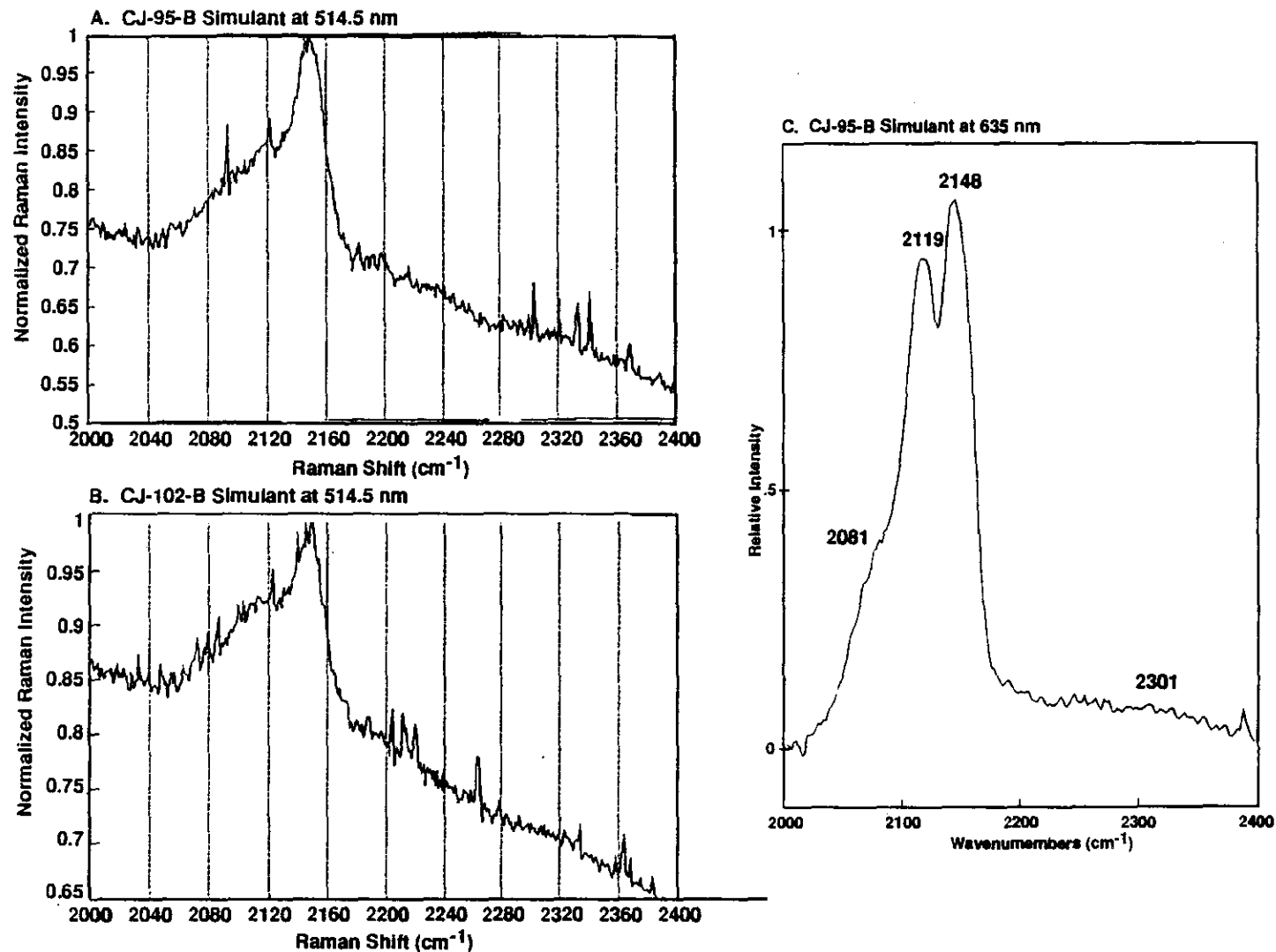
Centrifuged sludges from the ferrocyanide process samples were run via indirect methods by IC and FTIR spectroscopy. Quantitative results are reported in Table 4-1 by simulant name. Indirect methods performed at Pacific Northwest Laboratory (PNL) involve dissolution of the sample matrix before analysis in a solvent of 5 wt% ethylene diamine and 5 wt% ethylenediaminetetraacetic acid in water (Bryan et al. 1993). Resultant samples were analyzed for ferrocyanide ion, ferricyanide ion, and free cyanide and were representative of the anion found in the material analyzed because the oxidation state is preserved in this preparation.

Spectra of the ferrocyanide anion in solution taken with a FTIR in total attenuated reflectance mode are provided in Figure 6-5. These spectra show a single band at  $2,037\text{ cm}^{-1}$ , indicative of the ferrocyanide anion in solution. Spectra of the same simulants were analyzed by Raman spectroscopy at various wavelengths of excitation directly, as illustrated in Figure 6-6. Raman spectra were obtained from sample material mounted on a glass cover slip in a  $\sim 180^\circ$  backscattering geometry. Radiation was imaged into a 0.5-m focal length dispersive SPEX Industries triplemate spectrometer equipped with a liquid-nitrogen-cooled CCD detector. Approximately 35 mW of 634 nm radiation was generated from an argon-ion-pumped dye laser. This power was used to mimic power levels equivalent to the diode laser output. Results obtained on sample number CJ-95-B (early in-plant simulant) with 634 nm excitation are comparable to those obtained with 514.5 nm excitation, as shown, and are indicative of the ferrocyanide species as well in the form of the sodium mononickel salt.

Figure 6-5. FTIR Spectra of Ferrocyanide Process Simulants.



## In-Plant Ferrocyanide Process Simulants





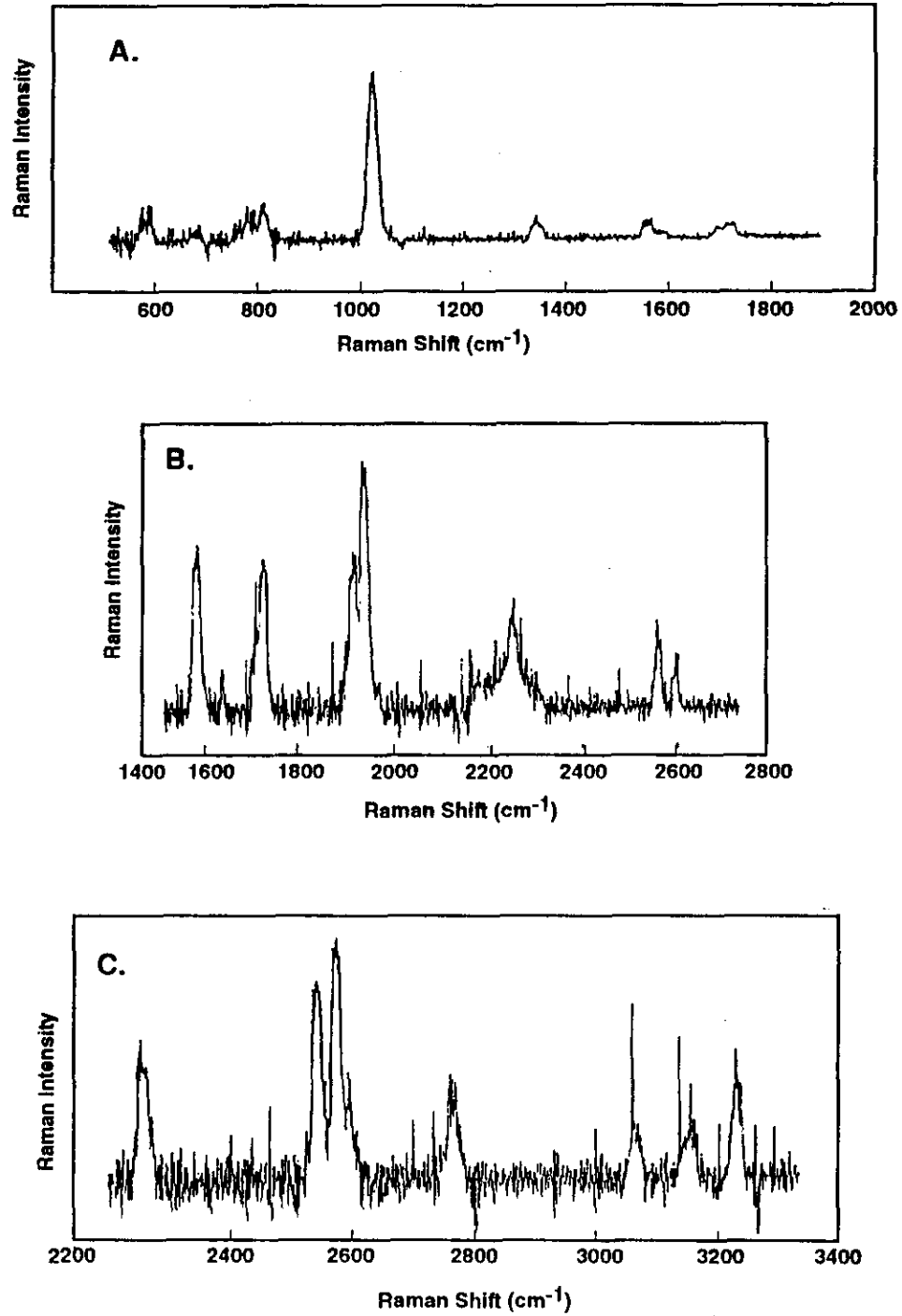
Finally, spectra of samples taken from ferrocyanide Watch List tanks 241-BY-104 and 241-T-107 were obtained from the hot cell with the argon ion laser (see Figure 6-4 for tank 241-BY-104 spectra and Figure 6-7 for 241-T-107). Material from tank 241-BY-104 did not show any Raman peaks in the ferrocyanide region. However, spectra were obtainable from the oxyanion region, which seemed to confirm the presence of nitrate and other components with peaks in the 100- to 900- $\text{cm}^{-1}$  range which may be attributed to chromate or aluminum species (Miller 1977). A 50-second exposure time was used with the CCD detector and 20 scans were averaged producing a clearly resolved spectrum. Detection of these species occurs at a frequency well within the 70 percent quantum efficiency of the CCD detector.

Spectra from the tank 241-T-107 sample were obtained over the spectral window from 600 to 3,200  $\text{cm}^{-1}$ . Figure 6-7 shows a spectrum taken over the 600- to 1,800- $\text{cm}^{-1}$  oxyanion region. Sodium nitrate appears to be a major constituent in this spectrum with the primary peak centered at 1,050  $\text{cm}^{-1}$ . Five other peaks not attributable to nitrate appear at 630, 850, 1,200, 1,590, and a doublet at 1,695 and 1,730  $\text{cm}^{-1}$ . The lower-frequency peaks may be caused by some form of phosphate in the sample, since phosphate is the major oxyanion present in this tank as analyzed (see Table 4-5). The peak at 650  $\text{cm}^{-1}$  may be caused by alumina, because the aluminum content found by ICP analysis is quite substantial (see Table 4-5). The peak at 850  $\text{cm}^{-1}$  may be caused by  $\text{CrO}_4^{2-}$  anion which has been used as an oxidizing agent in several processes and is prevalent in many waste tanks (Miller 1977). With more work a better understanding of these components is possible. Specifically additional matrix spikes and surveys of a collection of salts must be performed to delineate species identity.

The higher frequency peak at 1,590  $\text{cm}^{-1}$  in this tank 241-T-107 sample may be characteristic of an ionic form of an amine or a carbonyl stretch associated with the electron-attracting group on the nitrogen of an amine group (Lin-Vien et al. 1991). The bands at 1,730  $\text{cm}^{-1}$  are most likely caused by carbonyl moieties on imides or substituted amides. Spectra obtained from the 1,500 to 2,700  $\text{cm}^{-1}$  region and 2,300 to 3,300  $\text{cm}^{-1}$  region further indicate the presence of peaks that may be attributed to hydrolysis products of cyanides or ethylenediamine-type complexants in caustic mixtures. In particular, bands in the 1,900- to 2,000- $\text{cm}^{-1}$  region may be characteristic of types of conjugated long-chain hydrocarbons, bands in the 2,200- to 2,300- $\text{cm}^{-1}$  region may indicate the presence of cyanates and nitrilo compounds in the mixture, and bands from 2,500 to 3,250  $\text{cm}^{-1}$  may represent the presence of tertiary, secondary, and primary amines and ammonium ions in the tank matrix. It is impossible at this time to make definitive assignments of these constituents, and it may also be impractical to postulate true structures for these components that may be the fragmented components of many additives in the tank, none of which represent the original reagents. Further work is required to determine which constituents are present. However, continued study of these tanks and reagents expected in them may provide a basis for understanding the molecular dynamics at play in the mixtures found in many of these tanks.

691 502 16

Figure 6-7. Raman Spectra of Tank 241-T-107 Waste Sample.



29308093.5

## 7.0 MATRIX SPIKING

It was recognized that matrix effects could occur in Raman spectra of tank wastes as early as 1980, in studies performed on tank supernates (Miller and Macklin 1980). In these studies, line broadening and blue shifting were noted in lines of high symmetry oxyanions as sodium content was elevated. In addition, recent results from FSU have indicated major shifts that are not only caused by phase differences as dry salt is dissolved into its aqueous counterpart, but also by the cation associated with the salt (WHC 1992). When thoroughly understood, the noted spectral features may reveal much about the chemical and physical environment of analytes in the sample.

In early work with the oxyanions in solution, an internal standard of perchlorate was used (Miller and Macklin 1980). Perchlorate was observed to behave in a manner similar to the nitrate anion when increased sodium was added to the sample matrix, even though perchlorate does not form ion pairs as readily as nitrate in sodium matrices. Dry sodium chlorate was spiked into the tank 241-BX-107 matrix to check for similar response and provide a distinguishable internal standard for comparison with oxyanions. The spiked sample exhibited no broadening or shifting between the pure reagent and that observed in the tank matrix as illustrated in Figure 7-1. This standard was of limited use with this system because no other oxyanion peaks were detectable with the diode laser excitation; however, it may be used in further work as an internal reference standard with the argon ion laser.

Standard additions were further attempted using potassium ferrocyanide, sodium ferrocyanide, and sodium mononickel ferrocyanide to spike tank 241-BY-104 simulants and tank 241-BX-107 real tank waste materials (see Section 8.0). Spiking tank 241-BY-104 simulant with potassium and sodium ferrocyanide produced spectra in which peaks shifted to higher frequency (see Figure 7-2). In addition, the lower frequency peak in  $\text{Na}_4\text{Fe}(\text{CN})_6$  diminished as the peak at  $2,070\text{ cm}^{-1}$  increased in intensity. This was postulated to result from an aqueous form of the ferrocyanide anion. However, samples have been observed to undergo further decomposition over time as these spiked samples give off ammonia odor immediately after spiking. Figure 7-2 presents additional data that suggests that nickel may be removed from  $\text{Na}_2\text{NiFe}(\text{CN})_6$  when spiked into tank 241-BY-104 simulant, because the spiked spectrum resembles the  $\text{Na}_4\text{Fe}(\text{CN})_6$  spectrum much more closely than the  $\text{Na}_2\text{NiFe}(\text{CN})_6$  spectrum. Standard additions of both  $\text{Na}_4\text{Fe}(\text{CN})_6$  and  $\text{Na}_2\text{NiFe}(\text{CN})_6$  spiked into tank 241-BX-107 waste are provided in Figure 7-3. A large background was evident in the 241-BX-107 tank sample spectrum which produced poorer results than anticipated from the tank 241-BY-104 simulant data. The tank 241-BX-107 matrix provided additional challenges in data treatment and subsequent results should be compared with this in mind. After silica correction was used with these spectra, a similar result seemed to occur for  $\text{Na}_2\text{NiFe}(\text{CN})_6$  spiked into this matrix, as was observed in the tank 241-BY-104 matrix. This provided additional proof that the mononickel ferrocyanide salt is not stable in caustic matrices. In fact, this decomposition may be photoinitiated with 514.5 nm light, as is observed for the sodium and potassium ferrocyanide

Figure 7-1. Internal Standard  $\text{NaClO}_3$  with Diode Laser Excitation.

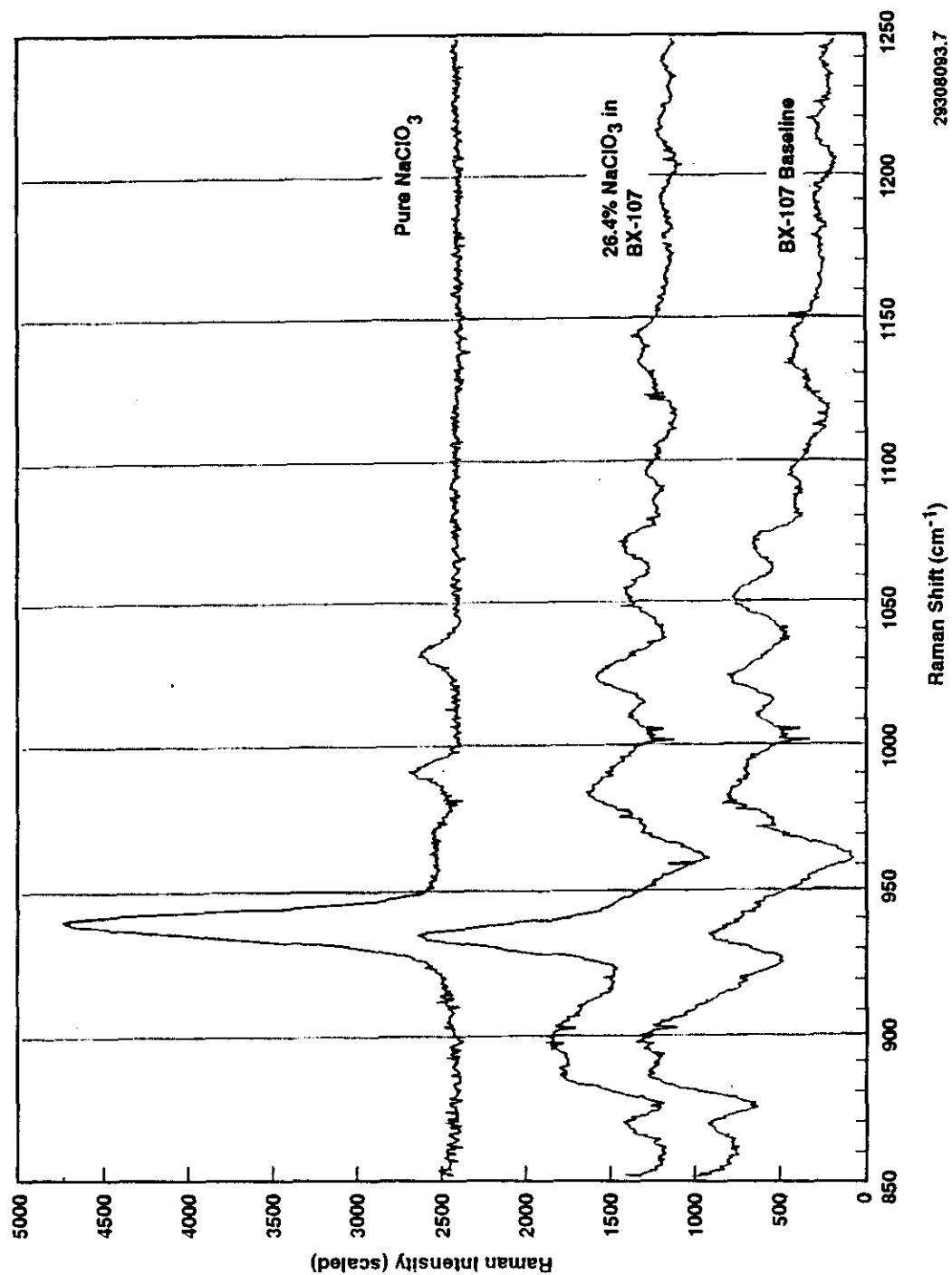


Figure 7-2. Spiking Tank 241-BY-104 Simulant  
with  $\text{Na}_2\text{NiFe}(\text{CN})_6$ .

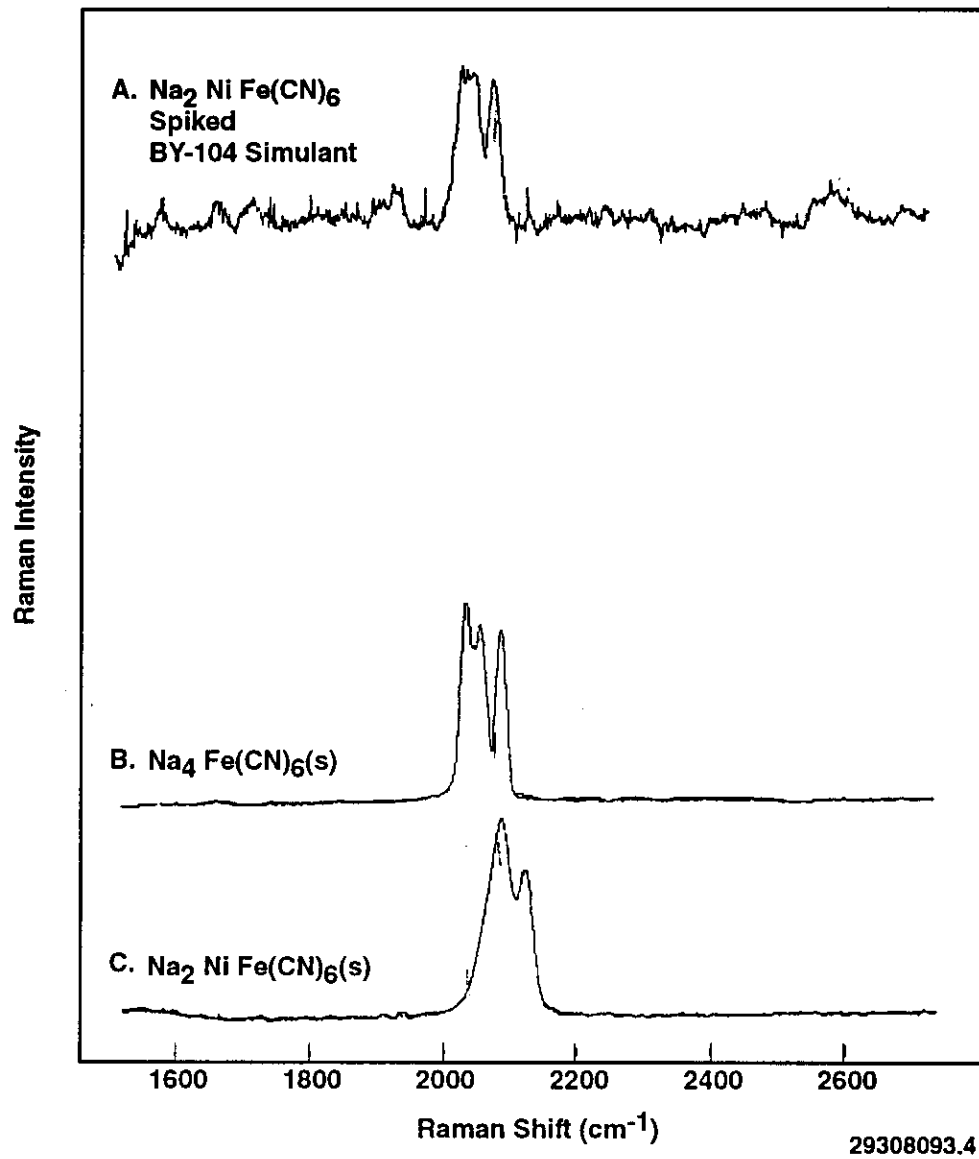
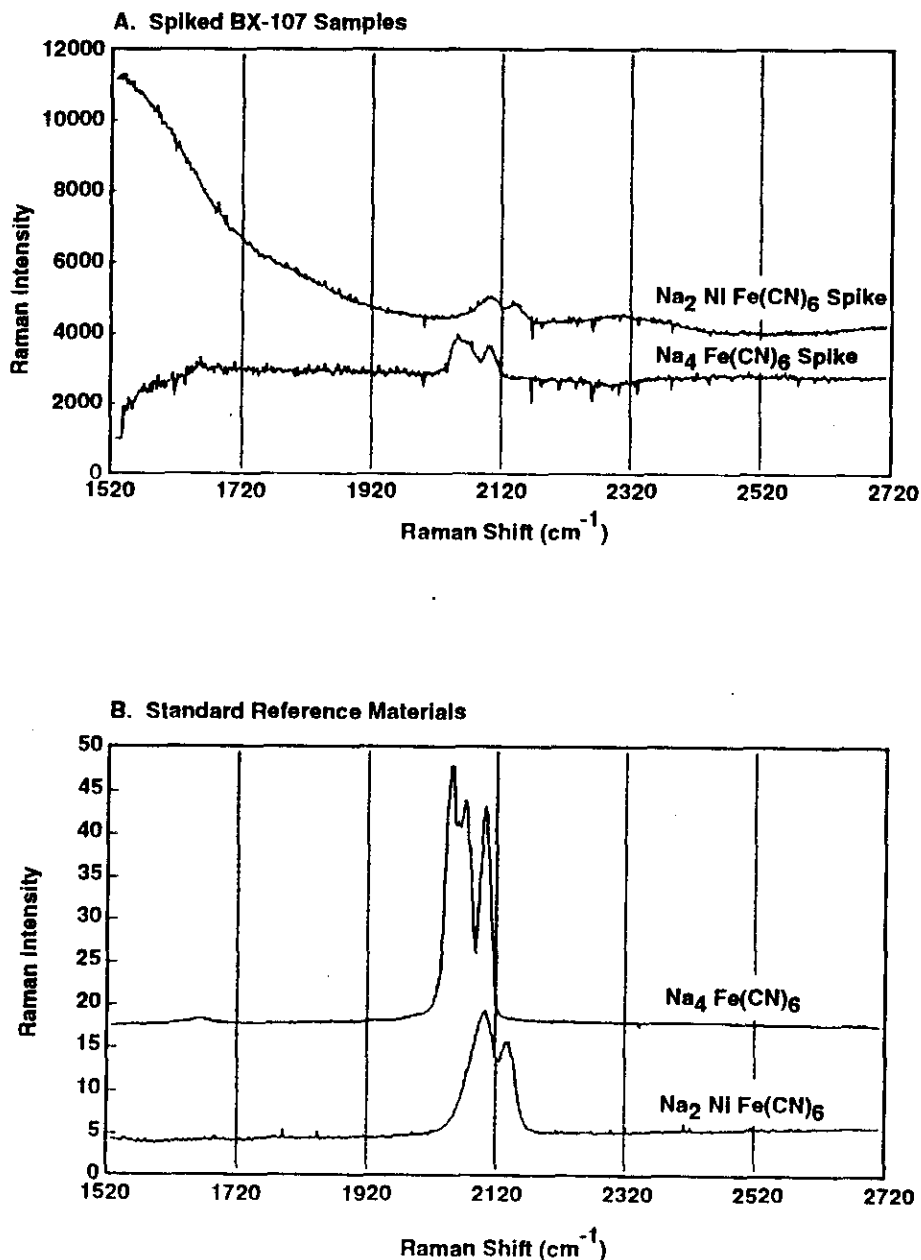


Figure 7-3. Spiking Tank 241-BX-107 Real Tank Waste.

## Ferrocyanide Spiking of BX-107



29308093.10

species (Meeussen et al. 1992, Villanueva et al. 1992). This must be substantiated and is impossible to determine spectrophotometrically. Therefore, it is suggested that the effect be studied with alternative methods in combination with exposure to visible light, such as IC or X-ray diffraction.

9413205.375

This page intentionally left blank.

913205-376



## 8.0 DETECTION LIMITS FOR CYANIDE SPECIES

Process knowledge indicates that tank 241-T-107 should contain 0.03 moles of Fe for each liter of waste (Hill 1992). Assuming a waste density of 1.4 g/mL, and all iron is in the form of ferrocyanide salt, a maximum concentration of 0.5 wt% ferrocyanide is possible in the tanks; this concentration is within the detection limit of the system. However, as shown in Table 4-5, the analyzed concentration of cyanide for tank 241-T-107 tank core 51 and core 52 composites is 0.01 and 0.006 wt%, respectively. Recent analysis of tank 241-BY-104 materials indicates concentrations of cyanide to be only 69  $\mu\text{g/g}$  of sample; equivalent to  $1 \times 10^{-3}$  wt%  $\text{Fe}(\text{CN})_6^{4-}$ . The previous detection limit for analysis of solid ferrocyanide salts in nitrate salt matrices, under ideal conditions (i.e., calibration via signal acquisition on a rotating sample), was 0.6 wt% ferrocyanide (WHC 1992). Spiking of tank 241-BY-104 saltcake simulant yielded a similar LOD for ferrocyanide species. A series of spikes were performed on simulated and real waste samples to determine detection limits in expected tank matrices. In addition, standard additions were also performed using potassium and sodium ferricyanide on simulants. In these preliminary studies, ferricyanide was found to be most stable in these matrices and provided the best analytical curve results.

Process simulants with ferrocyanide concentrations exceeding 0.5 wt% ferrocyanide-spiked 241-BY-104 simulant, and ferrocyanide-spiked 241-BX-107 tank material were analyzed to elucidate possible interferences to  $\text{Na}_4\text{Fe}(\text{CN})_6$  and  $\text{Na}_2\text{NiFe}(\text{CN})_6$  determinations. The potassium and sodium ferrocyanide salts were ground and gravimetrically weighed to concentrations of 10, 5, 2, 1, and 0.5 wt% ferrocyanide in sodium nitrate salt. These samples were then milled to a uniform particle size and consistency before spectral analysis was performed. Tank and simulant samples were spiked with ferrocyanide salt, which was added by weight. The samples were then stirred repeatedly until a uniform sludge was obtained with the consistency of loose peanut butter. All work was initiated on tank simulants before attempts at blending were made with the radioactive tank wastes in the hood.

Detection limits were based on American Society for Testing and Materials (ASTM) standard calculations using background noise and sample response to standards of known concentrations. Specifically, ten standard samples were analyzed. The resultant spectra were silica corrected and ensemble averaged to produce a single spectrum. The peak response and background statistics (i.e., background standard deviation and average background value for a known concentration) were used to calculate a linear slope and noise value or the average response for a set of known weight percent standards where the least squares fit standard deviation represented the noise response for the standard. The resultant detection limit value was calculated as 3 times the noise value divided by the slope or average response divided by the concentration (as shown in Equation 8-1).

$$\text{LOD} = \frac{3(\text{Noise})}{\text{Response}} \times \text{Concentration of Known}$$

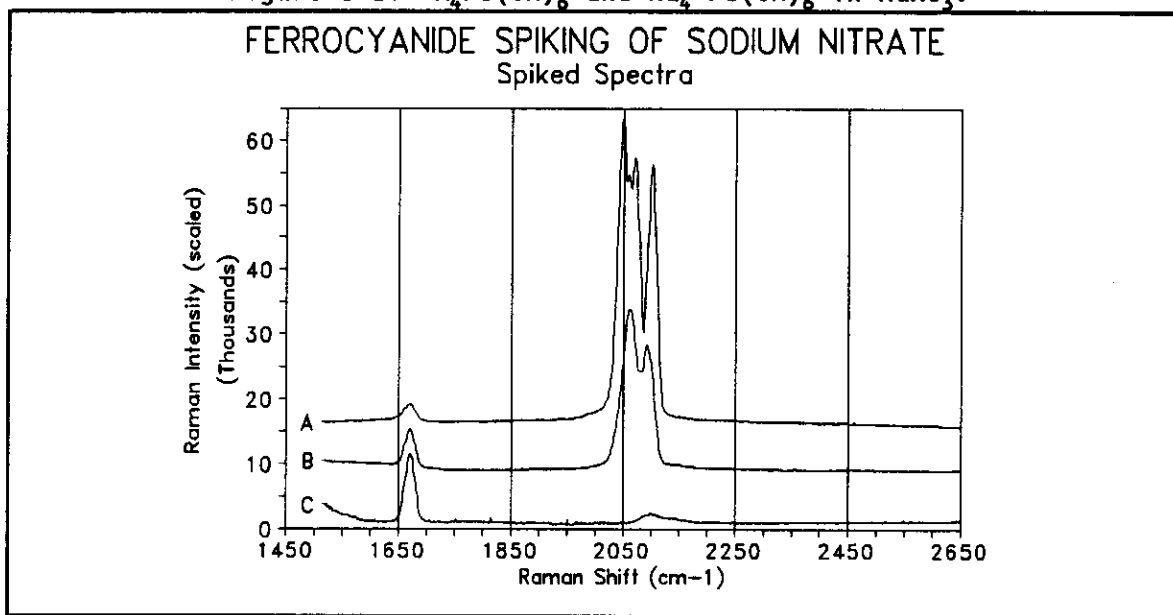
Equation 8-1

It was suspected that photoinitiated reactions were occurring in the caustic simulant as the presence of ammonia vapors were noticeable. Therefore, analyses of ferrocyanide salts in  $\text{NaNO}_3$  were first attempted. Results from ferrocyanide salts are provided in Figure 8-1. LOD were estimated from repeated measurements on samples containing a known concentration of a ferrocyanide. The collected data yielded a LOD of 0.28 wt% for  $\text{Na}_4\text{Fe}(\text{CN})_6 \cdot 10\text{H}_2\text{O}$ , and a LOD of 0.27 wt% for  $\text{K}_4\text{Fe}(\text{CN})_6 \cdot 10\text{H}_2\text{O}$ .

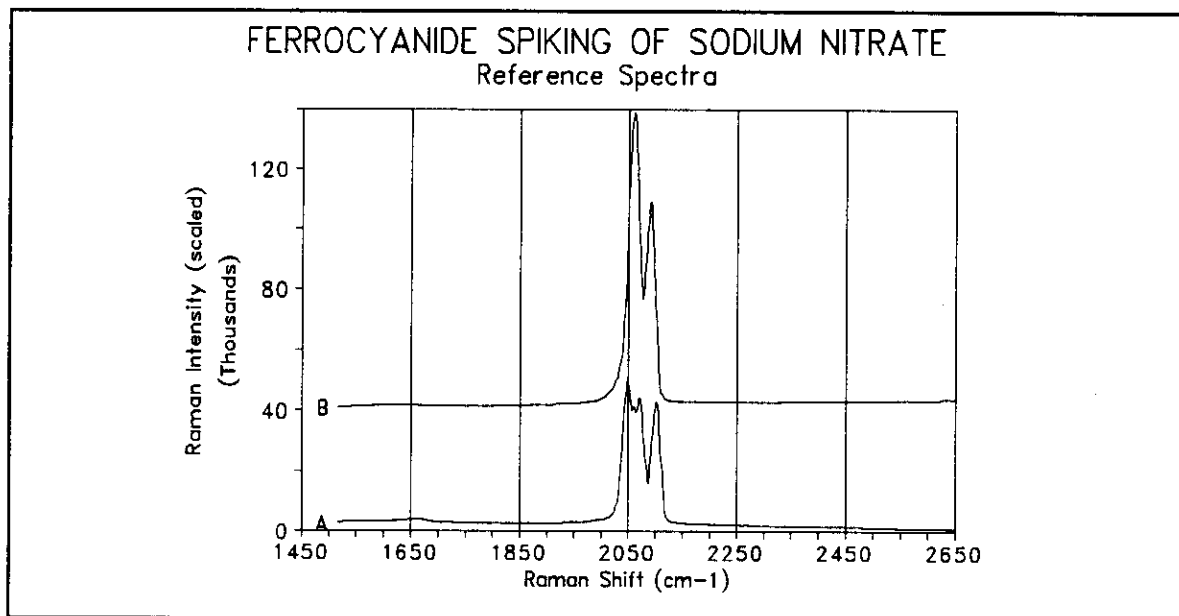
The tank 241-BY-104 simulant sample is dark brown in color, cohesive in consistency, and apparently poses a small problem with signal acquisition for sodium ferrocyanide. The LOD was estimated to be 0.63 wt% for data acquired during a 1-minute exposure. Spiking tank 241-BY-104 simulant provided spurious results, as shown in Figure 7-2, which were attributed to decomposition of the mononickel ferrocyanide species. However, potassium ferricyanide was found to be moderately stable in the tank 241-BY-104 simulant matrix. Therefore, a calibration curve based on five data points, using a set of ensemble-averaged spectra for each data point, was generated (see Figure 8-2). The correlation coefficient for the curve produced for these standards is 0.993. This value is reasonable for data obtained from a simulant tank matrix which is not known to be stable.

Spectra resulting from the standard addition of  $\text{Na}_4\text{Fe}(\text{CN})_6$  and  $\text{Na}_2\text{NiFe}(\text{CN})_6$  to tank 241-BX-107 materials are shown in Figure 8-3. These results show the uncorrected background from which the peaks were interactively subtracted from the silica and baseline background. The weak peaks in the  $2,050\text{--}2,150\text{-cm}^{-1}$  region are the original signals that were extracted resulting in the peaks shown in Figure 7-3. These results were used to estimate a detection limit for  $\text{Na}_2\text{NiFe}(\text{CN})_6$  of 9.9 wt% and for  $\text{Na}_4\text{Fe}(\text{CN})_6$  of 13.6 wt% in this real tank matrix. These results are quite poor, but in terms of data quality, clearly illustrate the effect of homogenization, chemistry, and data treatment, when extracting weak responses in the presence of large background, as in this technique.

Figure 8-1.  $K_4Fe(CN)_6$  and  $Na_4Fe(CN)_6$  in  $NaNO_3$ .



A = 31%  $Na_4Fe(CN)_6$       B = 5.41%  $K_4Fe(CN)_6$       C = 100%  $NaNO_3$



A = 100%  $Na_4Fe(CN)_6$       B = 100%  $K_4Fe(CN)_6$

Figure 8-2. Calibration Curve of  $K_3Fe(CN)_6$  in  
Tank 241-BY-104 Simulant.

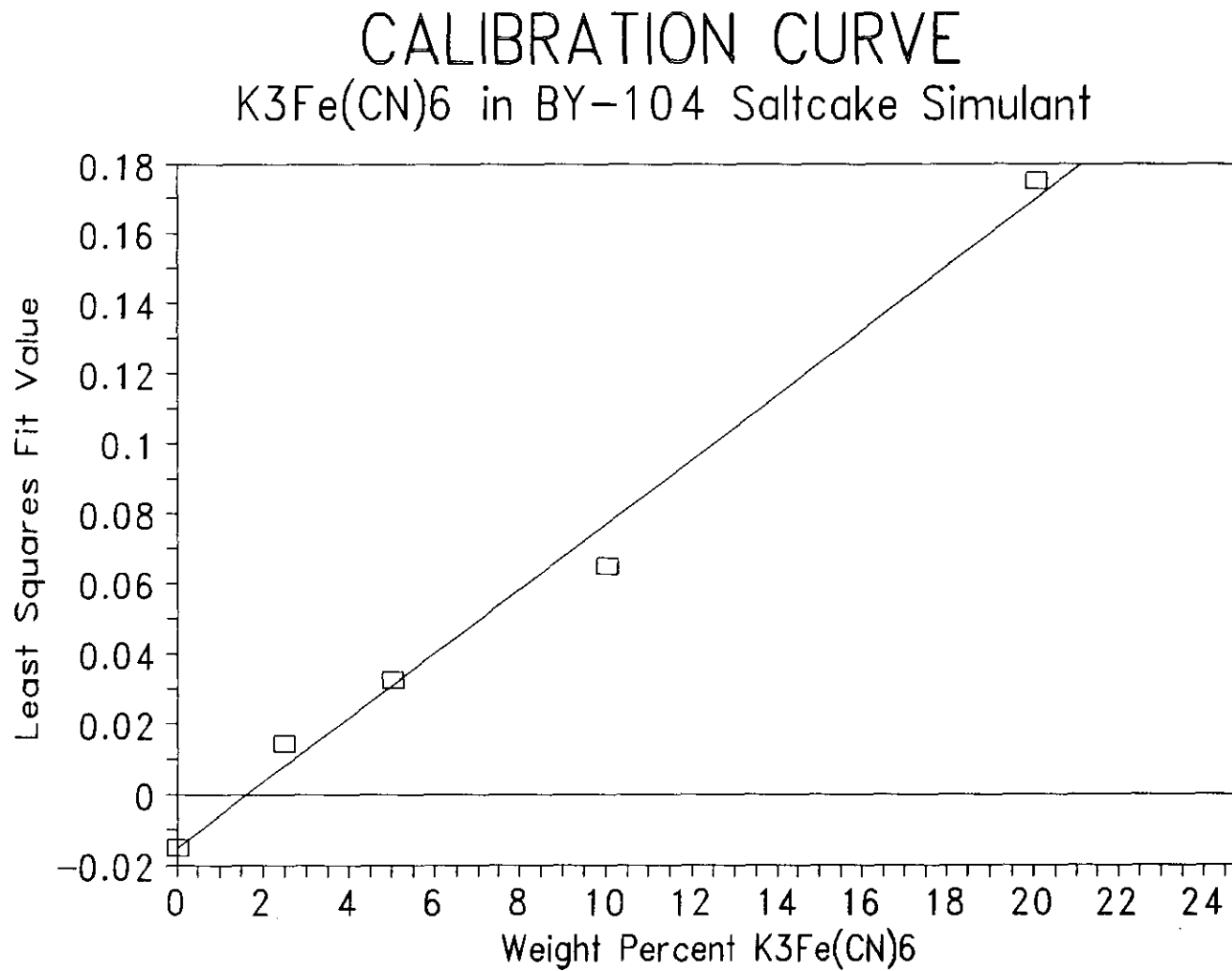
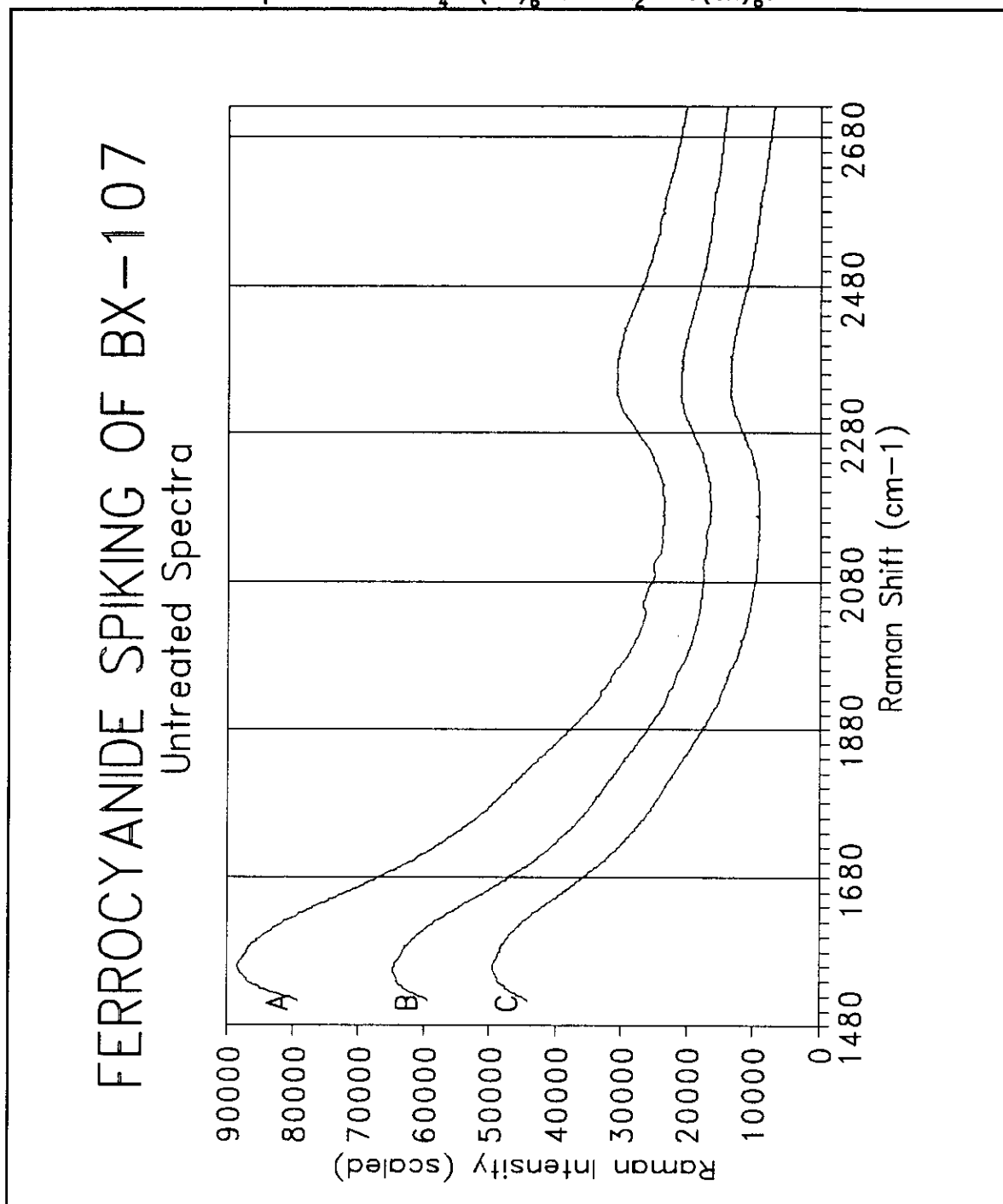


Figure 8-3. Tank 241-BX-107 Real Waste Sample  
Spiked with  $\text{Na}_4\text{Fe}(\text{CN})_6$  and  $\text{Na}_2\text{NiFe}(\text{CN})_6$ .



A =  $\text{Na}_4\text{Fe}(\text{CN})_6$  Spike B =  $\text{Na}_2\text{NiFe}(\text{CN})_6$  Spike C = BX-107

This page intentionally left blank.

91325-332

## 9.0 QUALITY ASSURANCE

Whenever applicable, standards and system performance checks used for this evaluation are based on either National Institute of Standards and Technology (NIST) or ASTM standards and practices. When standards were not available, peer reviewed results were used to provide validation through independently obtained data comparisons. Existing laboratory quality assurance methodology and procedures were used to obtain data provided in Tables 4-1, 4-3 and 4-4 in support of this qualification work (Moss 1992, WHC 1991).

Standards development is a parallel and ongoing process because application of Raman technology to waste tank characterization is in its early or initial program phases. Not all standards applicable to the measurement of chemical species in the waste tanks exist within the framework of NIST primary standards. Therefore, secondary traceability was obtained through the comparison of conventional laboratory methods to the NIST traceable elements from which the primary standards have been constructed. For example, NIST traceable standards are provided for ICP Fe analysis and spectrophotometric determination of  $\text{CN}^-$ . However, there are no standards for direct  $\text{Fe}(\text{CN})_6^{4-}$  analysis. Therefore, all standards prepared were analyzed via these traceable methods.

The goal of qualification has been to provide for the acquisition of Raman spectroscopy data from waste tank samples that are traceable and therefore, defensible (Crawford 1993c). This method of quality assurance has been applied to qualitative results. Defensibility has been defined through comparison of wavenumber assignments to a standard reference library. However, this reference library of Hanford Site waste constituents is in the initial phases of development for solids because there is a scarcity of literature on assignments for Raman peaks in solids. Therefore, all species of interest have been compared to results obtained by FSU in previous work (WHC 1992). It is anticipated that this library will be maintained and further comparisons will be made as data is collected from other U.S. Department of Energy laboratories. In this way, consensus assignments for many of the solid materials found in Hanford Site waste may be obtained. The implementation of further qualification will ultimately establish the validity and limitations of data obtained from the remote Raman screening system for quantitative analysis of ferrocyanide species in tank waste materials. Indeed, some of this work has provided a basis from which a program such as this may be initiated.

Qualification is divided into three parts: (1) spectrometer performance check, (2) speciation and software qualification, and (3) data qualification. A summary of these checks is provided in Table 9-1. A system of routine initial testing in a cold environment preceding the installation and operation of these systems, with ongoing calibration and performance checks is being established. The initial spectrometer performance check is based on the principles described in the *Standard Practice for Describing and Measuring Performance of Dispersive Infrared Spectrometers* (ASTM 1993). These tests verify and validate operation of the spectrometer. Data recordings that show trending are needed to maintain a historical record of accuracy and precision in system performance as comparable to baseline data obtained in initial

Table 9-1. Instrumental Parameters.

Testing phase	Environment	Qualification category	Parameter	Monitoring method	Logging requirements
Initial testing and optimization	Cold laboratory	Spectrometer performance	Light leakage optimum resolution	Record baseline	Chart in controlled notebook
				Plot Raman intensity vs. full width at half maximum resolution	Chart in controlled notebook
			Linear dispersion	Calibration with neon source	Spectra in notebook
			Stray radiant energy	-Radiation source response -Dark current response	Example spectrum to be posted in notebook
			Mechanical repeatability	Document results of 10 slews to same spectrometer position	Standard deviation of runs noted in notebook
		Species identification	Photometric accuracy	-Check laser frequency -Run pure standards for comparison -Determine instrumental limit of detection	Record in notebook
Weekly system checks	Hot hood or hot cell	Operations check and software algorithm check	Photometric accuracy	-Simulants determinations -Matrix spike -Blind samples	Response to results tracked and reported in logbook



Table 9-1. Instrumental Parameters.

Testing phase	Environment	Qualification category	Parameter	Monitoring method	Logging requirements
Daily operations check	Hot hood or hot cell	Species identification and software check	Photometric accuracy	-Signal-to-noise ratio -Check standard -Background subtraction -Blank determinations	Record in logbook
			Sample variance	-Signal averaging over small areas -Tracking of segment specific data	Perform analysis according to test plan and record in final report
		Operation check	Response time	Document acquisition time	Archive in notebook and file. Power obtained as presented to sample (at probe end)
			Ambient temperature	Document temperature in logbook	
			Laser frequency and power	Document frequency and power in logbook	
Final data validation	Arbitrary environment	Software and operations check	Data validity	-Compare pure reagent to real samples -Peer analysis of simulants -Compare real waste results to laboratory results -Compare simulants to real waste results.	Specified date recorded in final data package/report

\* data specified in statement of work or test plan.

checkout and optimization. Specifically, the initial performance check on wavenumber accuracy, mechanical repeatability, and precision is required using a neon standard. This performance check must be completed after optimization for maximum resolution after wavelength calibration and throughput is determined for the instrument. These initial performance parameters were, and will continue to be, documented in notebooks to become initial entries in a historical logbook which will be kept with the instrument at all times. All entries will be maintained in the same instrument logbook as the instrument proceeds into operation.

For future routine work, it is planned that performance checks will be performed on a weekly and daily basis as described in Table 9-1. All data collected for comparison of daily performance will be recorded in the instrument logbook that is kept with the instrument. Selected information will be entered in the electronic file copy of all spectra obtained. This selected information will also be cross-referenced to the laboratory logbook. Many of the parameters used to compensate for noise and background are archived in the file header information provided with the raw data. However, it is prudent to record some operations parameter measurements in the logbook kept with the instrument for easy access. Therefore, measurement and documentation of daily ambient temperature, response time, and signal-to-noise ratio will be provided in the instrument logbook.

The signal-to-noise ratio is reported for cyclohexane or acetonitrile and neat  $\text{NaNO}_3$  or  $\text{K}_4\text{Fe}(\text{CN})_6$ , depending on the spectral range of choice for the sample spectra. The liquid acetonitrile and cyclohexane standards may be run as homogeneous signal-to-noise ratioing standards. These pure liquid standards are inherently more homogeneous than the solid standards used. Sodium nitrate will be used for the spectral window centered at  $1,100\text{ cm}^{-1}$  and sodium ferrocyanide for the window centered at  $2,000\text{ cm}^{-1}$  for wavenumber accuracy and performance optimization on solids.

Spectra obtained during this work were tracked in laboratory notebooks (Crawford 1993b, and 1993d) and archived in compressed electronic files, by date, for future reference. All binary files were kept in archived electronic file format. Other processing files may have been added to those archived depending on data treatment required and are differentiated by extension assignment. The file name is indicative of the type of spectral data stored in the file. This format allows for other file forms to be added as needed, while traceable cross referencing is maintained in hardcopy format. These are tacked in laboratory notebook entries through the project. File extension assignments are shown in Table 9-2.

Notebooks include, but are not limited to, the parameters listed in Table 9-3 according to project and logbook.

Table 9-2. File Data Types and File Extensions.

File type	File extension
Binary files	.crd
Tungsten light (spectral response) files	.cnt
Dark current files	.drk
Dark white corrected files	.dwt
Summed input files	.sin
Spike-removed summed serial files	.sum
Fast fourier transformed files	.fft
Smoothed, noise-reduced summed files in final form	.trm

Table 9-3. Documentation Methods.

Medium	Parameters to be documented
System Logbook	Date Laser power Laser frequency Power measuring method Warm-up time Name of operator Filenames of spectra obtained Software Version Number Executable file date Date of software installation
Project Notebook	Date Observations Detailed description of methods used Sample identification and data Sample handling and system operation notes
Computer file	Date Laser Frequency Notebook reference numbers Spectrometer position Linear dispersion Laser power Operator Software name Version number Data reduction routine by extension

## 9.1 SOFTWARE QUALITY ASSURANCE

Because of the developmental nature of this work, results are not intended to be used to support safety or environmental quality decisions without additional data backing. Therefore, the use of both control and data acquisition software for this instrument has no impact on safety or financial or social welfare. This software is labeled noncritical by Institute of Electrical and Electronics Engineers standards (IEEE 1986) and data obtained from this system carries an Environment, Safety, Health, and Quality Assurance Impact Level 4 as stated in *Management Requirements and Procedures* (WHC-CM-1-3 1987).

## 9.2 QUALITY ASSURANCE IN RAMAN ANALYSES

These screening data support evaluation of technology development in the laboratory. Apart from this evaluation, analytical data derived from the Raman spectra of waste tank samples will ultimately support process decisions and safety assessments that must be made on feed for waste pretreatment, grouting or vitrification, and also on resolution of tank USQs. These data are not currently recognized by the Environmental Protection Agency as being a product of a valid certified laboratory method.

Sample analysis and data processing are based on species identification (qualitative analyses) and appropriate calibration curve generation. Species identification was based on spectral comparison with stored spectra from pure reagents, and from literature whenever possible (Herzberg 1945, WHC 1992, and Lin-Vien et al. 1991). System stability and reproducibility were checked via representative calibration either in matrices approximating real tank materials, or in real tank materials. Further verification was obtained with performance check standards such as cyclohexane, acetonitrile, sodium nitrate and sodium ferrocyanide.

Wavenumber calibration included correction for abscissa error. This calibration proceeded via assignment of neon standard lines to pixels on the CCD detector and reporting the center of mass for the peak by inspection or calculation. Neon lines were assigned for at least five spectrometer grating positions. Linear dispersion was determined for the operating range of the instrument as matched by laser source (Tseng et al. 1993). A reference spectrum, taken with the neon source, was obtained each time the spectrometer was set at a different center position. This spectrum was compared with spectra obtained from the last analysis performed in that spectral region. To account for discrepancies, spectral adjustments were made by wavelength shifting all spectra from common assignments to neon line standards. This ensured that the system wavelength accuracy was maintained.

Calibration for quantitative analysis was performed using analyzed standards that are traceable to NIST standards with certified cyanide and iron contents. Solid salt mixtures were constructed to mimic tank matrices as closely as possible. Therefore, ferrocyanide saltcake standards were added to sodium nitrate. These standards were made in 99.9 wt% pure sodium nitrate salt. Recent analytical efforts have shown that milling of solid standards

prepared for FTIR calibration produced results that are superior to direct mixing (Bryan et al. 1993); therefore, all standards were prepared gravimetrically and homogenized by milling.

Standard additions were performed on real tank wastes and LOD was derived from the resultant analytical curves as described in Sections 7.0 and 8.0. Results prove that detection limits for analytes in tank matrices are greater than for simple salt calibration. However, further work in establishing measurement accuracies on standards must be completed to provide a historical record of instrument performance in operation before quantitative measurements are performed in earnest.

Differences in aliquots or sample homogeneity, also known as presentation error, were eliminated by averaging multiple sample results and spinning the sample during analysis. The extent to which the sample in the hot cell represents the whole by this method remains to be measured, as sample spinning is impossible in the hot cell. Comparisons must be made with these calibration protocols before quantitative analysis is performed.

A series of comparisons was made to validate data obtained from both simulants and real tank wastes. Results of these analyses were traceable to NIST standards and are analyte specific. Whenever possible, laboratory methods were selected that most closely mimic the results expected. Specifically, when direct surface analyses were performed, such as Raman or FTIR on solids, a comparison method that included complete sample digestion was used and Raman spectra were obtained directly via an independent laboratory. Table 9-4 provides a summary of comparison methods used.

Peer analysis for validation of analytical data provided the best available comparison base because of the instability of simulant samples over time under present sample conditions.

Table 9-4. Data Comparisons by Analyte.

Analyte	Method of comparison
$\text{NO}_3^-$	Ion chromatography
$\text{NO}_2^-$	Ion chromatography
$\text{CO}_3^-$	Total inorganic carbon
$\text{SO}_4^-$	Ion chromatography
$\text{Fe}(\text{CN})_6^{4-}$	ICP-Fe CN <sup>-</sup> by distillation/colorimetry FTIR Ion chromatography
$\text{Fe}(\text{CN})_6^{3-}$	ICP-Fe CN <sup>-</sup> by distillation/colorimetry FTIR Ion chromatography

ICP = Inductively coupled plasma  
FTIR = Fourier transform infrared

This page intentionally left blank.

03205 390  
NOT CLAMEN  
03205 390  
03205 390

## 10.0 DATA TREATMENT PROTOCOLS AND NOISE SOURCES

Data was collected and treated as described in Appendix B. The general mathematical treatment involves spectral subtraction and ratioing to achieve the true spectrum. This spectrum is without noise and accounts for the spectral response of the instrument as shown in Equation 10-1.

$$\text{True Spectrum} = \frac{\text{Raw Spectrum}}{\text{Spectral Response}} - \text{Noise}$$

Equation 10-1

Tungsten light spectra were used to account for spectrometer spectral response and pixel-to-pixel variations. Initial spectra were archived as a record to be used to document spectrometer response as determined in initial testing. Subsequent electronic files of the spectra were used to ratio spectral response for each spectrum obtained. A dark spectrum was also collected at each sampling window to compensate for DC offset in the CCD detector. In general, the background response is additive and simple mathematics have been applied to eliminate it.

Spectrometer sensitivity and pixel-to-pixel variation, as determined from dark current and white light sources, was determined at each calibration setting. This was accomplished through spectral ratio. All raw data were stored and spectral correction was performed after data acquisition or was provided on a real-time basis as data were acquired.

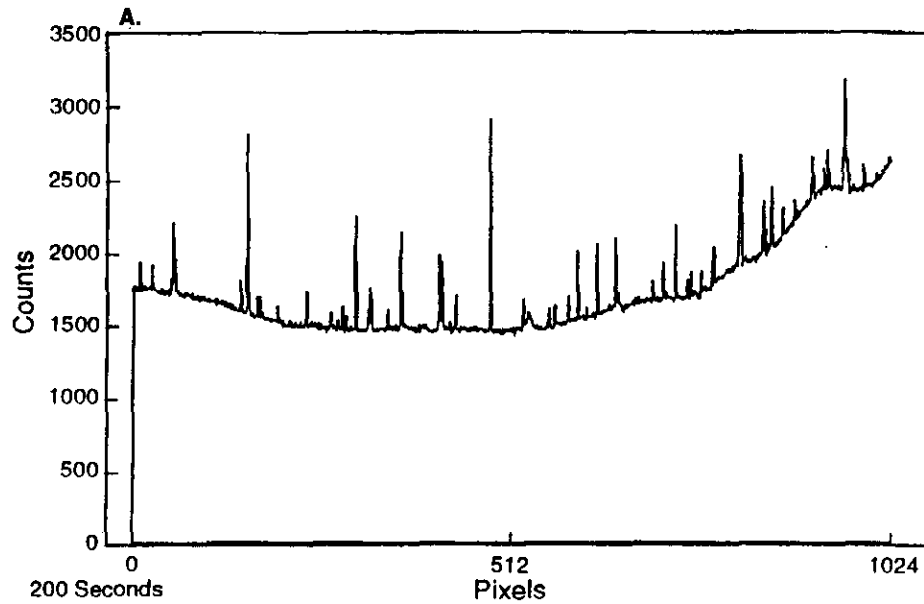
At low signal-to-noise ratios, the presence of noise spikes from radioactivity in the 222-S Laboratory became more visible. Background data obtained in the presence of a 5 mR/hr source indicated an increase from 17 to 72 events (spikes) in a 200-second acquisition spectrum (see Figure 10-1). The laboratory environment was expected to be a factor of 10 lower than this field. However, the amount of spike contamination observed in the laboratory was directly related to the number and type of samples in the vicinity of the detector and varied as work proceeded from day to day. The effects of these spikes were much more visible in the laser diode spectra than the argon ion spectra because of the comparative low signal levels of the laser diode compared with the argon ion laser results. However, detection of low concentration analytes using argon ion excitation is also compromised. Two approaches have been suggested to improve data acquisition in these conditions: (1) eliminate the gamma-induced noise by placing the detector in a low-background environment, and (2) use automated spike removal. Manual methods and an automatic spike removal technique were used with the laser diode results to obtain relatively noise-free spectra.

The spike removal method used included statistical filtering and summation of serially acquired spectra followed by data treatment as provided by FSU (WHC 1992). Spike rejection may be necessary for spectra containing weak signals before any data treatment (e.g., background removal and spectrometer response ratio) can be applied. This view is also shared by researchers in Germany, who have noted that the detection of weak signals by

Figure 10-1. Background with Known Sources.

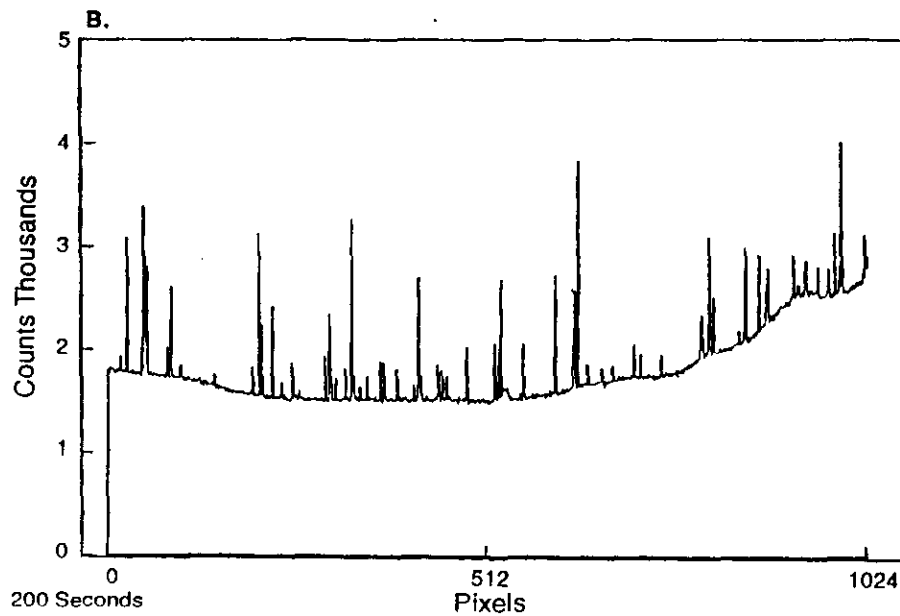
## Cobalt 60

1  $\mu$ Ci at 7" external



## Cesium 137

5  $\mu$ Ci at 7" external



29308093.2



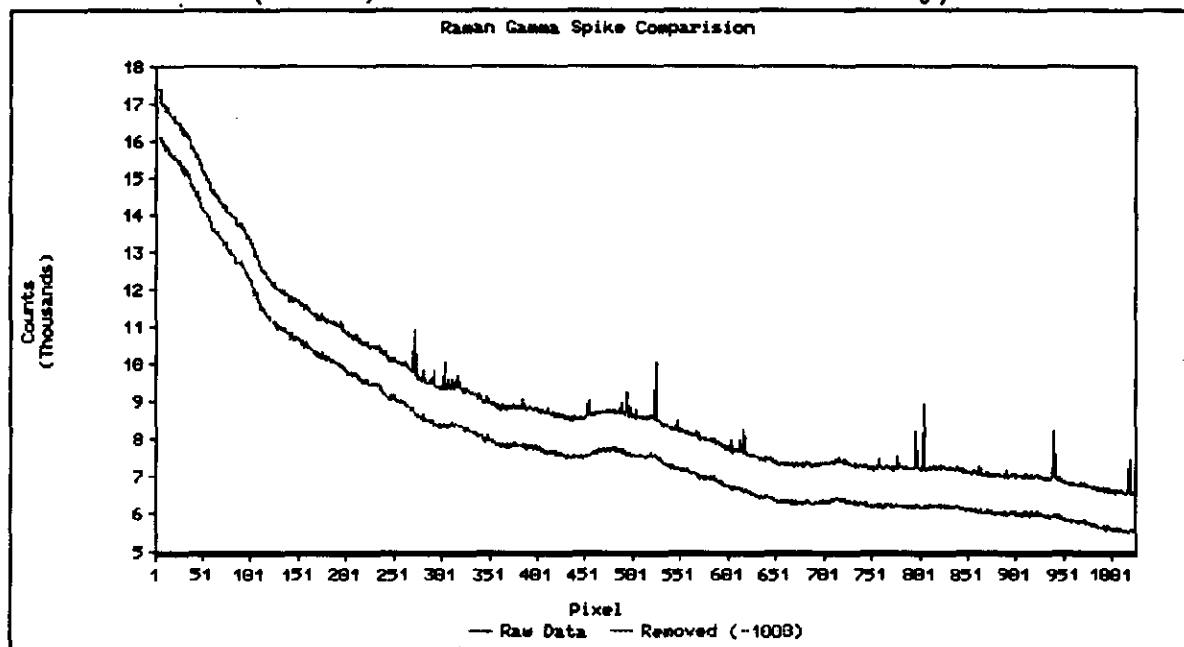
CCD detectors can be restricted by charge spikes often referred to as "cosmic rays" in nonradioactive backgrounds (Hill and Rogalla 1992). These restrictions in detection limits are normally above those caused by thermal background noise and are random in nature. In their approach, Hill and Rogalla (1992) used a multiple-missing-point method for correction of heavily contaminated data obtained in the presence of normal cosmic background with long exposure times. Data was collected with 1,000- and 100-second exposure times and averaged.

Gamma-induced spikes also reduce and impose limitations on the signal-to-noise ratio of the instrument, which ultimately compromises instrument sensitivity. It was also noted that cosmic rays, such as muons, can generate charge spikes of thousands of electrons on a single pixel element. When conditions are such that long integration times are required, these spikes can have a detrimental effect on data treatment and even interpretation of peaks. This problem is further amplified in the presence of gamma-emitting sources as illustrated in Figure 10-1. In similar work, Takeuchi (et al. 1993) pointed out that the practical limit to exposure time is determined by spike noise generated by cosmic rays, as well as gamma and alpha radiation from materials around the detector chip. Raman spectra observed by Takeuchi (et al. 1993) were contaminated with approximately 30 spikes in a 30-minute data acquisition, which represents about one-tenth of the spike contamination observed for some backgrounds in this work at the Hanford Site. Therefore, based on these studies (Hill and Rogalla 1992, Takeuchi et al. 1993), it seems prudent to continue using spike rejection when performing data treatment on heavily spike-contaminated data.

Gamma events or cosmic spikes are common to solid state detectors ranging from CCD arrays to large-volume (250-cc) devices. Background or naturally occurring high-energy gamma rays induce ionization tracks in the detector materials which become part of the signal of interest. The photon cross-section for thin, small-area CCD pixels is small, but when an event occurs, it can swamp the pixel dynamic range. A moderate case of sharp events riding on the general spectral shape is shown by the upper trace in Figure 10-2. These events can also be seen in the sodium nitrosylpentacyanoferrate spectrum shown in Appendix A (Page A-11). Given proper combinations of signal-to-noise ratios, frequency of occurrence, integration time, and spectral intensity, the events can be troublesome. For low amplitude signals, gamma event removal is desirable.

The approach tested for the data in Figure 10-2 is as follows. Successive 30-second exposures were acquired and stored. A moving window of five spectra were examined by comparing the upper  $3\sigma$  of the average of four outer points with the fifth central point. If the test point exceeded this criteria, the test point was replaced with the average. This method proceeded for each pixel and for the entire set of spectra. By using a  $3\sigma$  rule, <1 percent of the data will be arbitrarily and incorrectly removed. The removed data are replaced with a random value within a  $2\sigma$  range of the average, thus preserving the statistical noise of the baseline signal. It was noted that, as the signal integration time increased, the number of corrections for each spectrum increased. Correction rates of 10 to 15 percent was observed for 20-second scans, and nearly 30 percent for 1-minute scans.

Figure 10-2. Raman Gamma Spike Comparison: Upper Trace is Direct Sum of Unprocessed Scans; Lower Trace is Sum of Scans with Spikes Removed.  
(less 1,000 counts offset for trace clarity)



Calculations for signal-to-noise were taken as the total signal minus the background divided by the standard deviation of the background (i.e., noise specific to sample matrix). Clearly, signal-to-noise levels, and ultimately detection limits, will degrade with increased spike contamination and noise in spectra. These factors become more influential as analytes at low concentration are analyzed.

## 11.0 RECOMMENDATIONS AND CONCLUSIONS

This report provides observations and delineates areas requiring further evaluation after preliminary testing of the Raman Spectrometer on simulants and tank waste samples. Indications from these tests support the conclusion that programmatic issues can be mitigated by deployment and implementation of this instrument. Data that is currently available is not sufficient to completely address identification and resolution of all operational parameters. The next phase of this study will focus on collecting spectra on a large number of tank waste samples that have been homogenized and stored in the laboratory. Evaluation of these spectra is expected to define instrument and data handling requirements (e.g., sensitivity, resolution, signal-to-noise, spectral interpretation, reliability, and limitations of the methodology).

A number of protocols are amenable to the use of Raman spectroscopy in the laboratory; the most prominent candidate pertaining to sample screening. The utilization of the system may serve the purpose of 1) identifying cyanide breakdown products and/or oxyanions in high-level waste tank samples, 2) process monitoring for sampling purposes, and 3) monitoring homogeneity during core extrusion processes. Of course, the above-listed applications by no means define the limits for laboratory uses. With preliminary detection limits for ferrocyanide species, in most tank matrices, of approximately 0.5 to 10.0 wt%, the use of 514.5 nm Raman excitation provides mixed results for in situ quantitative ferrocyanide analysis in Hanford Site waste tanks. Therefore, efforts for remote Raman analysis uses should begin with qualitative monitoring, eventually evolving into a quantitative analytical process.

The work performed for the completion of this project serves as an initial technical assessment of both diode and argon ion laser-based remote Raman spectrometers for use in radioactive hot cells and hoods. Work should be directed at either development of longer wavelength laser sources, as demonstrated on simulants at PNL, or demonstration of robust data manipulation software that does not include functions that are subjective in nature. Specifically, oxyanions and ferrocyanide anions have been identified qualitatively in real tank matrices with argon ion excitation. Semi-quantitative analysis of these anions, based on nitrate concentrations, were not performed using the diode-based system as originally intended because of problems with frequency shifting in the laser. This phenomenon, known as "mode hopping," produces conditions in which it is impossible to distinguish signals with accurate Raman shift frequencies. Furthermore, with laser frequencies between 820 and 860 nm delivering less than 50 mW of laser power to the sample, the detectability of some ferrocyanide species is either diminished or impossible. The region of interest is near the extreme limit of acceptable quantum efficiency of the CCD detector for adequate determination of the mononickel ferrocyanide species in particular. Based on these observations, the most viable laser source used during these studies was the argon ion laser. However, the use of this laser source is not without problems as many of the tank samples analyzed exhibited fluorescence at this wavelength.

These tests successfully indicated that identification of oxyanions, ferro/ferricyanide, organics and breakdown products of cyanide are possible. Further studies are required to determine feasible detection limits for these analytes in waste tank matrices. The detection limits of ferrocyanide reported here, indicate that the system would not provide low concentration information on ferrocyanide salts in tank matrices without significant improvement. Standard additions have proven that there is some difference in detection limits in real tank waste vs. pure salt matrices. These interferences are likely to be the result of ion pairing and pH effects. In some cases these effects are detrimental, as in the case of tank 241-BY-104 simulant, where sample chemistry appears to be affecting results. In other cases, minimal sample preparation seems to have provided reasonable results, as in determination of oxyanions and organic species. Most tanks contain an appreciable amount of nitrate salt and nitrate signals have been easily identified using both argon and diode laser excitation.

The test work indicated the need for peak identification software for dispersive Raman systems, and for a Raman spectral library. Therefore, peak identification is preceded by observation and comparison with archived spectra of pure solids. Target anions (e.g., nitrates, nitrites, sulfates, and carbonates) are included as primary screening points. Addition of organic species, complexants, and other analytes must be added to this collection of spectra to better understand some of the breakdown products and other constituents in the tanks.

For this characterization application, it is imperative that instrument performance be judged in terms of factors that impact analysis and analytical accuracy. Work must progress toward better definition and modeling of those variables to be included in system calibration sets. It is impossible to measure all factors, such as homogeneity, without collecting large amounts of data over time and specifying target species for analysis. Based on present understanding, there are two sample variances possible in tank core segments, as extruded in the hot cell, that impact the Raman system performance. These variances are based on spectral changes observed over small sample surfaces which are postulated to result from particle size phenomena in a small sampling area and spectral changes attributable to analyte concentration differences throughout the core segments.

Continued efforts are also required to address the effects that color and physical character of samples have on spectral efficiency of samples. The physical form of the waste must be accounted for as work progresses. The physical form of the wastes depends on the water content of the wastes, and ranges from dry saltcake to near-liquid slurries. Calibration standards must be developed to account for these waste forms and must be based on addition of water to the calibration matrix, followed by a percent-of-water analysis by gravimetry in order to more nearly represent the material analyzed.

Data reduction methods must be determined that provide fast and accurate results based on quantitative standards. Future software development should focus on automation of data acquisition and data treatment. This will assist in placing the Raman instrument into a routine operations setting where a minimum of expertise is required for collection of spectra. Appropriate statistics and chemometrics techniques should be applied to verify the quality of final results. In addition, verification of these approaches must be

provided through peer review and recommendation of accepted experts familiar with the methods.

Data validation must be investigated. Sources of error in any calibration result from sample inhomogeneity and nonrepresentative sampling in the training or calibration set. These errors can be better understood and/or eliminated through development of complete calibration sets, statistical tracking, and mathematical comparisons of the data. Errors caused by sample inhomogeneity are stochastic and therefore, can be determined statistically. Nonrepresentative sampling of calibration sets is more subtle and requires a thorough understanding of all variables related to the analysis. These variables must be accounted for within the calibration set to the extent possible. Two approaches are recommended: (1) analysis of the variances caused by these factors and (2) chemometrics verification of data sets to monitor representativeness of calibration sets with samples.

Calibration comparisons and tracking must continue with the analysis of more known mixtures until a baseline of confidence is established that will allow operations tracking within the laboratory information management system. These comparisons include chemometric analysis of standards and samples, with checks on accuracy of calibrations, and comparison of representative measure to real sample conditions.

This page intentionally left blank.

943205.398

## 12.0 ACKNOWLEDGEMENTS

The authors gratefully acknowledge the efforts of a group of dedicated support people whose expertise and input have been exceedingly valuable. Technical guidance from C. K. Mann and T. J. Vickers has been crucial to the welfare of this project. Assistance with funding and project management has been provided by W. D. Winkelman, T. Lopez, F. R. Reich, J. G. Douglas, and S. J. Mech. Technical review, overall support, scheduling and tracking for this project would not have been possible without the contributions of J. R. Jewett, J. P. Slougher, and J. W. Hunt. Valuable technical guidance, advice, and peer review were provided by S. A. Bryan, G. J. Exarhos, and K. H. Pool from PNL; and R. S. Addleman and T. V. Rebagay from Westinghouse Hanford Company. Information Release was provided by K. M. Broz, Publications Services were provided by P. S. Gregory and M. R. Turner, and Graphics services were provided by S. J. Green and J. P. Esparza. Finally, a special thanks to Process Chemistry Laboratory technicians who worked closest to the samples: J. R. Smith, J. M. Kunkel, and D. W. Edmonson.

9413205.1399

This page intentionally left blank.

943205.400



### 13.0 REFERENCES

- ASTM, 1993, *Standard Practice for Describing and Measuring Performance of Dispersive Infrared Spectrometers*, ASTM Standard E-932, American Society for Testing and Materials, Philadelphia, Pennsylvania.
- Bechtold, D. B., C. J. Jurgensmeier, 1992, *Report of Beaker Tests of Ferrocyanide Scavenging Flow Sheets*, WHC-SD-WM-TRP-071, Revision 0, Westinghouse Hanford Company, Richland, Washington.
- Beck, M. A., 1992, *Waste Tank Characterization Plan for Sampling and Analysis of Augered Surface Samples from Tanks containing Ferrocyanide Wastes*, WHC-SD-WM-TP-114, Revision 2, Westinghouse Hanford Company, Richland, Washington.
- Bryan, S. A., K. H. Pool, L. L. Burger, C. D. Carlson, N. J. Hess, J. D. Matheson, J. L. Ryan, R. D. Scheele and J. M. Tingey, 1993, *Ferrocyanide Safety Project - Task 3.5 Cyanide Species Analytical Methods Development FY 1992 Annual Report*, PNL-8399, Pacific Northwest Laboratory, Richland, Washington.
- Crawford, B. A., 1993a, *Preliminary Evaluation of Raman Spectroscopy for the Hot Cell*, WHC-SD-WM-TP-157, Rev. 0, Westinghouse Hanford Company, Richland, Washington.
- Crawford, B. A., 1993b, *Process Support II Notebook*, WHC-N-623, Westinghouse Hanford Company, Richland, Washington.
- Crawford, B. A., 1993c, *Qualification Plan for Remote Dispersive Raman Spectroscopic Analysis on Hanford High-Level Waste Samples*, WHC-SD-WM-TPI-006, Rev. 0, Westinghouse Hanford Company, Richland, Washington.
- Crawford, B. A., 1993d, *Raman Screening System Logbook*, WHC-N-718-1, Westinghouse Hanford Company, Richland, Washington.
- Greenwell, R. A., R. S. Addleman, B. A. Crawford, S. J. Mech, and G. L. Troyer, 1992, *A Survey of Fiber Optic Sensor Technology for Nuclear Waste Tank Applications*, Fiber and Integrated Optics, Vol. 11, Westinghouse Hanford Company, Richland, Washington.
- Gerrard, D. L., 1991, *Organic and Petrochemical Applications of Raman Spectroscopy in Analytical Raman Spectroscopy*, J. G. Gresselli and B. J. Bulkin, editors., John Wiley & Sons, Inc., New York, New York, B. P. Research Center, Middlesex, England.
- Herting, D. L., D. B. Bechtold, B. A. Crawford, T. L. Welsh and L. Jensen, 1992, *Laboratory Characterization of Samples Taken in May 1991 from Hanford Waste Tank 241-SY-101*, WHC-SD-WM-DTR-024 Rev. 0, Westinghouse Hanford Company, Richland, Washington.

- Herzberg, G., 1945, *Molecular Spectra and Molecular Structure II. Infrared and Raman Spectra of Polyatomic Molecules*, Van Nostrand Reinhold, New York, New York.
- Hill, J. G., 1992, *Tank Waste Remediation System Tank Waste Characterization Plan*, WHC-SD-WM-PLN-047, Revision 0, Westinghouse Hanford Company, Richland, Washington.
- Hill, W., and D. Rogalla, 1992, *Spike Correction of Weak Signals from Charge Coupled Devices and Its Application to Raman Spectroscopy*, Analytical Chemistry, Institut fur Spectrochemie und Angewandte Spektroskopie, Dortmund, Germany.
- IEEE, 1986, *IEEE Standard for Software Verification and Validation Plans*, Institute of Electrical and Electronics Engineers, IEEE Standard 1012.
- Lin-Vien, D., N. B. Colthup, W. G. Fatley, and J. G. Grasselli, 1991, *The Handbook of Infrared and Raman Characteristic Frequencies of Organic Molecules*, Academic Press, San Diego, California.
- Marston, A. L. 1975, *Analysis of Radioactive Waste Supernate by Laser-Raman Spectrometry*, Nuclear Technology, E. I. duPont deNemours and Company, Savannah River Laboratory, Aiken, South Carolina.
- Miller, A. G., 1977, *Laser Raman Spectrometric Determination of Oxyanions in Nuclear Waste Materials*, Analytical Chemistry, Research Department of Research and Engineering, Rockwell Hanford Operations, Richland, Washington.
- Miller, A. G., and J. A. Macklin, 1980, *Matrix Effects on the Raman Analytical Lines of Oxyanions*, Analytical Chemistry, Research Department, Rockwell Hanford Operations, Richland, Washington.
- Meeussen, J. C. L., M. G. Keizer and F. A. M. de Haan, 1992, *Chemical Stability and Decomposition Rate of Iron Cyanide Complexes in Soil Solutions*, Environmental Science and Technology, Department of Soil Sciences and Plant Nutrition, Wageningen Agricultural University, Wageningen, The Netherlands.
- Moss, S. S., 1992, *Quality Assurance Project Plan for the Chemical Analysis of Highly Radioactive Mixed Waste Samples in Support of Environmental Activities on the Hanford Site*, WHC-SD-QAPP-002, Revision 0, Westinghouse Hanford Company, Richland, Washington.
- Robuck, S. J., and R. G. Luthy, 1989, "Destruction of Iron-Complexed Cyanide by alkaline hydrolysis," *Water Science and Technology*, Environmental Control Laboratory, Aluminum Company of America, Alcoa Center, Pennsylvania.
- Sasaki, L. M., 1993, *Tank Contents Overview presented at the Hanford Raman Workshop*, January 1993, Richland, Washington.
- Sloat, R. J., 1954, *TBP Plant Nickel Ferrocyanide Scavenging Flow Sheet*, HW-30399, General Electric Hanford Atomic Products Operation.

- Smith, R. E., E. A. Coppinger, 1954, *Nickel Ferrocyanide Scavenging Flow Sheet for Neutralized RAW*, HW-33536, General Electric Hanford Atomic Products Operation.
- Tseng, C. H., J. F. Ford, C. K. Mann and T. J. Vickers, 1993, *Wavelength Calibration of a Multichannel Spectrometer*, presented at the Raman Spectroscopy Workshop at Florida State University on January 25, 1993, Florida State University, Tallahassee, Florida.
- Takeuchi, H., S. Hashimoto, and I. Harada, 1993, *Simple and Efficient Method to Eliminate Spike Noise from Spectra Recorded on Charge Coupled Device Detectors*, Applied Spectroscopy, Pharmaceutical Institute, Tohoku University, Gobayama, Sendai, Japan
- Villanueva, R. M., J. M. Sanchis Mallols, E. F. Simo Alfonso and G. Ramis Ramos, 1992, *Photolytic and Transport Effects Produced by Argon Ion Laser radiation on Hexacyanoferrate (III) Solutions*, Analytica Chemica Acta, Department of Analytical Chemistry, University of Valencia, Burjassot, Spain.
- WHC, 1991, *Analytical Chemistry Services Laboratories Quality Assurance Plan*, WHC-SC-CP-QAPP-001, Westinghouse Hanford Company, Richland, Washington.
- WHC, 1992, *Detection and Quantitative Analysis of Ferrocyanide and Ferricyanide*, WHC-SD-TD-RPT-003, Revision 0, Westinghouse Hanford Company, Richland, Washington.
- WHC-CM-1-3, *Management Requirements and Procedures*, MRP 5.43, "Impact Levels," Westinghouse Hanford Company, Richland, Washington.
- Winters, W. I., L. Jensen, L. M. Sasaki, R. L. Weiss, J. F. Keller, A. J. Schmidt and M. G. Woodruff, 1990, *Waste Characterization Plan for the Hanford Site Single-shell Tanks*, WHC-EP-0210, Westinghouse Hanford Company, Richland, Washington.

This page intentionally left blank.

943205-10

943205 105  
943205 105  
943205 105

## APPENDIX A

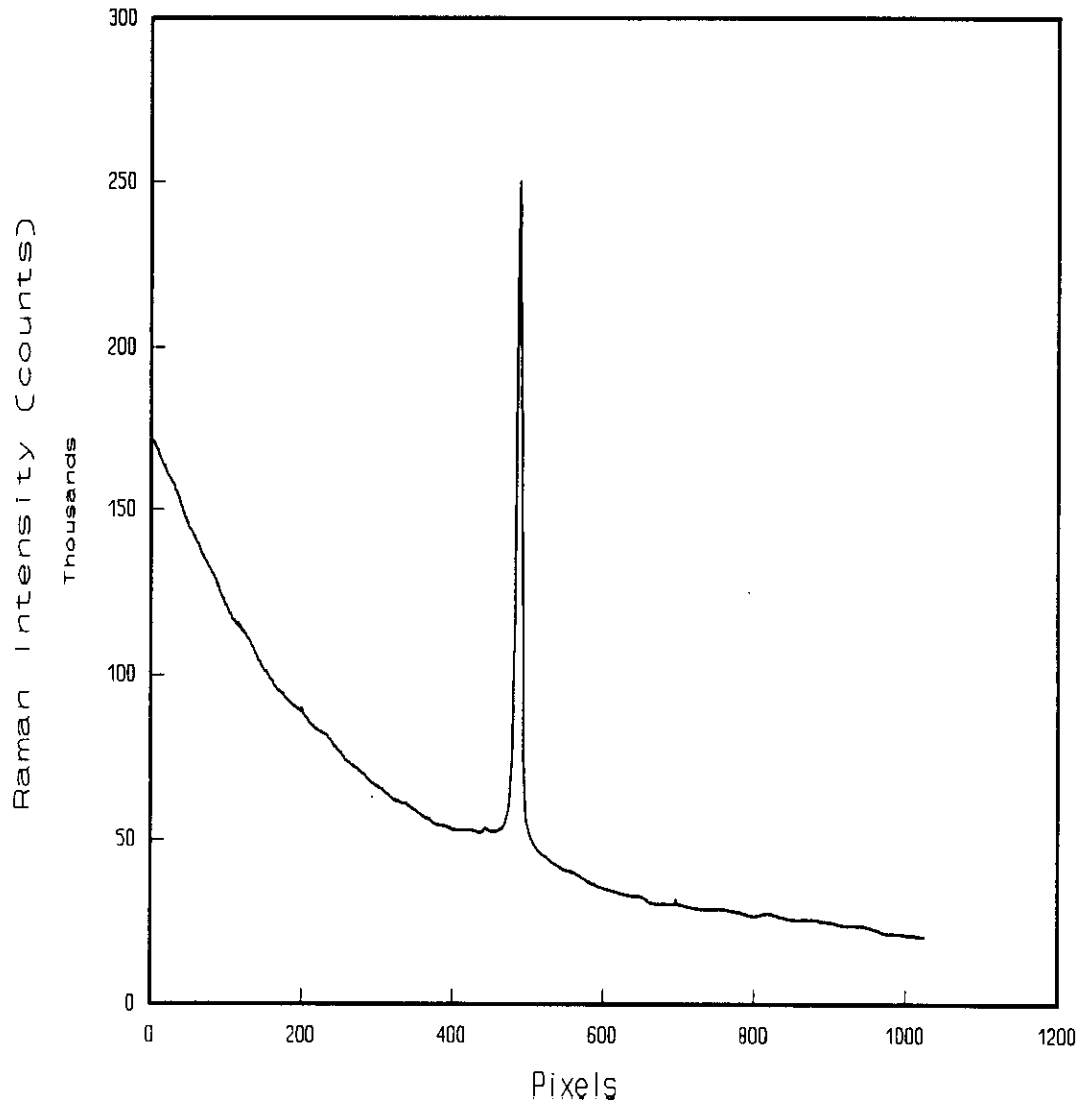
### SPECTRA OF PURE REAGENTS

This page intentionally left blank.

9443205 146

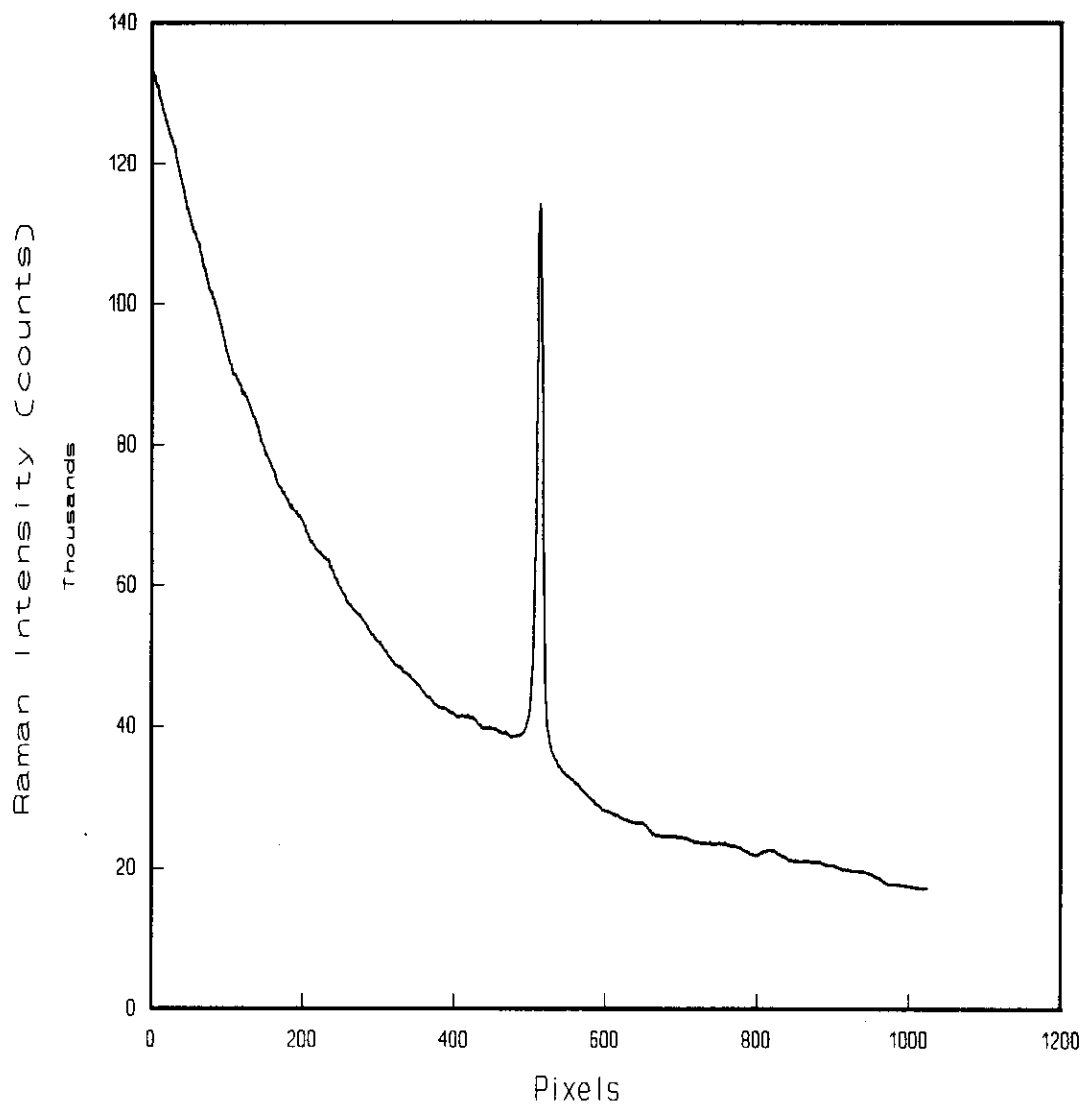
# Strontium Nitrate

centered at 900 nm



# Sodium Nitrate

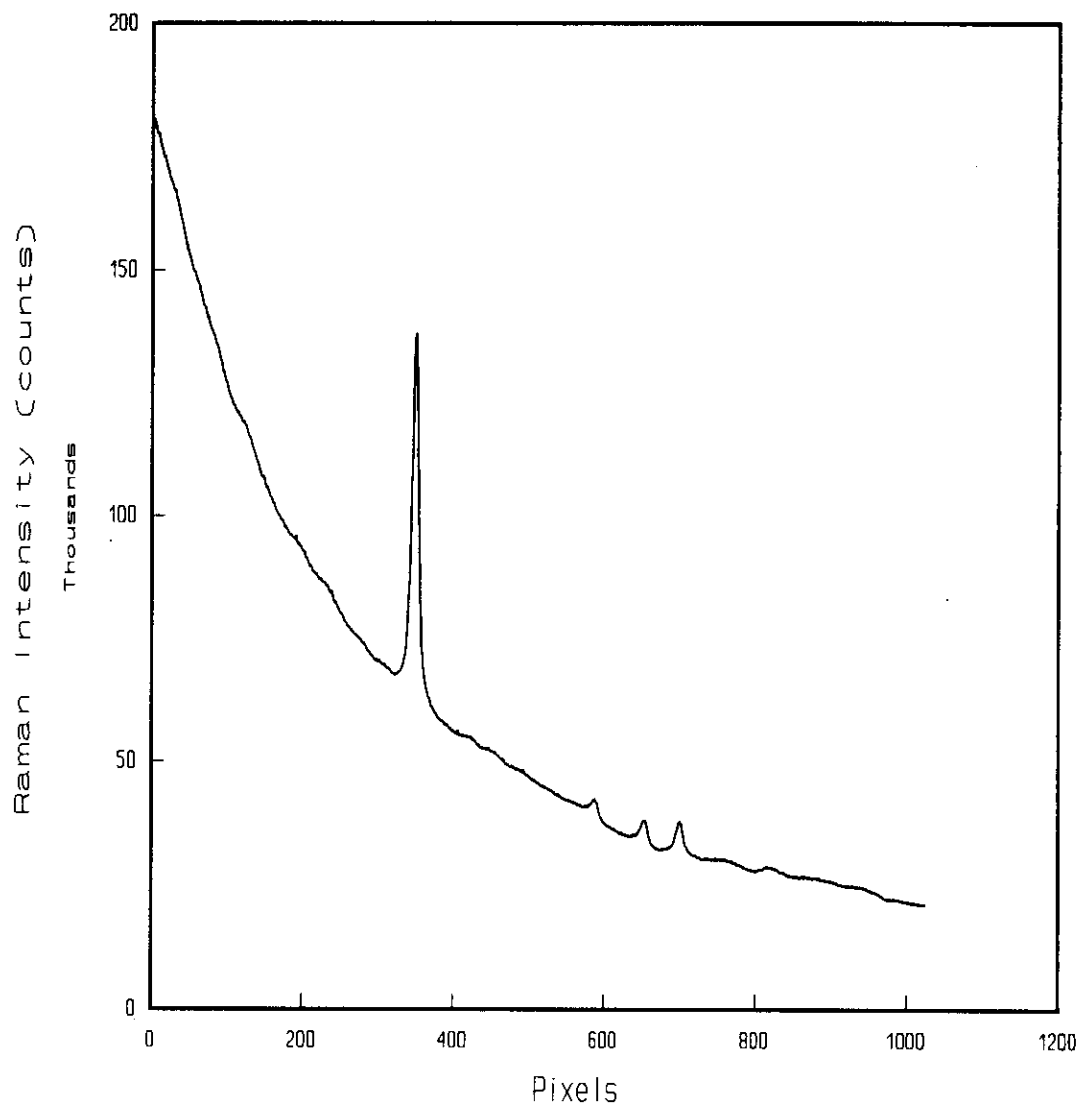
centered at 900 nm





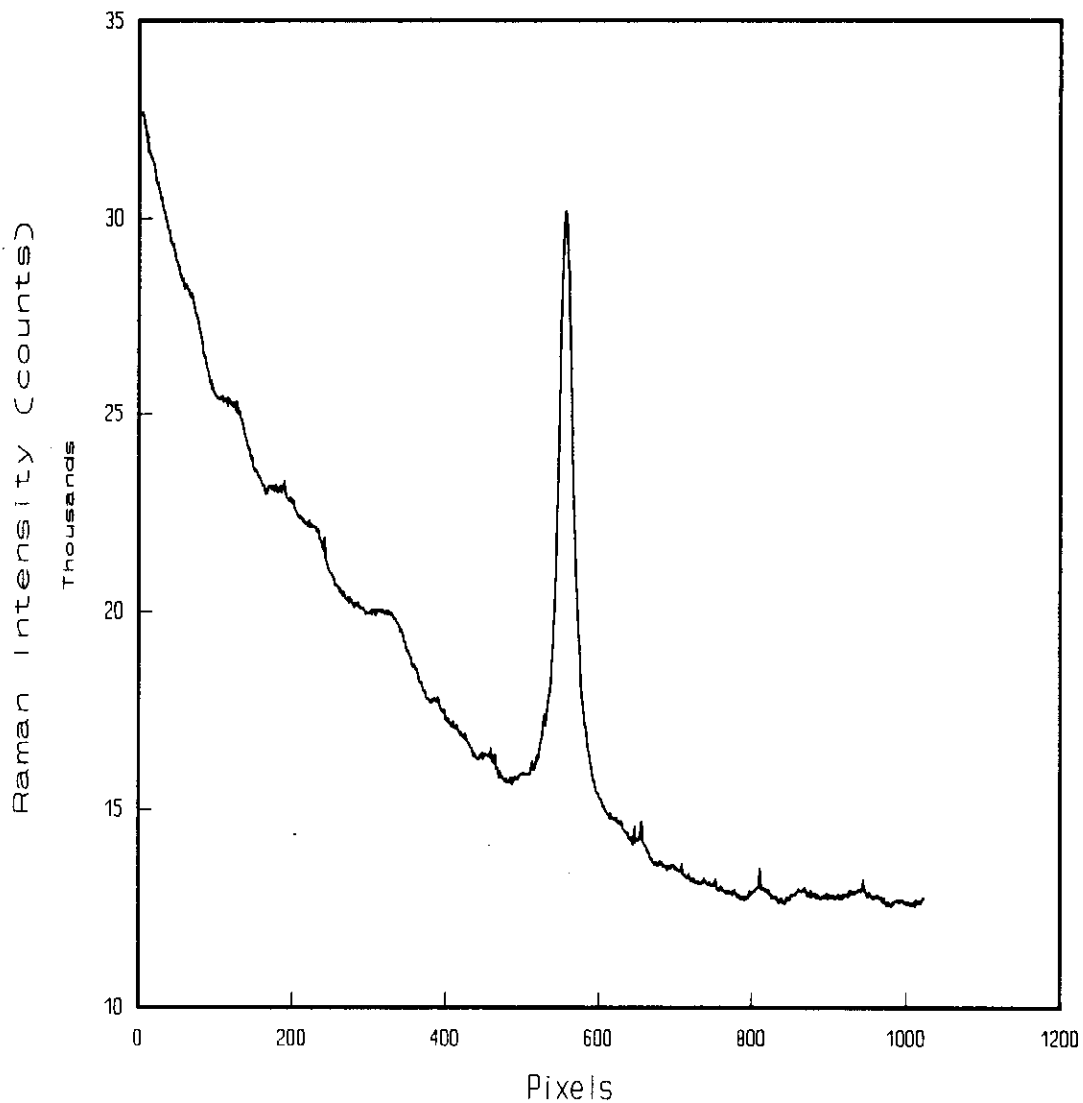
# Sodium Sulphate

centered at 900 nm



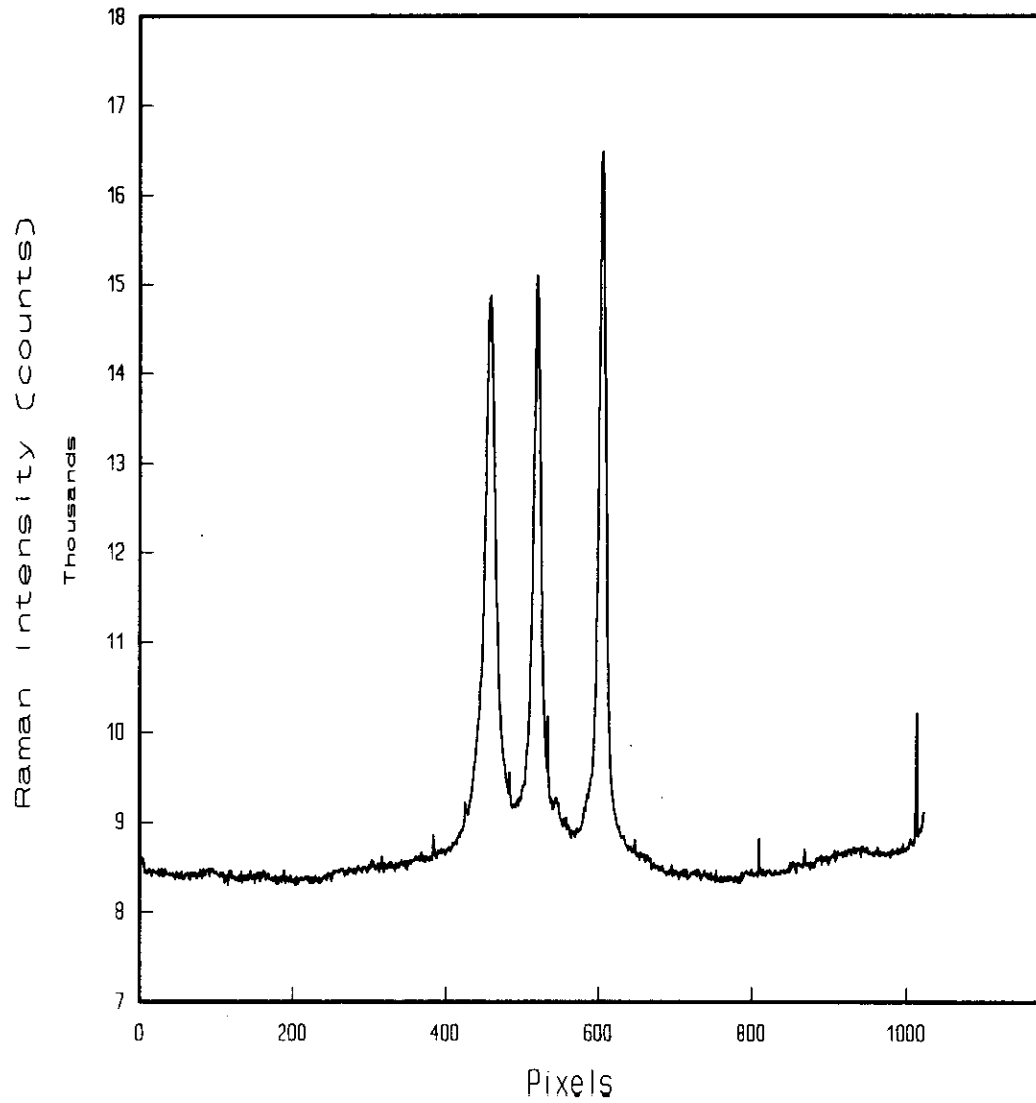
# Sodium Nitrite

centered at 920 nm



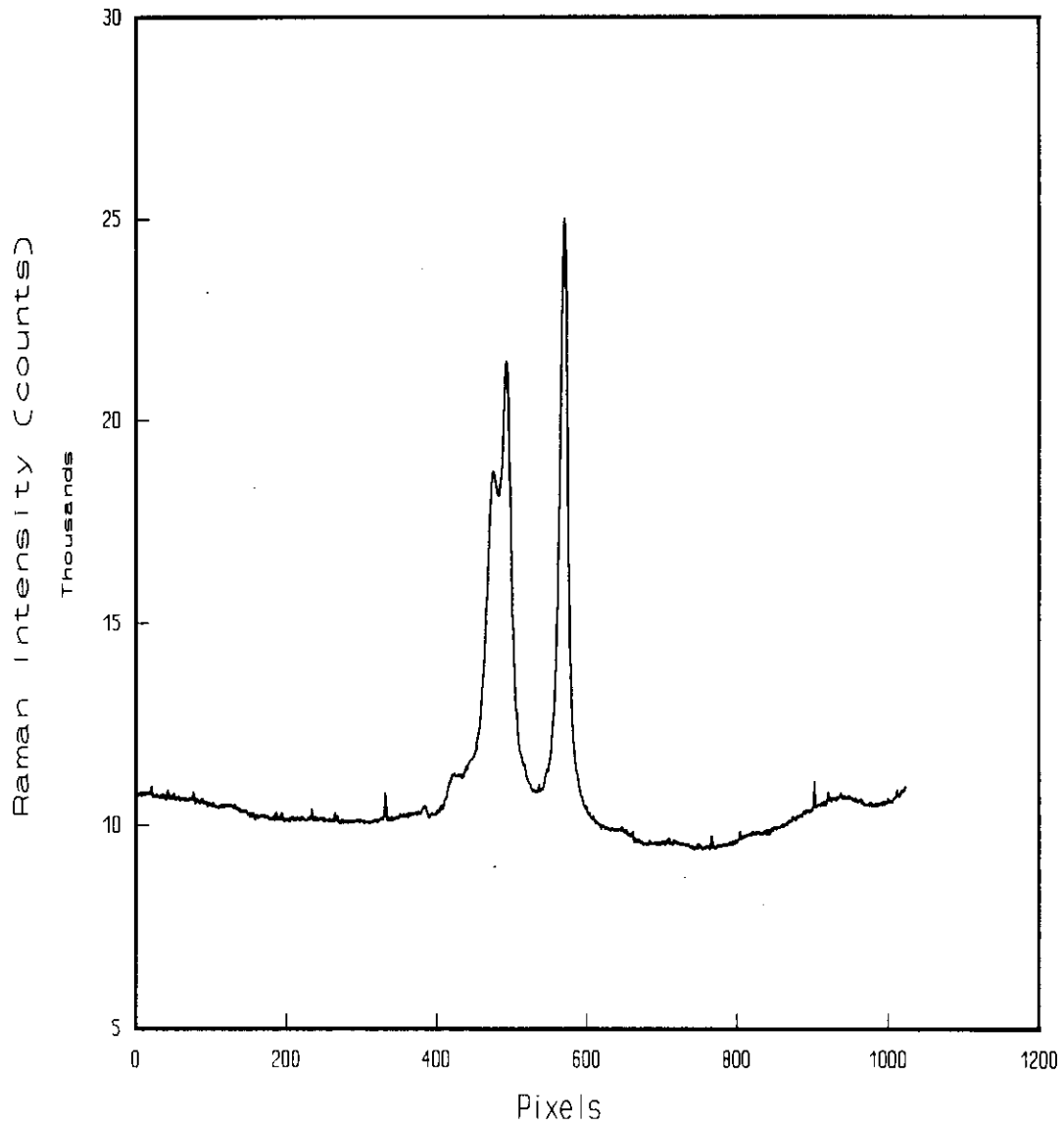
# Sodium Ferrocyanide

centered at 990 nm



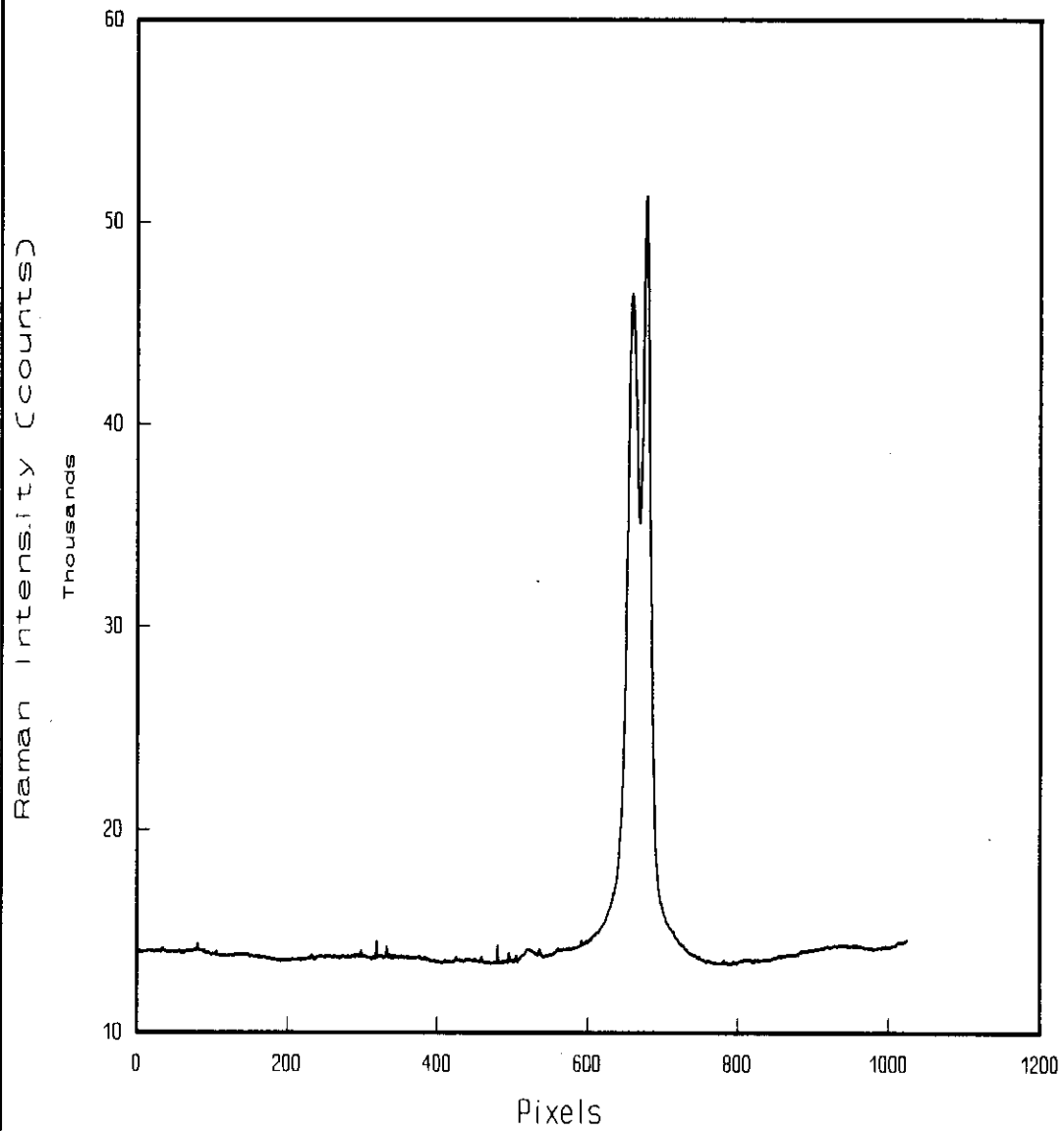
# Potassium Ferrocyanide

centered at 990 nm



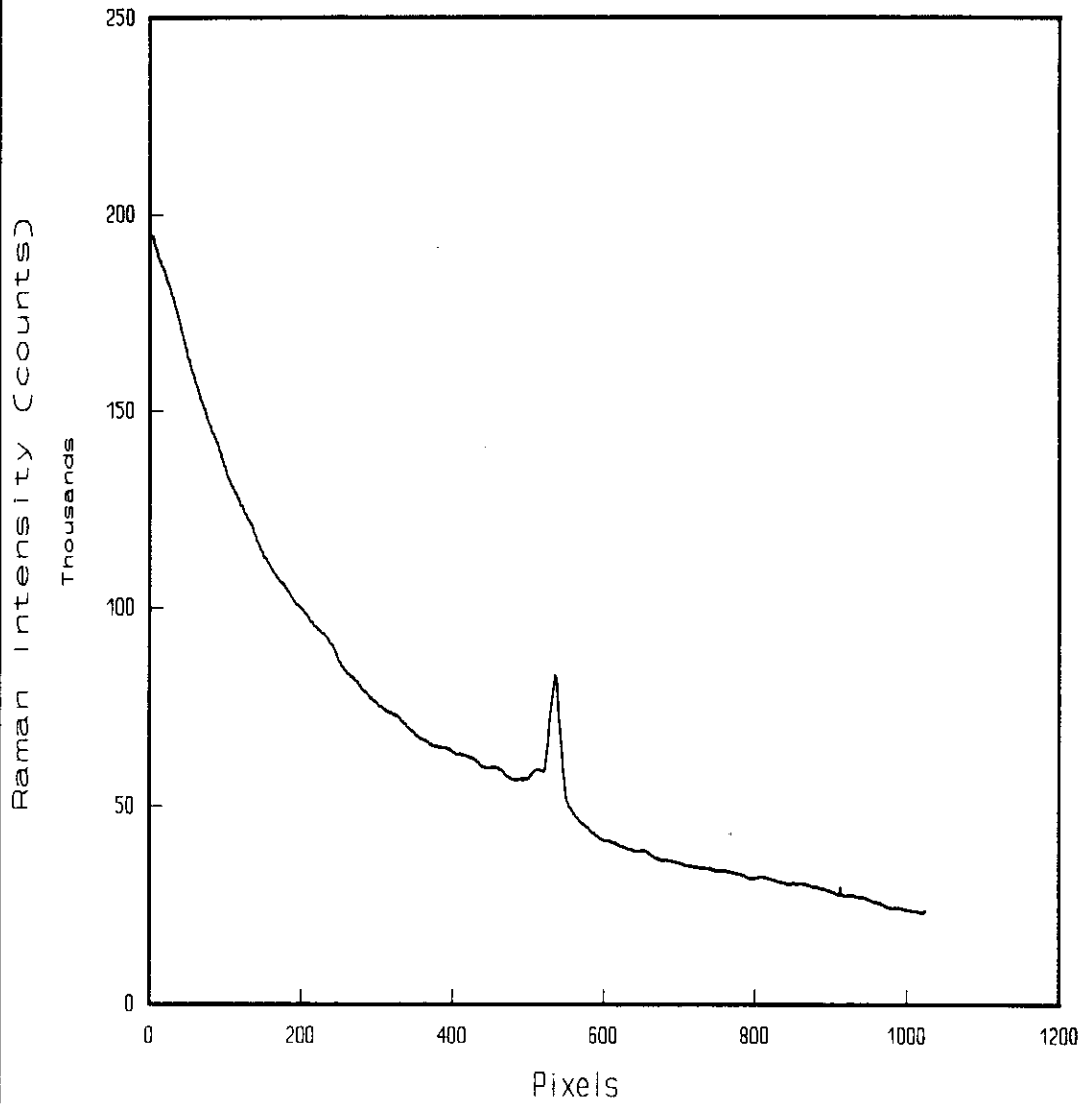
# Potassium Ferricyanide

centered at 990 nm



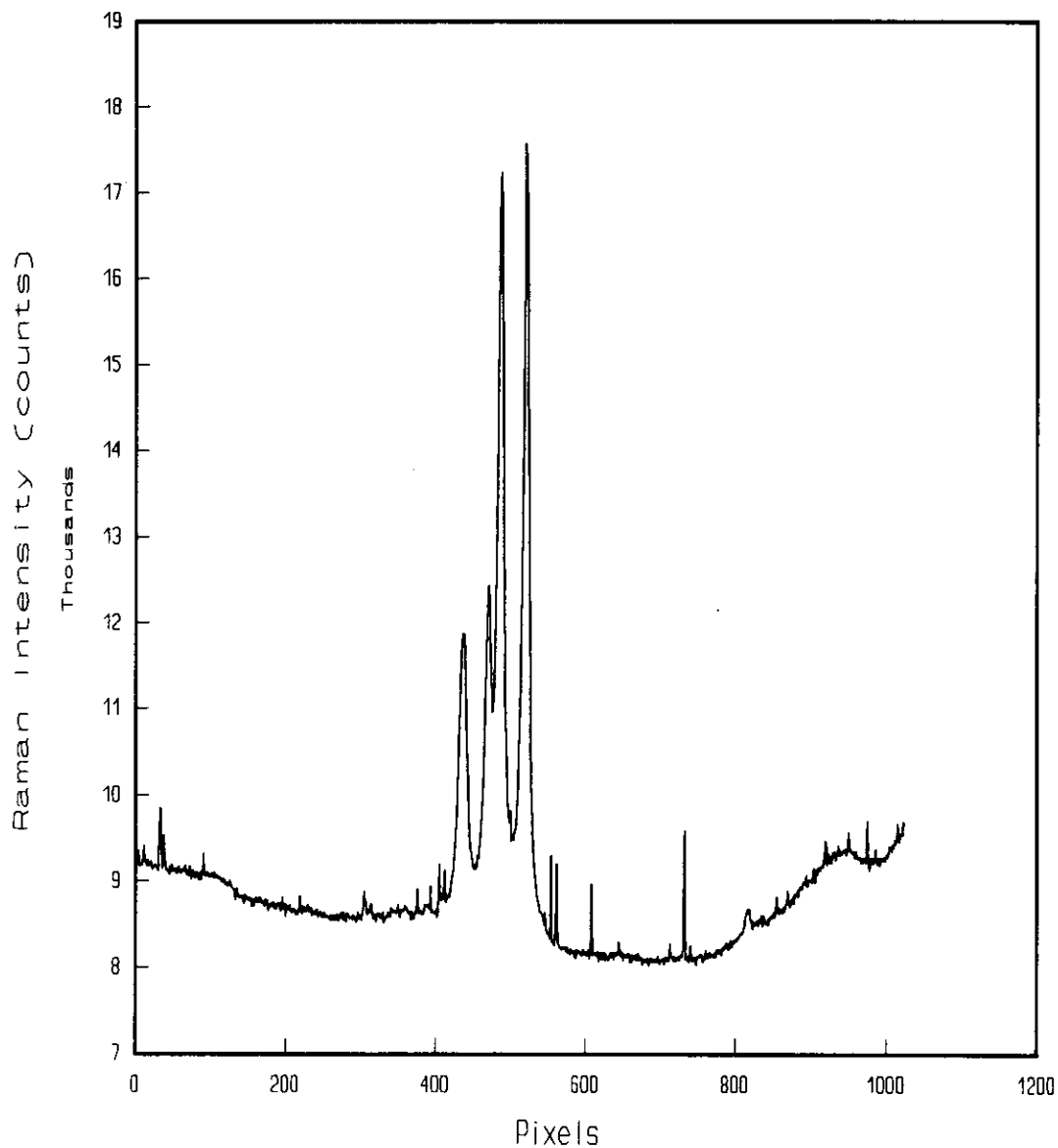
# Sodium Carbonate

centered at 900 nm



# Sodium Nitrosylpentacyanoferrate

centered at 1000 nm



This page intentionally left blank.

94325.446



913205-417

## APPENDIX B

### PRELIMINARY LABORATORY TECHNICAL PROCEDURE

This page intentionally left blank.

1  
2  
3  
4  
5  
6  
7  
8  
9  
10  
11  
12  
13  
14  
15  
16  
17  
18  
19  
20  
21  
22  
23  
24  
25  
26  
27  
28  
29  
30  
31  
32  
33  
34  
35  
36  
37  
38  
39  
40  
41  
42  
43  
44  
45  
46  
47  
48  
49  
50  
51  
52  
53  
54  
55  
56  
57  
58  
59  
60  
61  
62  
63  
64  
65  
66  
67  
68  
69  
70  
71  
72  
73  
74  
75  
76  
77  
78  
79  
80  
81  
82  
83  
84  
85  
86  
87  
88  
89  
90  
91  
92  
93  
94  
95  
96  
97  
98  
99  
100

## OPERATION OF DISPERSIVE LASER RAMAN SPECTROMETER

### SUMMARY

This procedure is used to operate the Dispersive Raman System in the 222-S or 222-SA laboratory in support of sample screening and process analysis.

### APPLICATIONS/LIMITATIONS

This procedure applies to the work performed by Process Analytical Chemistry Laboratories (PCL) personnel during analysis of tank core samples using the Dispersive Raman instrument. Some phases or parts of analysis are under development; therefore, some flexibility must be maintained to allow for modifications while the system is placed into operation. Any deviations from this procedure will be documented in controlled laboratory notebooks and/or data sheets. If these deviations involve safety concerns not already covered by approved procedures, safety approval will be obtained on a Job Safety Analysis form before performing the work.

This procedure is currently limited to the operation of the instrument only, and does not include extensive data interpretation and customer results communication. The instrument data acquisition is performed via menu-driven software that includes extensive data treatment algorithms. All data interpretation and treatment must be performed by cognizant scientists. Only after peer review should data be released for use by the customer.

The current system is capable of detecting oxyanions and ferrocyanide species and may be used to provide an overview of types of organic species suspected in tank or process samples. The current detection limit of this system is 0.5 wt% for ferrocyanide species. As with all other laboratory methods, this detection limit is extremely matrix dependent.

### SAFETY

Before using this procedure, the user should review the equipment list and ensure familiarity with laser safety regulations and electrical hazards. The physical location where analysis is to be performed should be restricted to those personnel who have obtained a laser eye exam and laser safety training. The area must be posted for operation of a Class IIb laser. All applicable laboratory safety precautions for handling radiological samples, hazardous chemicals, and hazardous wastes shall be followed.

All radiological concerns shall be covered by approved Radiation Work Permits (RWP). Before this system is used on radiological samples, the user should review all applicable radiological guidelines. Health Physics Technicians (HPT) may specify additional requirements, as needed.

## EQUIPMENT

Pigtails fiber optic  
SPEX single-stage monochrometer  
Omnichrome argon ion laser  
Princeton Instruments charge-coupled device (CCD) detector with liquid nitrogen dewar  
Computer

## PRESTART CONDITIONS

The cognizant scientist should know as much as possible about the sample before analysis in order to judge:

- Region of interest to acquire sample
- Special handling instructions (hot cell vs. hood)
- Amount and type of information required from the sample

Some samples may come with test plans or statements of work that will provide guidance for analysis and/or screening.

## PROCEDURE STEPS

### A. SYSTEM START UP

NOTE: Instrument may be installed at either a hood or at the hot cell.

1. Plug in instrument power strip and turn on power.

CAUTION: Thermal hazards exist with the use of liquid nitrogen. Wear asbestos gloves or suitable thermal insulation on hands when handling liquid nitrogen dewars and stand away from spilling if it occurs.

2. Fill the detector nitrogen dewar with liquid nitrogen.

NOTE: Argon ion laser requires 208 V output and must be plugged in separately.

3. Plug in argon ion laser if this laser is being used.
4. Turn on the computer, spectrometer controller (at center-back), and detector controller.
5. Turn on red A/C line switch to the argon ion laser.

CAUTION: Ensure that the laser shutter (small blue box) is turned off.

6. Insert key into laser lock and turn clockwise 180 °, then turn counterclockwise 90 °.

7. Make a directory on the "D drive" (D:) according to date and session.

example:

where AR0730a

AR = Argon ion laser  
0730 = July 30th  
a = Session a

8. Type **C C F Return** from within the directory created in step 7.
9. Follow software direction and add initials to the file to log on.

#### B. OBTAIN A NEON STANDARD LINE MARKER

1. Set spectrometer to desired wavelength.
2. Connect fiber optic for obtaining neon and white light to spectrometer.
3. Plug in neon standard source and place distal end of fiber optic over the source.
4. Press **F** for "free run."

NOTE: Use free run at first to check spectra and exposure time.

5. Set exposure time to time last used in logbook.
6. Press **R** for "run" and check spectra. If OK, press **Esc**.
7. Select "timed-measure mode."
8. Press **S** for "spectroscopic conditions."
9. Press **E** for "exposure time" and enter time for last neon in logbook.
10. Press **N** for "number of coadds," and enter the number for the last neon in logbook.
11. Press **Q** for "quit."
12. Press **C** for "composition."
13. Enter 1st as Neon, press **Enter**, and press **E** for "exit."
14. Press **A**, and then press **E** until screen reads "disabled."
15. Press **Q** for quit.
16. Press **H** for "header information."

17. Press **[N]** and enter the "notebook number." Press **[P]** for "page" and enter the page number of the logbook.
18. Press **[R]** for "record and exit."
19. Press **[T]** for "type of set."
20. Select **[S]** for "spectrum."
21. Select filename NEON1 with no numeric.
22. Enter the date, material or sample description, filename, spectrometer wavelength, exposure time (seconds), number of coadds, sequential spectra directory, and comments.
23. Press **[R]** for run, and answer the questions as they progress until a blank run screen shows on the monitor.

C. OBTAIN A WHITE LIGHT SPECTRUM FROM STANDARD TUNGSTEN SOURCE

1. Connect fiber optic to the tungsten source holder.
2. Plug in the tungsten source.
3. Press **[F]** for free run.

NOTE: Use free run at first to check spectra and exposure time.

4. Set exposure time to time last used in logbook.
5. Press **[R]** for run and check spectra. If OK press **[Esc]**, and press **[Q]** for quit.

NOTE: The spectrometer software must be in the timed-measure mode menu to proceed. When spectral acquisition is complete the software will quit in this menu.

6. Press **[T]** for timed-measure mode.
7. Press **[S]** for spectroscopic conditions.
8. Press **[E]** for exposure time, and enter time last used in logbook.
9. Press **[N]** for number of coadds and enter number last used in logbook.
10. Press **[Q]** for quit.
11. Select **[C]** for composition.
12. Select 1st and enter tungsten lamp.
13. Press **[E]** for exit.

14. Select "file type" by pressing **[T]** to "white light" by pressing **[W]**.
15. Select "filename" by pressing **[F]**, and enter the spectrometer position followed by a **[W]** for white light spectrum.
16. Press **[N]** for "numeric" to use.
17. Press **[N]** for "no numeric."
18. Press **[R]** for run, and answer the check questions accordingly.

#### D. OBTAIN A DARK CURRENT SPECTRUM

1. Close the spectrometer entrance shutter at the slits.
2. Press **[T]** for timed-measure mode.
3. Press **[S]** for spectroscopic conditions.
4. Press **[N]** for number of coadds and enter number last used in logbook.
5. Press **[E]** for exposure time and enter time last used in logbook.
6. Press **[Q]** for quit.
7. Press **[C]** for composition.
8. Select 1st and then type "NONE."
9. Press **[T]** for type of spectrum and **[D]** for "dark."
10. Select **[F]** for filename and enter sample ID for the filename.

101SY.drk

└── 101SY = Sample ID  
 └── .drk = Extension for dark current file type

11. Select **[N]** for numeric to use and **[N]** for no numeric.
12. In the logbook, enter the date, filename, spectrometer position in Å, exposure time (seconds), number of coadds, sequential spectra directory, and comments.
13. Press **[R]** for run and answer the check questions accordingly.

#### E. CHECK THE LASER POWER

1. Connect the power meter pigtail to the laser head.
2. Open laser shutter at the electronic box.
3. Turn on the power meter.

4. Read the laser power in mW and record in the logbook under "comments" for the date entered.
5. Close the laser shutter and disconnect the power meter fiber optic from the laser head.

F. RUN A SILICA BACKGROUND, REFERENCE STANDARD, AND SAMPLE

NOTE: This is to obtain data for signal-to-noise ratio.

1. Open the spectrometer shutter.
2. Connect the probe fiber optic to the laser head.
3. Place the fiber optic in a nitrate, ferrocyanide, or other suitable standard depending on spectral window selected.
4. Press **[F]** for free run.
6. Select **[P]** for laser power and enter the power value obtained in part E.

NOTE: Use free run at first to check spectra and exposure time and to optimize signal.

7. Set exposure time to time last used in log book.
8. Place the probe in NaCl for a silica spectrum.
9. Press **[R]** for run and check spectra.
10. When an optimized spectrum is achieved, press **[Esc]** and then press **[Q]** for quit.
11. Press **[T]** for timed-measure mode.
12. Press **[S]** for spectroscopic conditions.
13. Press **[N]** for number of coadds and enter number.
14. Press **[E]** for exposure time and enter time.
15. Press **[Q]** for quit.
16. Select **[C]** for composition and enter 1st as NaCl or sample identification.
17. Enter 2nd and describe the sample settings if appropriate (i.e., vertical or horizontal).
18. Select **[L]** for "laser on/off/power."
19. Enter laser on.



20. Press **[G]** for "give laser power reading" and enter the laser power.
21. Press **[E]** for exit.
22. From the timed-measure mode, select **[A]** for "auto dark/white correct" and toggle **[E]** until the screen shows "enabled."
23. Press **[W]** for "get white set."
24. Press **[R]** for "read binary files."
25. Type \*.cnt in response to the question asked.
26. Select the tungsten file with the .cnt extension that was obtained in part C by highlighting the file.
27. Press **[F10]** to accept and press **[F10]** again to return to the previous menu.
28. Press **[D]** for "drk set."
29. Select **[R]** for read binary files, and type **\*.DRK****[Return]** in response to the question asked.
30. Select the dark set obtained in part D by highlighting the file.
31. Press **[F10]** to accept and then press **[F10]** again to return to the previous menu.
32. Select **[O]** for "operand dark set" and select the same dark set as in steps 16 through 18 by highlighting the file.
33. Press **[F10]** to accept and then press **[F10]** again to return to the previous menu.
34. Press **[E]** for exit.
35. Select **[T]** for "type of spectrum" and **[S]** for spectrum.
36. Press **[F]** for filename and enter NaCl.
37. Press **[N]** for numeric and **[N]** for no numeric.
38. Press **[R]** for run and answer the check questions accordingly.
39. Select a reference standard for the spectral window of interest.
40. Type **[N]** for numeric to use, press **[S]** as 1 for the first spectrum of the day, and add one to this number for every sequential spectrum obtained for the day.
41. Enter filename as NANO3\_, or name of appropriate standard. This will provide a filename with the last digit showing the sequential number of the last nitrate spectrum run.

9443205-125  
521 50816

42. Enter **[C]** for "composite" and 1st as NaNO3 ("s" or "l" depending on the phase of the sample used).
43. Press **[E]** for exit.
44. Select **[R]** for run and answer the check questions accordingly.

G. DETERMINE THE SIGNAL-TO-NOISE RATIO  
FOR A STANDARD IN THE SPECTRAL WINDOW  
OF INTEREST AND RECORD IN THE LOGBOOK

1. Exit to the main menu.
2. Subtract the silica from the reference sample spectrum, by selecting **[I]** for "interactive subtract."

NOTE: Subtract the silica from your reference standard.

3. Select **[I]** for "ID operator set," and read-in or select the corresponding silica spectrum.
  - a. Press **[R]** for "read binary files."
  - b. Type **\*.\*Return**.
  - c. Select set by highlighting file (file having .DWT filename extensions). Press **[F10]** to accept and then press **[F10]** again.
4. Select **[L]** for "locate the operand," and read-in the reference standard spectrum.
  - a. Press **[R]** for read binary files.
  - b. Type **\*.\*Return**.
  - c. Select set by highlighting file (file having .DWT filename extension). Press **[F10]** to accept and then press **[F10]** again.
5. Select **[D]** for "do subtraction" and use the right and left arrow keys or the page up and page down keys to bring in the subtracted spectrum in a series of selections until the background is no longer evident and there are no negative-going peaks in the spectrum.
6. Press **[F10]** and then press **[E]** for exit.

NOTE: This brings you back to the main menu.

7. Press **[V]** for "video display."
8. Press **[G]** for "get data."
9. Press **[S]** for "save sets."
10. Press **[I]** for "ID file type." Press **[F]** for "float."
11. Press **[C]** to select current set names, press **[P]** for "proceed," press **[Enter]**, and then press **[F10]**.

NOTE: When any key is pressed the computer will return to the "Save Sets Menu."

12. Press **[E]** for exit.

13. Press **[R]** for "report results," press **[S]** for "standard deviation," and press **[G]** for "get data."

NOTE: Set to use should already be highlighted.

14. Highlight file having .REL filename extension, then press **[F10]**.

NOTE: Range is area where there are no peaks.

15. Press **[I]** for "ID range" (use page up, page down, and arrow keys to select Range). Press **[S]** to set ends of range, and press **[F10]** to accept.

16. Press **[R]** for "results storage," press **[G]** for "get set," and press **[D]** for "do calculation."

17. Write average, standard deviation, and variance in logbook.

18. Press **[E]** for exit, press **[M]** for "main menu," and press **[V]** for video display.

19. Press **[G]** for get data. Select (highlight) file having .REL filename extension and then press **[F10]** to accept.

20. Press **[D]** for "display data."

21. Press **[R]** for "data range."

22. Use the page up, page down, and arrow keys to locate marker on the largest peak. Write the value in the logbook.

23. Press **[F10]**, press **[Esc]**, and press **[E]** for exit.

24. Subtract the average obtained in step 15 from the value just obtained in step 22, then divide by the standard deviation also obtained in step 16. The answer is the signal-to-noise ratio. Record this in the logbook.

25. Record the ambient temperature, the laser head voltage, and original power reading in the notebook for the date.

H. RUN A SAMPLE IN THE SAME FORMAT AS THE REFERENCE SPECTRA WITH A SAMPLE ID AND NUMERIC FOR ALL COADDS

I. RUN A NEON SPECTRUM AFTER EVERY BATCH OF SAMPLES OR AT LEAST AFTER EVERY 5 SAMPLES ANALYZED

J. SUBMIT SPECTRA TO COGNIZANT CHEMIST FOR DATA PROCESSING

## DISCUSSION

The Raman system is primarily used as a screening tool for analytical samples in the laboratory. The detection limit for ferrocyanide is currently below those results being obtained using EPA-approved methods. However, some oxyanions are present in tank waste samples at concentrations of weight percent. Therefore, this instrument has potential in directing subsampling and sample preparation activities in the hot cells.

Hanford Site programs have resulted in the identification of the need for a screening methodology to quickly identify chemical heterogeneities within specimens from larger waste containers.

9413205-428

ONSITE

9

U.S. Department of Energy,  
Richland Field Office

R. F. Christensen (4)		R3-72
R. E. Gerton	R3-72	
A. G. Krasopoulos	A4-81	
Public Reading Room	H2-53	
RL Docket File (2)	H5-36	

8

Pacific Northwest Laboratory

R. T. Allemann	K7-15	
S. A. Bryan	P7-25	
B. M. Johnson	K1-78	
M. A. Lilga	P8-38	
R. D. Scheele	P7-25	
G. F. Schiefelbein	P8-38	
D. M. Strachan	K2-38	
Hanford Technical Library		P8-55

21

Westinghouse Hanford Company

S. J. Mech	L5-55
N. J. Milliken	H4-62
A. F. Noonan	R2-12
R. S. Popielarczyk	R1-30
T. V. Rebagay	T6-30
F. R. Reich	L5-63
C. P. Schroeder	L7-06
B. C. Simpson	R2-12
J. P. Sloughter	T6-07
H. E. Smith	R2-12
J. P. Summerhays	R2-85
H. Toffer	H0-38
G. L. Troyer	T6-50
W. T. Watson	H0-38
W. D. Winkelman	L5-55
D. D. Wodrich	H0-30
W. F. Zuroff	R2-14
Central Files	L8-04
EDMC	H6-08
IRA (3)	R1-05
TFIC	R1-20

9413205.1429

**THIS PAGE INTENTIONALLY  
LEFT BLANK**